

SOLID-STATE PROCESSING OF THERMOPLASTIC POLYMERS

by

Linda Wagnez Vick

*Dissertation submitted to the Faculty of the
Virginia Polytechnic Institute and State University
in partial fulfillment of the requirements for the degree of:*

Doctor of Philosophy

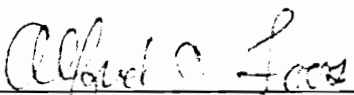
in

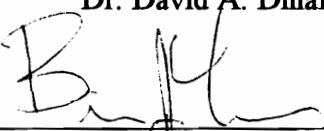
Materials Engineering Science


Approved:


Dr. Richey M. Davis


Dr. David A. Dillard


Dr. Alfred C. Loos


Dr. Brian J. Love


Dr. Ronald G. Kander, Chairman

Key Words: Compaction, Sintering, Consolidation, Polycarbonate, Powder

SOLID-STATE PROCESSING OF THERMOPLASTIC POLYMERS

by

Linda Wagnecz Vick

Ronald G. Kander, Chairman

(ABSTRACT)

Although compaction and sintering of polymeric powders has been investigated since the early 1970's, this processing method is not widely used, possibly because the fundamental mechanisms which control compaction and sintering have never been fully understood. This study has made significant contributions to our understanding of compaction and sintering of polymers. It was demonstrated that mechanical properties (yield strength, modulus) and physical characteristics (degree of physical aging, glass transition temperature, presence of crystallinity) of the particles, and thus, powder processing, storage, and handling techniques, affect the ability of the polymer to be successfully compacted. The difficulties encountered in sintering polymeric compacts were explained in terms of a loss of configurational entropy of the polymer molecules during compaction, which caused large-scale dimensional recovery in the particles upon heating above T_g . Hot compaction (above room temperature, but below T_g) was not found to be useful in eliminating recovery during pressureless sintering. However, consolidation of compacts formed at room temperature (by heating 10-20°C above T_g and applying a small pressure (less than 50 kPa)) was shown to be a promising processing method.

Acknowledgments

The author would like to express thanks and appreciation to the following people for both directly and indirectly supporting this research:

- Dr. Ronald G. Kander, for all the time and effort he spent as committee chairman, offering guidance and encouragement when I needed it most.
- Dr.'s Rick Davis, David Dillard, Alfred Loos, and Brian Love, for serving as committee members.
- The Virginia Institute for Material Systems and the Charles E. Minor Fellowship Program, for partial financial support of this research.
- The members of *Kander's Group*, for technical advice, assistance with equipment, and friendship. You guys were lots of fun to work with!
- Dr. Gang Chen, Mr. Steve McCartney, Mr. Mack McCord, for technical advice and assistance with the environmental scanning electron microscope.
- Dr. Pamela Percha, for training and guidance on the use of the thermomechanical analyzer, and Dr. David Dillard, for allowing me to use this equipment.
- Mr. Peter Dunn of the Mining Engineering Department, for assistance in wet sieving polycarbonate powder for use in examining particle size effects.
- Amy of the Chemistry Department for performing gel permeation chromatography experiments on the sieved polycarbonate powder.
- Glen and Laura Wagnecz, for being a great brother and sister.

- Al and Sylvia Wagnecz, the author's parents, for many years of love and encouragement.
- Alison and Everett Vick, born on February 26, 1996, for forcing their mom to stay home and write her dissertation while *patiently* awaiting their arrival.
- Kristen (age 6) and Kelsey (age 5), for teaching their mom patience and helping her keep her sense of humor.
- Dr. Brian "Mate" Vick, for being a great husband and dad. I couldn't have done it without you!!!

Table of Contents

Abstract	ii
Acknowledgments	iii
List of Figures	viii
List of Tables	xiii
I. Introduction	1
Background	1
Problem Statement	3
Goals	4
Technical Approach	4
II. Literature Survey	8
Powder Metallurgy	8
Compaction and Sintering of Polymeric Powders	11
Introduction	11
Compaction	12
Sintering	21
Theoretical Models for Strength Development at	
Polymer-Polymer Interfaces	29
Strength Development through Reptation	29
Intimate Contact Formation	32
Summary	36
III. Experimental Methods	38
Materials	38
Processing	42
Equipment	42
Compaction	42
Room Temperature Compaction	42
Hot Compaction	43
Pressureless Sintering	44
Consolidation	45
Preparation of Thin Films	46
Physical Aging of Powders and Films	47

Characterization	47
Density Measurement	47
Thermal Properties	52
Thermomechanical Behavior	53
Microtensile Testing	53
Characterization of Particle Size Effects	54
Environmental Scanning Electron Microscopy	57
IV. Room Temperature Compaction	58
Compaction of Polycarbonate Powder	58
Effect of Compaction Time on Density	58
Effect of Thickness on Density and Porosity	59
Effect of Compaction Pressure on Density - Unaged Polycarbonate	61
Effect of Compaction Pressure on Density - Aged Polycarbonate	62
Effects of Physical Aging on Densification Mechanisms	63
Effect of Physical Aging on Microstructure	65
Effect of Compaction on Thermal Properties	66
Room Temperature Compaction of Semicrystalline Polymers	71
Linear Low Density Polyethylene	71
Nylon-11	73
Poly(ether ether ketone)	75
Summary of Room Temperature Compaction Results	77
V. Sintering of Compacts Formed at Room Temperature	80
Isothermal Pressureless Sintering of Polycarbonate Compacts	80
Density Changes during Pressureless Sintering	80
Microstructural Changes during Pressureless Sintering	83
Dynamic Sintering of Polycarbonate Compacts	83
TMA of Bulk Polycarbonate Films	85
TMA of Room Temperature Compacted Polycarbonate	86
Transition from Reversible to Irreversible Recovery	86
Expansion Above the Transition Temperature	89
Effect of Compaction Pressure on Recovery	91
Effect of Physical Aging on Recovery	94
Dynamic Sintering of Semicrystalline Polymers	98
Nylon-11	98
Poly(ether ether ketone)	100
Discussion	103
Summary	106
Possible Ways to Improve the Compaction and Sintering Processes	107

VI. Hot Compaction of Polycarbonate Powder	109
Hot Compaction of Polycarbonate Powder	109
Isothermal Pressureless Sintering of Hot Compacted Polycarbonate	113
Effect of Compaction Temperature on Sintered Density	113
Effect of Compaction Pressure on Sintered Density	115
Microstructural Changes during Pressureless Sintering	115
Effect of Processing on Microtensile Strength	118
Dynamic Sintering of Hot Compacted Polycarbonate	121
Effect of Compaction Temperature on Recovery	121
Effect of Compaction Pressure on Recovery	124
Summary	125
VII. Consolidation of Cold Compacted Polycarbonate	127
Isothermal Consolidation of Polycarbonate Compacts	127
Dynamic Consolidation of Polycarbonate Compacts	130
Difficulties in Theoretically Modeling the Consolidation Process	137
Summary	140
VIII. Summary and Conclusions	141
Room Temperature Compaction	141
Unaged Polycarbonate	141
Physically Aged Polycarbonate	141
Semicrystalline Polymers	143
Sintering of Compacts Formed at Room Temperature	144
Polycarbonate Compacts	144
Semicrystalline Polymers	146
Hot Compaction of Polycarbonate Powder	147
Consolidation of Polycarbonate Powder	148
Possible Applications of Compaction and Sintering Technology	149
Contributions of this Research	150
References	151
Vita	156

List of Figures

Figure 1 -	The effect of compaction pressure on the green density of UHMWPE from several manufacturers [11].	14
Figure 2 -	Green strength as a function of densification parameter for the UHMWPE powders from different manufacturers whose green densities are plotted in Figure 1 [11].	15
Figure 3 -	Schematic showing the neck radius, x , and the particle radius, a , used in the sintering equations described in the text.	23
Figure 4 -	Effect of sintering time and temperature on (a) the tensile strength and (b) the thickness of UHMWPE precompacted at 75 ksi at compaction rates of 0.71 and 0.78 inches per minute [9].	25
Figure 5 -	ESEM micrograph of as-received LPC3000 polycarbonate	39
Figure 6 -	GPC results for coarse and fine polycarbonate particles	57
Figure 7 -	Effect of compaction time on the normalized density of polycarbonate compacts (compaction pressure: 40 MPa, compact mass: 1.5 gram).	59
Figure 8 -	Effect of compact thickness on the volume fraction of open and closed porosity in polycarbonate compacts (compaction time: 5 minutes.).	60
Figure 9 -	Effect of compaction pressure on the normalized density of polycarbonate compacts (compaction time: 5 minutes, compact mass: 1.5 gram).	61
Figure 10 -	Effect of compaction pressure on the normalized density of compacts made from unaged and aged polycarbonate powder (compaction time: 5 minutes, compact mass: 1.5 gram).	63
Figure 11 -	Stages of compaction for metals, ceramics, and polymers.	64
Figure 12 -	ESEM micrographs of polycarbonate compacts made from (a) unaged and (b) aged powder having densities of 85% of the theoretical density of polycarbonate (compaction time: 5 minutes, compact mass: 1.5 gram, compaction pressure: (a) 60 MPa and (b) 140 MPa).	67

Figure 13 -	Differential scanning calorimetry traces for as-received and aged polycarbonate (first and second scans) obtained at a heating rate of 10°C/minute.	68
Figure 14 -	Effect of compaction pressure on the thermal properties of unaged (as-received) polycarbonate powder (compaction time: 5 minutes, compact mass: 1.5 grams).	69
Figure 15 -	Effect of compaction on the thermal properties of aged polycarbonate powder (compaction time: 5 minutes, compact mass: 1.5 grams).	70
Figure 16 -	Effect of compaction pressure on the normalized density of Nylon 11 compacts as measured using the geometric technique at various times after removal of the compaction pressure (compaction time: 5 minutes, compact mass: 1.5 grams).	74
Figure 17 -	Effect of compaction pressure on the normalized density of PEEK compacts (compaction time: 5 minutes, compact mass: 1.5 grams).	76
Figure 18 -	Effect of pressureless sintering at 165°C on the normalized density of polycarbonate powder compacted at room temperature at compaction pressures of 40, 80, and 160 MPa (compaction time: 5 minutes, compact mass: 1.5 grams).	81
Figure 19 -	ESEM Micrographs of polycarbonate compacts made from (a) unaged and (b) aged powder after pressureless sintering for 20 minutes at 165°C (compaction time: 5 minutes, compact mass: 1.5 grams, compaction pressure: 60 MPa, density prior to sintering: 85% of the theoretical density of polycarbonate.)	84
Figure 20-	TMA trace for bulk (unaged) polycarbonate film scanned at heating and cooling rates of 5°C/minute (pressure exerted by probe: <40 Pa (0.006 psi)).	85
Figure 21 -	(a) Thickness change and (b) estimated normalized density (fraction of theoretical density) during TMA testing of polycarbonate compacts formed at room temperature at a compaction pressure of 80 MPa from unaged powder (compaction time: 5 minutes, compact mass: 1 gram, pressure exerted by probe: < 40 Pa (0.006 psi).	87
Figure 22 -	Schematic showing transition from reversible to irreversible expansion which occurs at about 50°C in cold compacted polycarbonate.	89

Figure 23 -	Change in thickness as a function of time during TMA testing of room temperature compacted polycarbonate (compaction time: 5 minutes, compaction pressure: 80 MPa, pressure exerted by probe: < 40 Pa (0.006 psi)).	90
Figure 24 -	Normalized density (fraction of theoretical density) estimated from TMA data for compacts formed from unaged polycarbonate powder at room temperature at compaction pressures of 40, 80, and 160 MPa (compaction time: 5 minutes, compact mass: 1 gram, pressure exerted by probe: < 40 Pa (0.006 psi)).	92
Figure 25 -	Normalized density (fraction of theoretical density) estimated from TMA data for compacts formed from aged and unaged polycarbonate powder at room temperature at a compaction pressure of 80 MPa (compaction time: 5 min., compact mass: 1 gram, pressure exerted by probe: < 40 Pa (0.006 psi)).	95
Figure 26-	Effect of physical aging of polycarbonate particles prior to compaction on the dimensional changes during TMA analysis for compaction pressures of 40, 80, and 160 MPa (compaction time: 5 minutes, compact mass: 1 gram, TMA load: < 0.2 kPa (0.03 psi)).	97
Figure 27 -	Estimated normalized density (fraction of theoretical density) during TMA testing of Nylon-11 compacts formed at room temperature for isothermal hold temperatures of 100, 150, and 180°C (compaction pressure: 160 MPa, compaction time: 5 minutes, compact mass: 1 gram, pressure exerted by probe: <40 Pa (0.006 psi)).	98
Figure 28 -	Estimated normalized density (fraction of theoretical density) during TMA testing of PEEK compacts formed at room temperature for isothermal hold temperatures of 100, 150, and 180°C (compaction pressure: 80 MPa, compaction time: 5 minutes, compact mass: 1 gram, pressure exerted by probe: <40 Pa (0.006 psi)).	101
Figure 29 -	Extruded polycarbonate rod as cut, after compression to 50% of its original length, and after recovery at 170°C for 30 minutes.	105
Figure 30 -	Effect of compaction temperature on the normalized density of polycarbonate powder as a function of compaction pressure and temperature (preheat time: 5 minutes, compaction time: 5 minutes, compact mass: 1.5 grams).	110

Figure 31-	ESEM micrograph of polycarbonate compact formed at 125°C using unaged powder. (compaction time: 5 minutes, compact mass: 1.5 grams, compaction pressure: 80 MPa, green density: 96% of the theoretical density of polycarbonate).	111
Figure 32 -	Effect of compaction temperature on the normalized density of polycarbonate compacted at 80 MPa during pressureless sintering at 165°C (compaction time: 5 minutes, compact mass: 1.5 grams).	114
Figure 33	Effect of compaction pressure on the normalized density of polycarbonate compacted at 125°C during pressureless sintering at 165°C. (compaction time: 5 minutes, compact mass: 1.5 grams).	116
Figure 34-	ESEM micrograph of polycarbonate compact hot compacted at 125°C made from unaged powder following pressureless sintering for 20 minutes at 165°C (compaction time: 5 minutes, compact mass: 1.5 grams, compaction pressure: 80 MPa, density prior to sintering: 96% of the theoretical density of polycarbonate.)	117
Figure 35 -	Microtensile strengths of polycarbonate compacts at various stages of processing: CC - cold (room temperature) compacted, HC - hot compacted at 125°C, PS -following pressureless sintering for 20 minutes at 165°C, aged - powder aged before compaction. (compaction pressure: 160 MPa for all specimens; all powder unaged prior to compaction unless otherwise noted)	119
Figure 36 -	Normalized density (fraction of theoretical density) estimated from TMA data for compacts formed from unaged polycarbonate powder at room temperature, 100°C, and 125°C at a compaction pressure of 80 MPa (compaction time: 5 min., compact mass: 1 gram, pressure exerted by probe: < 40 Pa (0.006 psi)).	122
Figure 37 -	Normalized density estimated from TMA data for compacts formed from unaged polycarbonate powder at 100°C at compaction pressures of 40, 80, and 160 MPa (compaction time: 5 min., compact mass: 1 gram, pressure exerted by probe: <40 Pa (0.006 psi)).	124
Figure 38 -	Effect of consolidation pressure on the dimensional recovery of polycarbonate compacts consolidated at 162°C for 15 minutes following room temperature compaction at 80 MPa (compaction time: 5 min., compact mass: 1.5 grams, initial compact density: 87% of the theoretical density).	129

Figure 39 - Effect of TMA load on dimensional recovery during TMA scan with 152°C isothermal hold and temperature profile as shown. (compaction pressure: 80 MPa, compaction time: 5 min., compact mass: 1 gram, initial compact density: 87% of the theoretical density).	131
Figure 40 - Effect of TMA load on dimensional recovery during TMA scan with 162°C isothermal hold and temperature profile as shown. (compaction pressure: 80 MPa, compaction time: 5 min., compact mass: 1 gram, initial compact density: 87% of the theoretical density).	133
Figure 41 - Effect of the consolidation pressure on the maximum thickness change measured during thermomechanical analysis. (Data taken from Figures 35-36.)	134
Figure 42 - Percent thickness increase measured after 15 minute hold at the indicated temperature (compaction pressure : 80 MPa, compaction time: 5 minutes, compact mass: dynamic -1 gram, isothermal - 1.5 grams). (Data taken from Figures 34-36.)	136

List of Tables

Table I -	Summary of Theoretical Treatments of Strength Development at Polymer-Polymer Interfaces	30
Table II -	Laserite™ LPC3000 Polycarbonate Properties Supplied by DTM Corp.	39
Table III -	Laserite™ LN4010 Nylon-11 Properties Supplied by DTM Corp.	41
Table IV -	Victrix PEEK Powder Properties Supplied by Manufacturer	41
Table V -	Summary of TMA thermal expansion data obtained on room temperature compacted (unaged) polycarbonate powder (compaction time: 5 minutes, compact mass: 1 gram).	94
Table VI -	Summary of TMA recovery data obtained on room temperature compacted unaged polycarbonate powder (compaction time: 5 minutes, compact mass: 1 gram).	94
Table VII -	Summary of TMA thermal expansion data obtained on room temperature compacted aged polycarbonate powder (compaction time: 5 minutes, compact mass: 1 gram).	96
Table VIII -	Summary of TMA recovery data obtained on room temperature compacted aged polycarbonate powder (compaction time: 5 minutes, compact mass: 1 gram).	96

I - Introduction

Background

Thermoplastic polymers with superior mechanical properties, thermal stability, and solvent resistance have been developed for high-performance engineering applications. However, high melt viscosity, thermal degradation near the melting temperature, and processing temperatures exceeding the limits of conventional processing equipment can make these polymers very difficult and expensive to melt process.

Solution processing, which involves dissolving a polymer in a compatible solvent, is an alternate processing method which avoids the difficulties involved with melt processing. However, with recent efforts to make manufacturing more environmentally-friendly, some of the most effective solvents for solution processing can no longer be used. The chlorofluorocarbon solvents, which are non-flammable, non-toxic, and highly solvating at low temperatures for many polymers, have also been determined to be the most harmful to the environment and are being banned from use.

With the difficulties encountered in melt processing and the environmental problems associated with solution processing, solid-state polymer processing is becoming a more attractive alternative. Here, the term *solid-state* means that the polymer is processed under conditions where bulk flow of the material does not dominate the strength

development process, generally at temperatures just above the glass transition temperature of amorphous polymers or melting temperature of semicrystalline polymers.

Concepts from powder metallurgy have been applied to the solid-state processing of polymers. A number of studies on polymer *compaction* (applying pressure to form contacts) and “*sintering*” (applying heat to promote bonding) have been performed, and a good review of this research is presented by Jog [1]. A majority of the literature is concerned with compaction, but not “sintering,” although it has been known since the earliest studies that heat treatment can greatly improve mechanical properties [2].

Note that in metal and ceramic processing, *sintering* means that processing is performed below the bulk melting temperature. However, the term *sintering* is frequently used to describe heat treatment at temperatures above the glass transition temperature of amorphous polymers or above the melting temperature of semicrystalline polymers and will also be used in this manner in this document. The word *consolidation* will be used to describe heat treatment of previously compacted powder with or without the application of external pressure.

Experiments have shown that processing variables (sintering and compaction times, temperatures, and pressures) and powder characteristics (size, size distribution, and particle morphology) affect the processing of polymer powders as they do in metals and

ceramics.[1] However, it has not been demonstrated that polymers can be processed below their melt temperature without a sacrifice in mechanical properties, as can be done with metals and ceramics. Although the compaction and sintering of polymers has been investigated since the early 1970's, this processing method is not widely used, possibly because the fundamental mechanisms which control polymer compaction and sintering are not well understood, making it difficult to choose appropriate processing conditions.

Problem Statement

From a review of the literature and preliminary results from this study it was apparent that pressureless sintering of room temperature compacted polymers at relatively low temperatures (just above the glass transition temperature of amorphous polymers or melting temperature of semi-crystalline polymers) is not feasible. When thermoplastic polymers are compacted at room temperature, they deform both plastically and viscoelastically, with dimensional changes observed upon removal of the room temperature compaction pressure or upon heating of the compact to relatively low temperatures.

Strength development at polymer-polymer interfaces depends on two processes occurring: the formation of intimate contact between particles and the development of strength through the diffusion of chains across the contact surface. In processes based on powder metallurgy technology, compaction is performed to create (intimate) contacts between

particles and to obtain an acceptable handling strength. However, when healing is attempted at elevated temperatures in the absence of pressure, viscoelastic recovery of the particles takes place, and intimate contact is lost. Sintering temperatures must then be raised well above the glass transition or melt temperature, where coalescence of the particles occurs through viscous flow and is driven by the reduction of surface area. The recovery of deformation by the particles, therefore, prevents compaction and pressureless sintering of thermoplastic polymer powders from being a useful manufacturing process.

Goals

The goals of this study were to:

1. Characterize the recovery process which occurs during the pressureless sintering of cold compacted thermoplastic polymer powders, and
2. Use these results to help modify the compaction and/or sintering processes, with the objective of maintaining the intimate contact between particles, which was achieved through compaction, during the consolidation process.

Technical Approach

Polycarbonate powder was chosen as the primary material for this study. Although polycarbonate does not have some of the processing difficulties (e.g., extremely high melt viscosity, degradation at processing temperatures, or extremely high processing

temperatures) which motivate this study, this polymer was chosen as a model amorphous system. Semicrystalline polymers which are currently processed through compaction and coalescence, such as polytetrafluoroethylene [3], are much more difficult to study, as changes in density due to phase transformations, crystallization, and melting make simple indicators of consolidation, such as volume and density, ambiguous. Also, a large quantity of polycarbonate (from a single processing lot) having a particle size distribution which promotes high packing was donated by the DTM Corporation for use in this study.

To study the recovery process which occurs during the healing of interfaces between particles, two sets of experiments were performed. First, the *room temperature compaction* process was studied by:

- Characterizing the effects of varying compaction time, compaction pressure, and compact thickness.
- Examining the effects of the compaction processing parameters on the thermal properties, physical properties, and morphology of the resulting compacts.
- Investigating the effects of material properties on the room temperature compaction process by studying physically aged polycarbonate and semicrystalline polymers having glass transition temperatures well below, just above, and well above room temperature.

After these experiments were completed, the *pressureless sintering* process was studied by:

- Investigating the effects of isothermal sintering on the density, porosity, morphology, and strength of room temperature compacted polycarbonate.
- Examining the kinetics of pressureless sintering through thermomechanical analysis, which simulates dynamic sintering with a controlled temperature ramp.

Possible methods of controlling particle recovery during sintering are *hot compaction* (compacting the powder at elevated temperatures) and *consolidation* of room temperature compacted powders (heating just above the glass transition temperature with a very small applied pressure). *Hot compaction* was studied by performing the following experiments on polycarbonate:

- Investigating the effects of the compaction temperature and/or pressure on the physical properties, strength, and morphology of the resulting compacts.
- Examining the effects of the compaction temperature on the degree of recovery which takes place during isothermal and dynamic pressureless sintering.

Consolidation was studied by:

- Characterizing the effects of the consolidation pressure on the density, porosity, and the degree of recovery which takes place during isothermal pressureless sintering.
- Studying the effects of consolidation on strength and morphology.

- Examining the effects of the consolidation pressure and temperature on the degree of recovery which takes place during dynamic pressureless sintering.
- Determining the order of magnitude of the consolidation pressure that must be used to successfully prevent the recovery of room temperature compacted polycarbonate.

In the next chapter, a literature survey discussing previous research related to the compaction and sintering of polymeric powders is presented. Then, the experimental methods are described. Experimental results are summarized in the next four chapters according to topic: room temperature compaction, pressureless sintering, hot compaction, and consolidation. In the final chapter, a summary of the results presented in this dissertation and conclusions that can be made based on these results is presented. Potential applications for the compaction and sintering of polymeric powders and contributions of this research are also described.

II. Literature Survey

Several related research areas have been studied which give insight to the compaction and sintering of polymer powders. The concept of using fine particles to decrease processing temperature was first used in powder metallurgy. This technique has been highly developed for metals and has been modified for processing ceramics below their melting temperatures. The following review of the literature begins with a brief description of powder metallurgy and identifies some of the processing parameters and powder characteristics that have been found to affect the behavior of metal and ceramic powders (and are expected to affect the processing of polymer powders). A summary of research investigating the compaction and sintering behavior of polymer powders, which is primarily experimental in nature, is then presented. The final section summarizes theoretical treatments of polymer strength development, which address the mechanisms that control the compaction and sintering of polymeric powders, including neck growth, reptation, and intimate contact development.

Powder Metallurgy

As early as 3000 BC, the Egyptians produced the first known powder metallurgy parts. Because they were unable to heat iron above its melting point, the Egyptians reduced it to powder form to lower its processing temperature.[4] Increasing the surface area of the iron raised the free energy of the material, creating a large driving force for the particles to chemically bond to each other at elevated temperatures. Since the early 1800's, technical

understanding of powder metallurgy has grown vastly. Mass production of large, complex, high-quality powder metallurgy parts is now possible. Variations of this process are currently being used to sinter ceramics at relatively low temperatures.

Powder metallurgy involves two basic steps: *compaction* and *sintering*. Compaction involves the application of pressure to the loose powder to consolidate it into a *green body* having the desired shape, an acceptable level of porosity, and sufficient handling strength. Processing parameters that affect the compaction of metal powders include the magnitude of the applied pressure, the speed of pressure application, the temperature of the powder during compaction, and the nature of the mold. Powder characteristics that promote bulk movement or deformation and fracture of the particles improve the effectiveness of compaction, resulting in high green strength and green density.

Following compaction, the green bodies are sintered at elevated temperatures (below the melting point of the material) to form chemical bonds between the particles. This step generally increases both the strength and the density of the compact. As mentioned earlier, the primary driving force for sintering is the large amount of surface area present in the powder. Particle characteristics that increase the surface area to volume ratio of the powder, the number of contacts between neighboring particles, and material transport and diffusion lead to higher sintered strength and density.

The size, shape, and morphology of the powder particles have been found to greatly affect both the compaction and sintering behavior of metal powders. The following is a list of powder characteristics and how they tend to affect these processes in metals [4]:

- **particle size** - The smaller the particle size, the larger the frictional surface area, and the less effective the compaction, but the larger the driving force for sintering.
- **particle size distribution** - Uniform particle sizes tend to decrease the ability of the material to pack efficiently during compaction, leading to less contact area and poorer sintering. By mixing small and larger particles with the proper volume fraction of small particles, the packing of the particles can be improved, resulting in more efficient compaction and sintering.
- **particle shape** - As the particle shape departs from spherical, the higher the surface area per volume of the powder and the larger the driving force for sintering.
- **particle roughness** - The rougher the particle, the larger the frictional forces during compaction and the lower the green density, but the larger the surface area per volume and the greater the driving forces for sintering.
- **grain size** - Smaller grain sizes promote more uniform sintering. In bulk metals, smaller grain sizes are associated with improved mechanical properties.
- **powder porosity** - The higher the porosity within the particles, the larger the driving force for sintering, but the lower the green and sintered densities.
- **cold working** - Cold working reduces the amount of deformation that occurs during compaction and leads to lower green density, but dislocations associated with cold working can increase the driving force for sintering.

In addition to the powder characteristics described above, processing parameters greatly affect the compaction and sintering processes. [4] Factors that improve the green density tend to improve the sintered density and strength. For example, decreasing the speed of

pressure application and increasing the maximum pressure (up to a threshold level) lead to improved green and sintered densities and strengths. Sintered properties increase as sintering occurs. Longer sintering times and higher sintering temperatures allow sintering to proceed towards completion.

Adjustments to the process can also improve the quality of the sintered material.[4] For example, vibrating the powder in the mold prior to compaction promotes bulk motion and settling of the particles, which increases the apparent density of the powder and leads to higher green and sintered densities and strengths. This is particularly effective for powders with very small particle sizes and rough particle surfaces.

In summary, a variety of processing parameters and powder characteristics affect the compaction and sintering behavior of metal powders. As will be seen in the following sections, there are many similarities between the compaction of metals and the compaction of polymers, while many differences exist in the sintering of these two different classes of materials.

Compaction and Sintering of Polymeric Powders

Introduction

With the development of high-performance thermoplastic polymers, solid-state processes based on powder metallurgy principles have the potential to improve the cost-effectiveness

of some polymer processes. Reducing the processing temperature at which high pressures (above 100 psi) are applied to polymers and adding a post-compaction, lower pressure, higher temperature “annealing” step has the potential to lower tooling and equipment costs for polymers which require excessive processing temperatures. Solid-state consolidation can also reduce processing difficulties in polymers which have a very high melt viscosity, such as ultra-high molecular weight polyethylene, or those which exhibit thermal degradation near the melting temperature, such as polytetrafluoroethylene. In the next sections, experimental research on the compaction and sintering of thermoplastic polymer powders is reviewed.

Compaction

For metals, processing parameters that were found to affect compaction included the magnitude of the applied pressure, the speed of pressure application, the temperature of the powder during compaction, and the nature of the mold; the same has been found for polymer powders. The stages of compaction of polymeric powders were described by Crawford and Paul [5] as being the same as those described for metals [4]: particle rearrangement, elastic deformation at contact points, plastic deformation at contact points, and bulk compression. However in the case of some brittle polymers, such as polyamide-imide (PAI), the most important mechanism of densification during compaction appears to be fracture of the larger particles [6].

The effect of room temperature compaction pressure on green density has been investigated for polyvinylidene chloride (PVDC) [7], polyvinyl chloride (PVC) [7], polypropylene (PP) [7,8], polystyrene (PS) [9], ultra-high molecular weight polyethylene (UHMWPE) [10,11], polytetrafluoroethylene (PTFE) [8,12], polyphenylene sulfide (PPS) [13], poly (ether ether ketone) (PEEK) [14], polyimide (LaRC TPI) [6], and PAI [6,8]. In all cases, the green tensile strength was found to increase quickly with increasing compaction pressure for low pressures and to level off at higher pressures. (As noted by Crawford and Paul [15], the pressure applied to the powder is not exactly equal to the applied pressure. Pressure gradients exist along both the axis and radius of a cylindrical die and are affected by the size of the mold and by the friction between the polymer powder and the mold.)

Halldin and Kamel [11], who studied cold compaction of UHMWPE, introduced the concept of a terminal green density to polymer compaction. This density, which is below the polymer's theoretical density, cannot be exceeded during compaction for a given powder, another similarity between the compaction of metals and polymers. The theoretical density for a polymer is considered to be the density of the polymer in bulk, void-free form, having the same morphology as that of the powder. (The theoretical density is affected by the degree of crystallinity, since there is a small difference between the density of the amorphous and crystalline phases.)

The terminal density for UHMWPE powders was between 80% and 90% of the theoretical density for several powders from different manufacturers having similar molecular weights, but differing particle morphology and particle size distributions. A typical green density versus compaction curve for UHMWPE powders from several manufacturers is shown in Figure 1 [11].

Other researchers also noted terminal densities when high enough compaction pressures were used. The highest terminal density was reported to approach 100% of theoretical density for PTFE [8], however, most published values are between 85% and 90%.

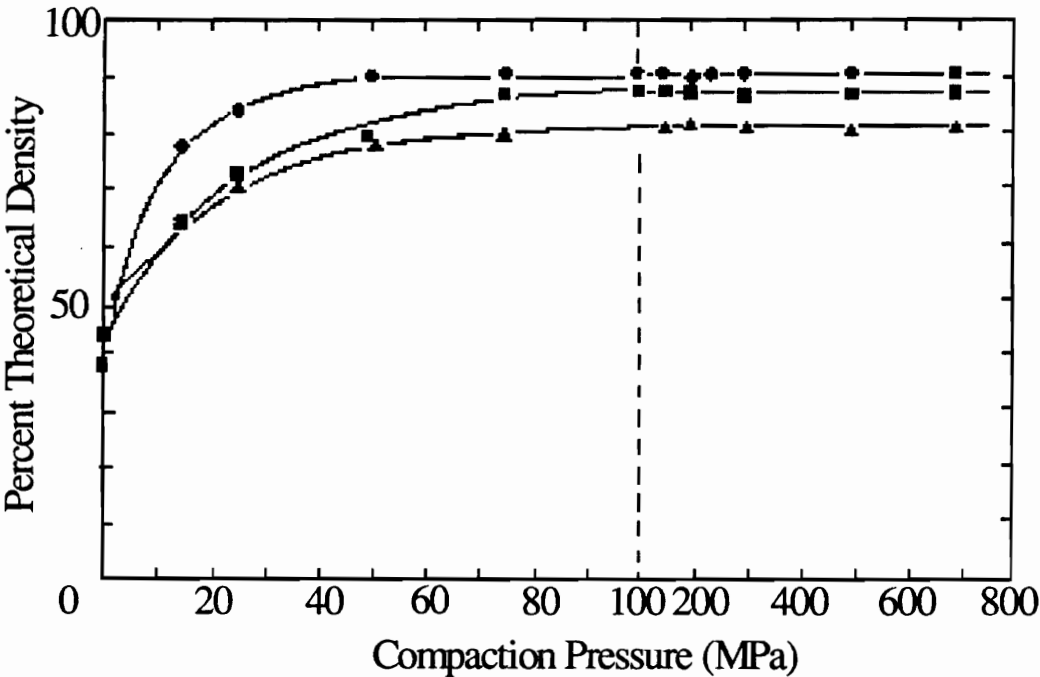


Figure 1 - The effect of compaction pressure on the green density of UHMWPE powder from several different manufacturers [11]. (Note change in abscissa scale.)

Terminal densities are generally obtained at compaction pressures in the range of 100 to 500 MPa at room temperature.

The green tensile strength tends to increase with increasing green density. It was found that the green strength of some polymers, including UHMWPE [11] and PEEK [14], could be plotted versus a densification parameter to obtain a master curve for the green strength of a given polymer under various compaction conditions. Figure 2 [11] shows a plot of green strength versus densification parameter for the UHMWPE powders whose densities were plotted as a function of compaction pressure in Figure 1. The densification parameter, which is commonly used in powder metallurgy to quantify compaction

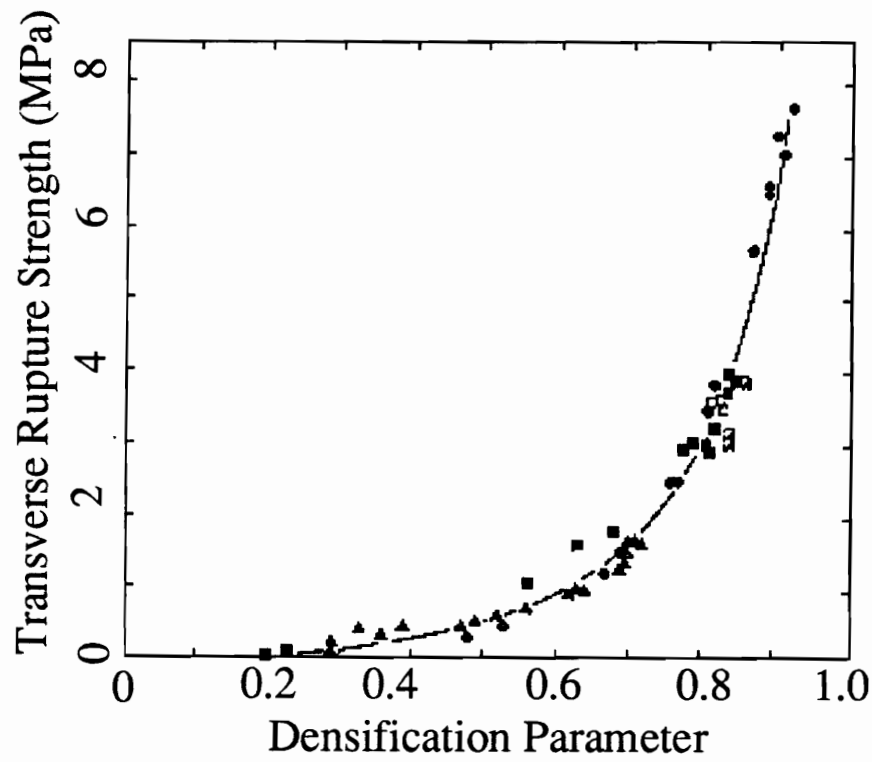


Figure 2 - Green strength as a function of densification parameter for the UHMWPE powders whose green densities are plotted in Figure 1 [11].

effectiveness, is the ratio of the change in density during compaction to the maximum theoretical change in density during compaction.

In addition to the maximum applied compaction pressure, time and rate effects influence the green density and green strength of a compact. For very short compaction times and low compaction pressures, the peak pressure dwell time may affect the green density. Jayaraman, et al, [9] found that for PS, the maximum green density was achieved in less than one minute for all conditions tested, with the lowest pressure being 30 ksi and the lowest piston speed at 0.71 inches/minute. They also found that coining, or repeating the pressure application cycle, increased the green density and strength, but did not affect the sintered properties [9].

Crawford and Paul [7] confirmed that dwell time is more likely to affect green properties for lower peak pressures and noted that higher rates of compaction (between 1 and 20 MPa/sec) resulted in higher green density and green strength for PVDC. Microstructural observations revealed that the particles became less distinct as the compaction speed increased. This was attributed to differences in energy dissipation, with dynamic compaction resulting in higher temperature rises in the compacts. Maeda and Matsuoka [2] found that dynamically compacted medium density polyethylene (MDPE) had higher green and sintered tensile strengths than statically compacted MDPE.

Following removal of the compaction pressure, some polymer compacts were found to change dimensions, with expansion occurring along the axis of the applied compressive stress, and contraction observed perpendicular to the direction of the applied load. This effect was described in the literature for semicrystalline polymers, such as UHMWPE [11] and PEEK [14], with increases in thickness of as much as 2.5% having been measured for UHMWPE. Relaxation of amorphous polymer compacts at room temperature following removal of compaction pressure has not been reported.

Material properties are also expected to influence or to be influenced by compaction. Halldin and Kamel [11] found that for UHMWPE with molecular weights greater than 2 million, molecular weight did not significantly affect powder compressibility. However, for lower molecular weight MDPE in the range of 1.5×10^4 to 5.3×10^4 , Maeda and Matsuoka [2] concluded that increasing the molecular weight improved the green and sintered tensile strengths (possibly because these molecular weights are on the order of the critical molecular weight for entanglements). In later studies, Really and Kamel [14] found that grades of PEEK powder with higher viscosity were more difficult and sometimes impossible to compact. They concluded that the particles did not deform sufficiently during compaction for green strength to develop.

For UHMWPE powders having a percent crystallinity in the range of 57 to 75%, crystallinity was not found to significantly affect compaction [11], while compaction was

found to alter the structure and decrease percent crystallinity in PPS [16,17]. Some polymers, including Nylon-11 [8] and polypropylene [7], have been described as being difficult or impossible to compact.

Particle size distribution and particle morphology have also been found to affect the compaction behavior of polymers. Conflicting observations have been made concerning the effect of particle size on green and sintered properties, possibly because the particle size distribution is more significant than the average particle size. Maeda and Matsuoka [2] found that the green and sintered tensile strengths of PP and high density polyethylene (HDPE) decreased with the average particle size, with the same trend observed for the impact strengths of PP, HDPE, and MDPE. In their study, the average particle sizes ranged from under 39 to over 88 microns for the PP, from under 39 to 127 microns for HDPE, and from 8 to 16 microns for MDPE. Reilly and Kamel [14] found that for PEEK with average particle sizes between 145 and 680 microns, compaction resulted in more deformation and mechanical interlocking of the larger particles, with higher strengths, but larger changes in dimensions, measured for larger average particle sizes.

Other researchers noted the opposite effect, including Bigg and Epstein [8], who concluded that smaller particle sizes led to higher green and sintered densities and strengths for a variety of polymers. Research on PS having average particle sizes of 125 and 250 microns by Jayaraman and coworkers [4] showed that smaller particle sizes

resulted in higher green and sintered densities and strengths. Studies on PVDC in the range of 10 to 90 microns by Crawford and Paul [7] also showed that green strength and density were higher when smaller particles were used. Hambir and Jog [12] noted no significant differences in green density between PTFE compacts having average particle sizes of 35 microns and 550 microns, but noted that sintered strength developed more quickly with the smaller particles.

In addition to particle size and size distribution, the particles morphology has also been observed to affect compaction behavior of polymer powders. Truss, et al, [10] noted that compacts made from particles with a fibrous morphology had higher green and sintered tensile strengths and deformed less during sintering than did those made from particles having a dense, nodular structure. This was attributed to a higher degree of mechanical interlocking and more contact points having been formed during compaction. Shiers, Bigger, and Delatycki [18] showed that altering the catalysts used during the synthesis of HDPE affected the particle morphology, which in turn affected compactibility and green strength. They, too, noted that fibrous particle morphologies resulted in higher green strength than did nodular ones.

Hot compaction, or compaction at elevated temperatures, can be used to increase green strength and density and to compact powders that are difficult to compact at room temperature. For example, Reilly and Kamel [14] were able to successfully compact the

high viscosity grades of PEEK they were unable to compact at room temperature by raising the compaction temperature to 210°C (which is above the T_g , but below the melting temperature of PEEK). It was reasoned that softening of the amorphous regions resulted in greater plastic deformation, and therefore, higher green strength. Mokashi and Jog [13] showed that raising the compaction temperature of PPS to 72°C and 120°C (compared to the T_g of 88°C) resulted in higher green density, with the highest densities achieved at the higher compaction temperature. However, when the PPS was compacted above its T_g and the pressure raised above a critical pressure (2500 kg/cm² for a compaction temperature of 120°C), the density began to decrease slightly, a phenomenon also observed in the current research. Throne [6] noted increases in green density when hot compacting LaRC TPI at 260°C, slightly lower than its T_g of 265°C. Maeda and Matsuoka [2] performed hot compaction on MDPE and observed large increases in green strength at compaction temperatures of 95°C.

From these studies, it can be seen that the compaction of polymeric powders has many similarities to the compaction of metal powders. Density versus compaction pressure curves have similar shapes to those obtained for metals, with a terminal density reached at higher pressures which is lower than the theoretical density. A densification parameter used to predict the green strength of metal compacts under a variety of compaction conditions was also found to work for some polymers. The rate of pressure application and peak pressure dwell time affected green properties under some conditions. Some

semicrystalline polymer compacts exhibited time-dependent relaxation at room temperature following removal of the compaction pressure; this has not been reported for metals or amorphous polymers. Hot compaction has been successfully used to improve green properties of polymer compacts and to successfully compact some polymers that could not be compacted at room temperature.

Sintering

Experimental research on polymer sintering can be divided into two categories. The more fundamental research examines the sintering of uncompacted, spherical particles, as a function of time, with the measurement parameter being a geometric factor, such as neck radius. Sintering tends to be performed at relatively high temperatures, involves bulk flow of the polymer, and is driven by the reduction of surface energy. The goal of this type of research is to determine the mechanisms of polymer powder coalescence.

The second and more applied research category focuses on the sintering of pre-compacted polymer powders. In these studies, mechanical and physical properties, such as strength and density, are used to quantify the degree of sintering. Lower sintering temperatures tend to be used, and sintering is more of a solid-state healing process (rather than a viscous flow process) which occurs at contact points that were previously formed during compaction. The goal of this type of research is to develop viable processing methods. The more fundamental sintering research will be discussed below, followed by a summary of the applied sintering research.

The earliest studies on polymer sintering found in the literature were performed by Kuczynski, Neuville, and Toner [19], whose work on poly(methyl methacrylate) (PMMA) was published in 1970. Spherical PMMA particles were sintered to flat, polished blocks of PMMA, and the radii of the necks that formed between the spheres and the plate were measured as a function of time and particle size at various sintering temperatures. A general expression was obtained relating the neck radius, x , to the particle radius, a ; surface tension of the polymer, γ ; time, t ; and an empirically determined rheological constant, n :

$$\left[\frac{x^2}{a} \right]^{\frac{1}{n}} = \frac{1}{2n} \left[\frac{8n\gamma}{K} \right]^{\frac{1}{n}} \cdot t$$

where K describes the temperature dependence in the relationship between shear stress, σ , and strain rate, $d\epsilon/dt$:

$$\sigma = K(d\epsilon / dt)^n .$$

The dimensions x and a are shown in the sketch in Figure 3. The empirically determined value of n describes the type of flow occurring during sintering. Based on this model and experimental data gathered above the T_g of 105°C , the sintering mechanisms of PMMA were found to be pseudo-plastic flow below 150°C and viscous flow above 170°C .

Rosenzweig and Narkis [20] developed a method for observing the sintering of two spherical particles, and published optical micrographs of the progression of sintering of two PMMA particles at 180°C [20] and three PMMA particles at 200°C [21] (both

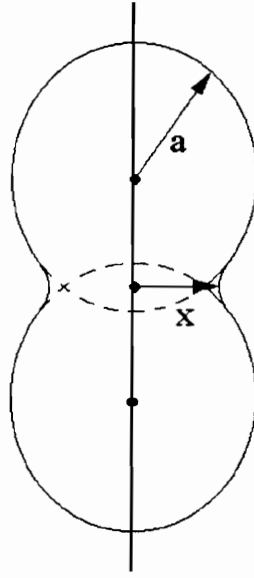


Figure 3 - Schematic showing the neck radius, x , and particle radius, a , used in the sintering equations described in the text.

temperatures well above the T_g of 105°C). They also showed the progression of sintering of two spherical PS particles at 180°C [22], again much higher than the T_g of 100°C.

During the sintering of spherical PMMA or PS particles at high temperatures, measurements of the neck dimensions showed that sintering occurs through viscous flow, in support of a simple model developed by Frenkel [23] in 1945 to describe the early stages of viscous sintering (which are driven by the reduction of surface area):

$$\left[\frac{x^2}{a} \right] = \frac{3\gamma}{2\eta} t$$

where η is the viscosity of the polymer. The conclusion that sintering occurs through viscous flow is also in agreement with Kuczynski, Neuville, and Toner's [19] findings for

PMMA above 170°C. Rosenzweig and Narkis [24] also developed a more detailed model to describe the sintering process.

Applied sintering studies have been performed on compacts made from a variety of polymers, including PS [9], UHMWPE [10], MDPE [2], PVC [2], PTFE [12], and PAI [6]. The most detailed sintering studies found in the literature were performed on PS by Jayaraman and coworkers [9], who tracked the tensile strength of the amorphous polymer with sintering time. They chose five sintering temperatures between 100°C (the T_g of PS) and 173°C. The average particle size of the PS was 250 microns. A plot of tensile strength versus time for the PS at the five sintering temperatures is shown in Figure 4a [9]. The room temperature compaction pressure for these specimens was 75 ksi. The two curves for each sintering temperature correspond to pressing speeds of 0.71 and 78 inches/minute.

Note that tensile strength increases rapidly with temperature for sintering temperatures 50°C or more above T_g , but does not change substantially for sintering temperatures less than 25°C above T_g . Sintering studies on PAI [6] and PVC [7] also showed that amorphous polymers could not be successfully sintered below T_g . Gale [25] found that various pre-treatments performed on poly(p-phenylene) powder, including heating and chemically or mechanically altering the particle surface, affected the sintered strength.

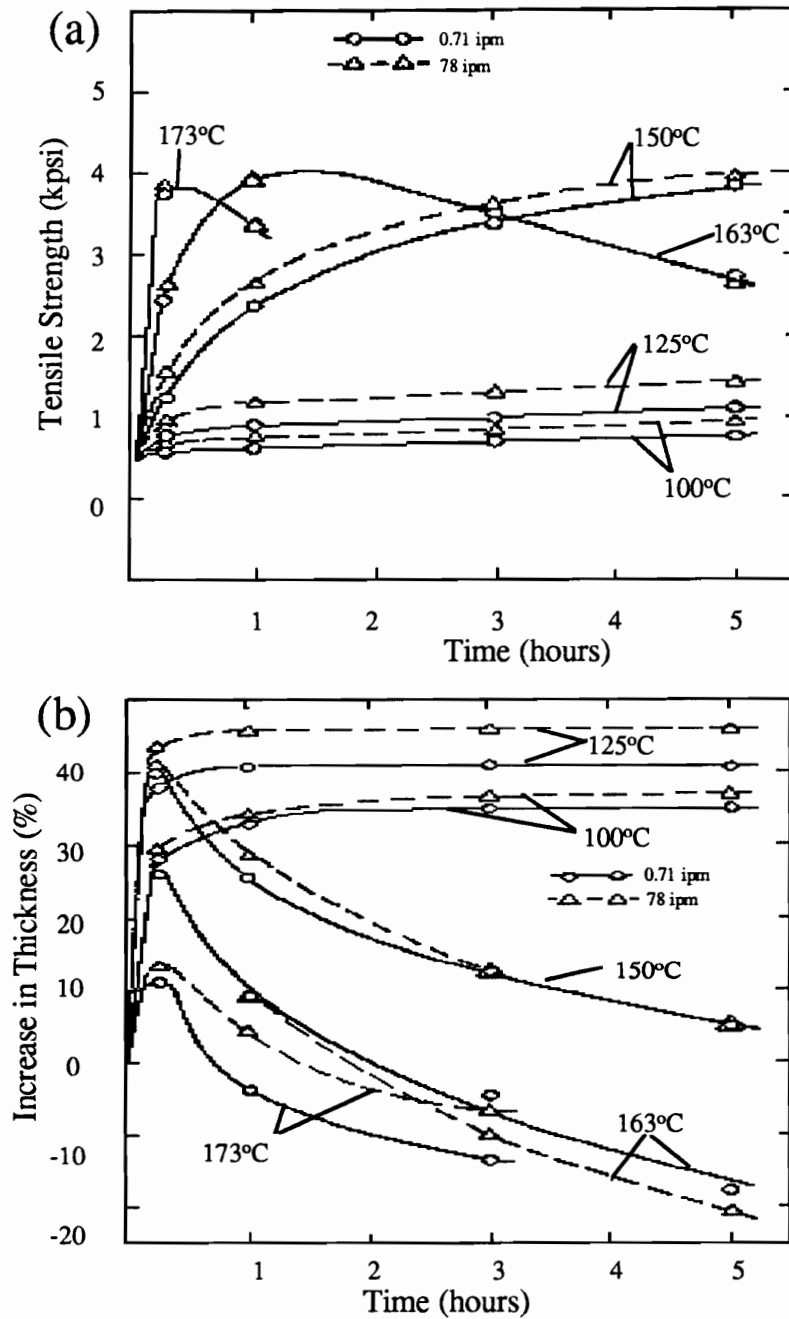


Figure 4 - Influence of sintering on (a) the tensile strength and (b) thickness change for polystyrene powder compacted at 75 ksi [9].

From Figure 4a, it is apparent that compaction rate did not significantly affect the sintered properties of PS, although it was found to affect the green properties [9]. Matsuoka and Maeda [2] found that the opposite was true for MDPE. As was the case with the green tensile strength, the sintered tensile strength was higher for dynamically compacted MDPE than for statically compacted MDPE. However, the compaction rates were unavailable and may have been quite different than those used by Jayaraman, et al [9].

Figure 4b [9] shows the thickness changes experienced by the compacts whose tensile strengths are plotted in Figure 4a. Note the large, rapid increases in thickness in the compaction direction, which were as high as 45%. At longer sintering times, the thicknesses eventually approach their original value or reach an even smaller thickness for sintering temperatures 50°C or more above T_g . The lower strengths for the PS sintered at and near T_g can be attributed to the expansion of the compacts and the resulting decrease in density. Strength data of the equivalent melt processed PS was unavailable for comparison.

Sintering of UHMWPE powders from several manufacturers was performed by Truss and coworkers [10], who made similar observations. They, too, measured large changes in thickness (up to 50%) during sintering and found these changes to be dependent on the particle size and morphology. Increases in the thickness, along with simultaneous decreases in the diameter of the cylindrical compacts, showed that distortion of the shape

of the compacts, rather than pure volume expansion, was occurring during sintering. As expected, the compact having the largest sintered tensile strength also had the largest sintered density. Sintering above the melting temperature of 140°C resulted in significantly higher strengths than achieved through sintering at lower temperatures; however, for sintering temperatures above 140°C, the strength dropped off, apparently due to oxidative degradation of the polymer.

Sintered properties may also be influenced by particle size. Strengths were found to be higher for PS sieved from the same lot as the 250 micron PS, but having an average particle size of 125 microns [9]. Later studies on semicrystalline polymers, including polyimides [26] and PTFE [12], also showed that smaller particles resulted in higher sintered strengths. Strength developed more quickly during the sintering of smaller particle sizes of PTFE [12], as predicted by models based on surface energy arguments [19,22,23]. The sintered strength of UHMWPE could be improved above that of an individual size range by mixing particles from two different narrow particle size ranges [10], supporting the conclusion by powder metallurgists that broad size distributions lead to more efficient packing and higher sintered properties [4].

The effect of compaction properties on sintered properties is not fully understood. Excessive compaction pressures (75 ksi compared to 30 ksi) were found to improve the green strength and density of PS, but did not significantly affect sintered properties [9].

However, Maeda and Matsuoka [2] found that samples of semi-crystalline MDPE and PVC compacted at higher compaction pressures had higher green and sintered strengths than did those compacted at lower pressures. This was also found to be the case in a study of PTFE [12].

General conclusions can be made from the polymer sintering literature. The sintering of spherical particles of amorphous polymers (PMMA and PS) was found to occur through viscous flow at temperatures well above, but not near, T_g . Particle coalescence at high temperatures is driven by the reduction of surface area, and geometric changes can be predicted by simple models, which also estimate an increase in sintering rate with decreasing particle size.

When particles are pre-compacted at room temperature, the sintered strength tends to improve with green density, sintering temperature, and sintering time, although excessive sintering temperatures and times can lead to strength degradation in some polymers. Large increases in thickness (up to 50%) and smaller decreases in dimensions perpendicular to the compaction direction lead to distortion of compacts and decreased density and strength during the early stages of sintering. Smaller particle sizes lead to higher sintered strength, which is achieved in shorter sintering times. Broader particle size distributions appear to improve strength and density. Sintering temperatures above the glass transition temperature of amorphous polymers and above the melting temperature of

semi-crystalline polymers are required to obtain strengths comparable to those achieved through melt processing.

Theoretical Models for Strength Development at Polymer-Polymer Interfaces

Several approaches have been used to model strength development at polymer-polymer interfaces. The models can be grouped by which mechanism is considered to be the limiting factor in strength development. Table I contains a summary of three models used to treat polymers and their important features. Note that for the various reasons listed, these models are not applicable to the current study. The following sections describe two of these models, which are related to the compaction and consolidation of thermoplastic polymer powders: intimate contact formation and strength development through reptation. The third, the application of neck growth models to sintering of polymeric powders, was discussed in the previous section.

Strength Development through Reptation. Strength development at a polymer-polymer interface has been described by Wool and O'Connor [28] as a healing process that occurs in five stages: (a) surface rearrangement, (b) surface approach, (c) wetting, (d) diffusion, and (e) randomization. The stages of interest in polymer compaction and consolidation are the wetting stage, which requires the formation of intimate contacts between the two surfaces, and the diffusion and randomization stages, which have been described as a reptation process [29].

Table I - Summary of Theoretical Treatments of Strength Development at Polymer-Polymer Interfaces

	Neck Growth Models	Reptation Theory	Contact Development Models
Limiting Factor	Neck radius between particles.	Diffusion time for polymer chains to form entanglements.	Formation of intimate contact between prepregs.
Processing Conditions & Assumptions	No pressure High temperature (well above T_g or T_m for polymers)	No pressure Moderate to high temperatures (above T_g or T_m) Assumes perfect initial contact; no residual stress; amorphous polymers only	High pressure High temperature (well above T_g or T_m for polymers)
Applications	Sintering of spherical metallic, ceramic, and polymeric powders	Healing of polymer-polymer interfaces.	Consolidation of composite prepregs.
Why Model is Not Applicable to This Study	Temperatures too high.	Do not have perfect contact between particles.	Temperatures too high; contacts are formed at elevated temperatures instead of at room temperature.
References	[19,23,24]	[27-32]	[33-37]
		Reptation & contact development: [38]	

Reptation theory was developed by de Gennes [27] to describe the movement of a long chain-like molecule in the melt. Constraints imposed by its surroundings force a chain to move in an imaginary tube, which follows the chain's contour, through local Brownian motion. The chain is free to jump randomly in either direction through the tube. As the chain ends exit the tube ends with time, memory of the initial positions of the tube ends is lost. At a time equal to the reptation time, memory of the initial tube configuration has been totally erased.

Reptation theory has been used by Kim and Wool [29] to predict strength development at interfaces between linear amorphous polymers as a function of time and temperature, provided wetting (and therefore, intimate contact) has occurred. In metals, full strength development would be achieved at the same time as intimate contact, but polymer chain segments must diffuse across the particle interfaces a sufficient penetration distance for the interface to obtain maximum strength [30]. Healing theories based on reptation assume that the amorphous polymer is linear, is above its glass transition temperature, and is at equilibrium. That is, there are no driving forces which bias motion of the chain in the tube towards one direction, as might result from residual stresses, applied pressures, or surface energy. Note that reptation theory does not apply to semi-crystalline polymers below their melting temperature, because the crystalline phase imposes constraints on the motion of the amorphous regions.

Scaling laws based on reptation theory for various relevant quantities in polymer healing have been reviewed by Wool, Yuan, and McGarel [31]. The average interpenetration depth of chains crossing the interface, or χ , is predicted to vary as:

$$\chi \propto \left[\frac{t}{M} \right]^{\frac{1}{4}}$$

where t is time and M is the molecular weight. For fracture by a chain pullout mechanism, the strength, σ , is predicted to be proportional to χ [29]:

$$\sigma \propto \left[\frac{t}{M} \right]^{\frac{1}{4}}$$

When healing proceeds for a time equal to the reptation time, t_r , the strength reaches its maximum value of σ_∞ . The reptation time can be shown to vary with the molecular weight to the third power. The degree of healing, D_h , defined as the ratio of the strength at time, t , to the infinite strength, can be expressed as:

$$D_h \propto \frac{\sigma}{\sigma_\infty} \propto (t)^{\frac{1}{4}} (M)^{-\frac{3}{4}}$$

The dependence of strength on time to the one-quarter power has been supported by experimental evidence, as reviewed by Wool et al [31] and Kausch and Tirrell [32].

Intimate Contact Formation

The *degree of intimate contact* quantifies the amount of physical contact that exists between surfaces. Because they are never perfectly flat, two surfaces will not be in perfect

contact with each other unless a high enough pressure is applied at the given temperature to produce deformation of the surface irregularities. The degree of intimate contact is a function of pressure, time, and temperature. As noted by Butler and coworkers [38], differences exist between wetting and intimate contact formation. *Wetting* occurs when surface asperities are very small, which allows the surfaces to be brought close enough together to interact through intermolecular forces. In the case where surface irregularities are much larger, external forces must be used to deform and reduce surface irregularities in order to obtain *intimate contact*, and wetting can be assumed to occur instantaneously.

Wetting was described by Wool and O'Connor [28] as being a nucleation and growth process. In order to predict the progression of healing with time, a wetting distribution function describing the rate of contact formation with time had to be known. For early healing studies, wetting was assumed to occur instantaneously, a reasonable assumption in cases where contact development is aided by an applied pressure and the time to develop intimate contact is much smaller than the time scale of reptation.

More detailed models of intimate contact formation were developed to account for the pressure and temperature dependence of thermoplastic composite consolidation at elevated temperatures. Loos and Dara [33] modeled contact development as a viscous flow process, in which the applied pressure was carried evenly by the portion of the composite plies that had achieved contact. The variation in prepreg height was

represented by a wave formed by rectangular elements of varying height and thickness. A two-parameter Weibull distribution function, whose parameters were chosen based on the degree of contact measured from ultrasonic C-scans, quantified the wave. The effective viscosity of the fiber/matrix system was also adjusted based on the experimental results. This model was used to describe contact development in a graphite fiber-reinforced polysulfone composite.

Lee and Springer [34] developed a more simple model for contact formation in which the prepreg topography was described as consisting of a series of rectangular slabs of uniform height and equal spacing. Laminar flow was assumed to occur as a result of the applied pressure, with the slabs becoming shorter and wider until they touched at the point of 100% intimate contact. When a viscosity was chosen to match the measured and predicted degrees of intimate contact as a function of time, this model was able to successfully describe intimate contact formation for a graphite fiber-reinforced PEEK composite. Note that other sub-models were included in the theoretical treatment, including impregnation, or flow of the matrix into the spaces between fibers, and time and temperature dependent crystallization.

Li and Loos [35] used a two-stage contact formation model based on Lee and Springer's approach [34] to predict contact development in angle ply laminates. They found that the development of intimate contact was strongly affected by the orientation between adjacent

plies, with cross ply laminates (having 0 and 90 degree plies) taking more than ten times as long to achieve full intimate contact as unidirectional laminates made from fiber-reinforced graphite-polysulfone and graphite-PEEK prepregs.

Modifications were made to Lee and Springer's model [34] by Mantel and Springer [36] for use with other composite processing techniques, including tape laying and filament winding. This model, which includes provisions for time-dependent viscosity, temperature, and pressure, was experimentally validated on graphite fiber-reinforced PEEK composites by Mantel, Wang, and Springer [37].

Note that for all of the composite consolidation models, processing temperatures are assumed to be high enough for flow to occur. Air is assumed to escape through the channels without becoming trapped as voids, and prepregs are considered to be free of residual stresses. With some modifications, these models may be useful for predicting contact formation during hot compaction of polymer powders or consolidation of polymer powder compacts with an externally applied force.

A recent model by Butler, Pitchumani, Gillespie, and Wedgewood [38] combined the contact development by Mantell and Springer [36] with reptation scaling laws by Kim and Wool [29] to predict strength development in cases where contact development and reptation occur simultaneously. This model was experimentally validated for tow

placement in the manufacture of graphite-poly (ether ketone ketone) (PEKK) composites under a variety of processing conditions. Strength predictions for the coupled model were found to be more accurate than those based on healing theory alone.

In summary, strength development in interfaces between linear amorphous polymers above the glass transition temperature has been described by scaling laws, which correctly predict the time dependence observed experimentally. Theoretical models have been developed to predict the formation of intimate contact through the flow of thermoplastic polymers under applied pressures at elevated temperatures. A coupled model combining these two aspects of polymer strength development shows promise for predicting strength development in cases where both contact formation and reptation occur in similar time scales. Modified forms of these theoretical treatments might be used to model the behavior observed in the current study.

Summary

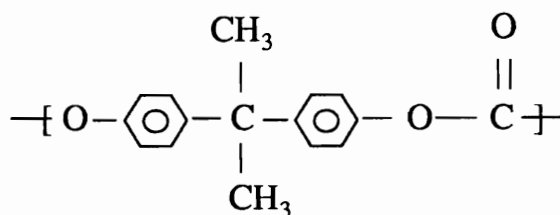
In summary, amorphous and semicrystalline thermoplastic polymers have been the subject of recent compaction and sintering studies. Published research has shown that processing variables (compaction and sintering times, temperatures, and pressures, etc.) and powder characteristics (size, size distribution, and particle morphology, etc.) affect the processing of polymer powders. Although there are many similarities that have been observed in the compaction behavior of metals and polymers, many differences in the sintering behavior

exist, including time and temperature dependent relaxation, which is observed in polymers. Strength development in polymer compacts has very different time and temperature dependencies than those observed in metals. These differences, which result from the long, chain-like structure and viscoelastic nature of polymers, have led to several types of theories which predict strength development at polymer-polymer interfaces under a variety of processing conditions. The conditions considered by these theories do not match those in the current study, however, these theories might serve as a basis for future modeling efforts.

III - Experimental Methods

Materials

The Laserite™ LPC3000 polycarbonate powder used in this study was donated by DTM Corporation of Austin, Texas. Properties of the LPC3000 provided by the manufacturer are summarized in Table II [39]. Polycarbonate is an amorphous polymer having the repeat unit:



The glass transition temperature (T_g) of the LPC3000 was found to be 142°C when characterized by differential scanning calorimetry (DSC) at a scan rate of 10°C/minute. Polycarbonate is also known to undergo a beta transition at -50°C which involves rotation of the backbone at the ether linkages.

The LPC3000 polycarbonate powder has a broad particle size distribution which promotes high packing in its intended selective laser sintering application. An average particle size of 90 microns and a particle size range of 30 to 175 microns were determined by the manufacturer through laser diffraction techniques. The particle shapes are irregular, as shown in Figure 5, due to grinding. To reduce and control absorbed moisture, the powder was stored in a dry box with desiccant for several weeks prior to use.

Table II - Laserite™ LPC3000 Polycarbonate Properties Supplied by DTM Corp.[39]

<u>General Properties</u>	<u>Value</u>	<u>Test Method</u>
Specific Gravity, 20°C	1.20 g/cm ³	ASTM D792
Moisture Absorption, 20°C, 65% relative humidity	0.35%	ASTM D570
Powder Tap Density	0.62 g/cm ³	ASTM D4164
Volume Average Particle Size	90 microns	laser diffraction
Particle Size Range, 90%	30-175 microns	laser diffraction
<u>Thermal Properties</u>		
Glass Transition Temperature	150°C (302°F)	differential scanning calorimetry
DTUL, 66 psi (0.45 MPa)	138°C (280°F)	ASTM D648
DTUL, 264 psi (1.82 MPa)	136°C (277°F)	ASTM D648
<u>Mechanical Properties of Selective Laser Sintered Parts</u>		
Tensile Strength at Yield	23 MPa (3400 psi)	ASTM D638
Tensile Modulus	1220 MPa (177000 psi)	ASTM D638
Tensile Elongation at Break	5.0%	ASTM D638
Flexural Modulus	1050 MPa (152000 psi)	
Impact Strength		
Notched Izod	53 J/m (1.0 ft-lb/in)	ASTM D256
Unnotched Izod	107 J/m (2.0 ft-lb/in)	ASTM D256

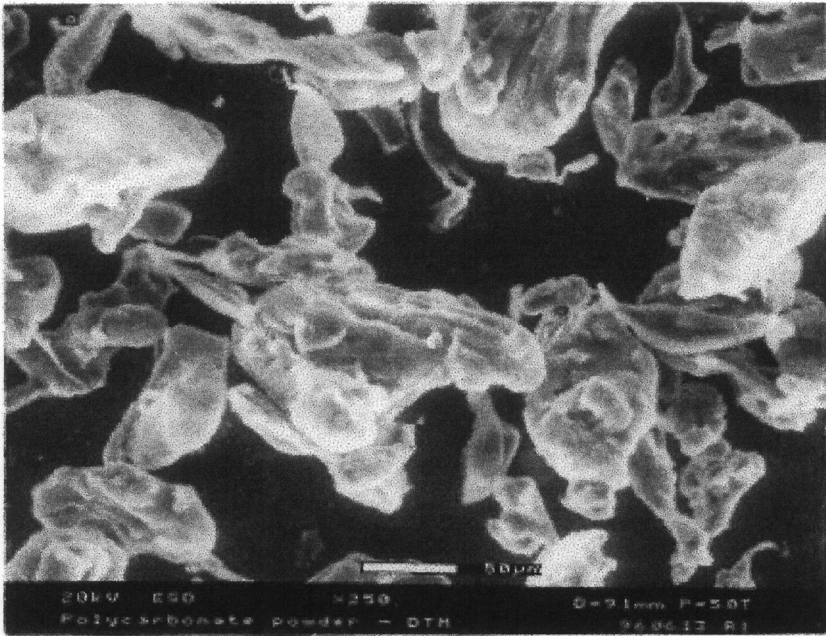


Figure 5 - ESEM micrograph of as-received LPC3000 polycarbonate.

Selected experiments were performed on semicrystalline polymers having a variety of glass transition temperatures (all determined through DSC at a heating rate of 10°C/minute). An experimental lot of linear low density polyethylene (LLDPE) powder donated by DTM Corp. was known to have a T_g well below room temperature and a melting temperature of 135°C. The average size of the LLDPE particles was approximately 200 microns, with 90% of the particles between 125 and 300 microns. No other properties for this polymer were available from the manufacturer.

Laserite™ LN4010 Nylon-11 powder, also donated by DTM Corp., had a T_g of 55°C and a peak melting temperature of about 190°C. Properties provided by the manufacturer for the Nylon-11 powder are summarized in Table III [40].

Poly(ether ether ketone) powder, Victrex grade 150PF, purchased from ICI Advanced Materials was found to have a T_g of 145°C and a melting temperature of 340°C. Other properties for PEEK provided by the manufacturer are summarized in Table IV [41].

Table III - Laserite™ Nylon-11 Properties Supplied by DTM [40]

<u>General Properties</u>	<u>Value</u>	<u>Test Method</u>
Specific Gravity, 20°C	1.04 g/cm ³	ASTM D792
Moisture Absorption, 20°C, 65% relative humidity	1.0%	ASTM D570
Powder Tap Density	0.58 g/cm ³	ASTM D4164
Volume Average Particle Size	120 microns	laser diffraction
Particle size range, 90%	60-250 microns	laser diffraction
<u>Thermal Properties</u>		
Melting Point	186°C (367°F)	differential scanning calorimetry
DTUL, 66 psi (0.45 MPa)	163°C (163°F)	ASTM D648
DTUL, 264 psi (1.82 MPa)	44°C (111°F)	ASTM D648
<u>Mechanical Properties of Selective Laser Sintered Parts</u>		
Tensile Strength at Yield	36 MPa (5200 psi)	ASTM D638
Tensile Modulus	1400 MPa (202000 psi)	ASTM D638
Tensile Elongation at Break	32%	ASTM D638
Flexural Modulus	870 MPa (126000 psi)	
Impact Strength		
Notched Izod	70 J/m (1.3 ft-lb/in)	ASTM D256
Unnotched Izod	1370 J/m (25.7 ft-lb/in)	ASTM D256

Table IV - Victrex™ PEEK Properties Supplied by the Manufacturer [41]

<u>General Properties</u>	<u>Value</u>	<u>Test Method</u>
Specific Gravity, 20°C		ASTM D792
Crystalline	1.32 g/cm ³	
Amorphous	1.26 g/cm ³	
Typical Level of Crystallinity	35%	
Moisture Absorption, 73°F	0.5%	ASTM D570
Particle Size Range	< 90 microns	
<u>Thermal Properties</u>		
Melting Point	343°C (649°F)	differential scanning calorimetry
Glass Transition Temperature	143°C (289°F)	differential scanning calorimetry
DTUL, 264 psi (1.82 MPa)	155°C (311°F)	ASTM D648
<u>Typical Mechanical Properties</u>		
Tensile Strength at Yield/Break	100 MPa (14,500 psi)	ASTM D638
Tensile Elongation at Yield	4.9%	ASTM D638
Compressive Strength	~ 120 MPa (17,000 psi)	ASTM D695
Flexural Modulus	170 MPa (24,700 psi)	ASTM D790
Notched Izod Impact	60 J/m (1.12 ft-lb/in)	ASTM D256

Processing

Equipment

Compaction, consolidation, and hot pressing were performed using a Carver Laboratory Press (Model-C) capable of exerting a maximum force of 11 metric tons (24,000 pounds) with its 153 mm (6 inch) square platens. The applied pressure was controlled manually with the aid of either a 5000 pound or a 24000 pound force gage. The temperatures of the upper and lower platens were controlled by digital temperature controllers from Omega (model CN76000).

Compaction

Room temperature and elevated temperature compaction experiments were performed using a 28.6 mm (1.13 inch) diameter, single-action stainless steel cylindrical die commonly used for powder metallurgy. A light coat of Chem-Pak Shop Silicone™ mold release was applied to the mold prior to compaction to reduce the friction between the powder and the die.

Cold Compaction. Cold compaction was achieved by pouring the pre-weighed powder into the mold, manually applying the desired pressure for 5 minutes, then quickly releasing the pressure. The compacts were measured and weighed after removal from the die and remeasured at least one day later to check for short term recovery. It was found that changes in the dimensions of the compact following removal from the die were within

experimental error (approximately 0.1 mm or less than 2%) for the polycarbonate powder. Following cold compaction, compacts were stored at room temperature in a dry box for a minimum of 24 hours prior to final density measurement and subsequent testing.

Hot Compaction. For hot compaction, the hot press and cylinder die were preheated to the desired temperature prior to pouring the pre-weighed powder into the die. The loaded die was then placed in the preheated press, with the upper platen very close to, but not touching, the die. A fiberglass cloth was draped around the platens to reduce convective heat transfer. Note that the large thermal mass of the die prevented significant temperature fluctuations during hot compaction.

The powder was allowed to preheat for 5 minutes in the hot die before the desired pressure was manually applied and held for 5 minutes. The compacts were removed from the die and allowed to air cool for at least 10 minutes prior to being measured and weighed. As was the case for cold compaction, it was found that changes in the dimensions of the compacts after 24 hours were within experimental error for the polycarbonate powder. Compacts were stored at room temperature in a dry box and allowed to recover for at least 24 hours prior to subsequent testing.

Pressureless Sintering

Compacts made following the above procedures were used for pressureless sintering experiments. After a one day recovery period, the thickness, diameter, and mass of the compacts were measured and recorded. The density calculated based on the geometric technique (described in a later section) was used to estimate the initial density.

The hot press was used for short duration pressureless sintering tests, as it could be used to quickly apply and hold a constant temperature. Short term pressureless sintering was performed by placing a sheet of 0.05 mm (0.002 inch) thick Kapton™ film coated with Frekote 800-NC™ mold release on the bottom platen of the preheated hot press, waiting 1 minute for it to heat up, then placing the compacts on the Kapton™ film. The bottom platen was then raised until the top platen was within 1 mm of touching the compact. As the compact heated up and expanded, the bottom platen was manually lowered to prevent the compact from touching the top platen.

For a 2-3 mm thick polycarbonate sample (1.5 g powder), significant recovery was visually observed to occur between 45 and 50 seconds after the compact was placed in the hot press, indicating that the heat up time for such a compact was about one minute. This observation was confirmed by measuring thickness changes during pressureless sintering as a function of time. Because the heat up time was on the order of one minute, pressureless sintering experiments were conducted for at least 5 minutes.

For long term pressureless sintering experiments (one hour or longer), compacts were placed on a Kapton™ sheet coated with Frekote 800-NC™ mold release on a preheated aluminum plate and placed in a preheated vacuum oven at ambient pressure. After the sintering time had been reached, the compacts were removed from the oven and allowed to air cool to room temperature.

Consolidation

Consolidation was performed on room temperature compacted polycarbonate approximately 24 hours following compaction, after the thickness, diameter, and mass of the compacts were measured and recorded. The density calculated based on the geometric technique was used to estimate the initial density.

The hot press was used for a series of short term consolidation tests, as it could be used to quickly apply and hold a constant temperature. A sheet of 0.05 mm (0.002 inch) thick Kapton™ film coated with Frekote 800-NC™ mold release was placed on the bottom platen of the preheated hot press. Consolidation was accomplished by placing the compacts on the preheated platens and immediately applying a preheated block of steel of known mass, whose smooth contact surface was covered with a 0.05 mm thick Kapton™ film coated with Frekote 800-NC™ mold release. After the designated consolidation time had elapsed, the compacts were removed from the hot press and allowed to air cool in the absence of an applied pressure.

Although the average consolidation temperature could be fairly well controlled in the hot press, a temperature gradient of approximately 10°C was believed to exist between the top and bottom of the compacts. This was evident by the variation in color, morphology, and strength across the compacts (delamination of the layers sometimes occurred when the compacts were sliced with a razor blade). The hotter side, which rested against the bottom platen of the hot press, tended to be more transparent, appeared to have less visible interfaces between particles, and was stronger than the top side (which received no conductive heating during the test from the upper platen). A much better consolidation test would involve using the upper platen to apply the desired pressure, however, very sensitive pressure control and perfect platen alignment would be required. For the consolidation tests performed in this study, the maximum applied consolidation pressures were less than 10 kPa (1.5 psi), much too small for the hot presses available for use in this study.

Preparation of Thin Films

Thin films were prepared by using flat 3 mm thick aluminum plates and stainless steel shims as a simple “picture frame mold.” Prior to forming films, the polymer powders were dried in a vacuum at a temperature of 100°C for 2-3 days. Kapton™ films (0.005 mm thick) coated with Frekote 800™ mold release were placed between the aluminum plates and the polymer powder to act as a release cloth and to promote a smoother surface finish. The loaded mold was placed in a the preheated hot press, and a small force (less than 100

pounds) was applied to increase thermal contact. For polycarbonate, the hot press was held at 190°C, about 50°C above polycarbonate's glass transition temperature. The powder and mold were allowed to heat for 3 minutes prior to the application of a force of 1.4 metric tons (3000 pounds), which was held for 3 minutes and released. The films were quickly removed from the mold and allowed to air cool to room temperature.

Physical Aging of Powders and Films

Physical aging of polycarbonate powders and films was accomplished by heating the polymer to 130°C (about 10°C below its glass transition temperature) in a vacuum and holding this temperature for at least 200 hours. Physical aging, which involves a reduction in free volume in glassy polymers, occurs slowly at room temperature and more quickly at higher temperatures (below T_g). It is a thermally reversible process that causes polymers to become more brittle by increasing the modulus and yield strength and decreasing the strain to failure. By comparing unaged and physically aged polycarbonate powder, the affect of the modulus and yield strength on behavior during compaction and sintering could be investigated.

Characterization

Density Measurement

Two different techniques were used to measure the density of the compacted powder. The first was a geometric technique, while the second was based on the Archimedes

principle. The geometric technique was useful for obtaining a quick estimate of density, while the Archimedes technique provided more detailed information on the type of porosity present and was especially useful for measuring density on more complex shapes. The geometric technique was used primarily to estimate the initial density of a compact prior to further processing, such as consolidation, while the Archimedes technique was used following final testing. Results from both techniques were compared on cold compacted polycarbonate and found to be within the experimental error of the geometric technique (2% of the measured value).

Geometric Technique. Because the shape of the cylindrical compacts were very well controlled following compaction, density could be accurately found by dividing the measured mass by the volume calculated using measured dimensions. Rather than reporting actual density values, a dimensionless density is used.

The *normalized density*, N , is obtained by dividing the actual density by the theoretical (maximum) density, ρ_{th} , (taken as the specific gravity, which is 1.2 g/cm^3 for bulk polycarbonate):

$$N = \frac{\text{mass}}{\frac{\pi}{4} \rho_{th} \cdot \text{thickness} \cdot (\text{diameter})^2} \quad (1)$$

Archimedes Method. The Archimedes density measurement technique is based on the fact that when an object is placed in a fluid, it undergoes a weight loss equal to the weight of the fluid it displaces. When the fluid is water (with a specific gravity of 1 g/cm³) and when metric units are used, several equations can be derived to calculate the volume of the object, the volume fraction of open porosity, and the volume fraction of closed porosity. To quantify the amount of porosity present, three quantities must be measured: (1) the dry mass of the object; (2) the saturated mass of the object, after it has been soaked in the water a sufficient amount of time for the maximum amount of water to be absorbed into the open pores; and (3) the suspended mass, measured while the saturated object is suspended in water.

A Mettler AE-50 millibalance, which reads to the nearest 0.1 milligram was used to measure the three masses. After the dry mass was measured, the compacts were placed in a beaker of room temperature water with 1-2 drops of Joy dishwashing soap to act as a surfactant. The beaker was placed in a vacuum desiccator and a vacuum was applied and released several times in the first 10 minutes, then held for an additional hour to help fill the open pores with the water. It should be noted that increasing the soaking time to as much as 24 hours did not affect the measured values of open porosity, although it did systematically affect the values of closed porosity.

Following the vacuum soak, the suspended mass was then measured using a suspension apparatus (available through Fisher Scientific) which fits onto the platform of the Mettler balance. Each compact was quickly removed from the water it was soaking in and placed in a second beaker of water on the suspension apparatus using a pair of tweezers. After its suspended mass was measured, it was allowed to remain soaking in the second beaker while other compacts were measured. The saturated mass was then found by removing one compact at a time from the water, quickly patting it twice with a damp paper towel to remove excess of water from the surface, and measuring the mass within 5 seconds.

From ASTM standard C-373 written for porosity measurement in ceramics, the following equations can be derived for the Archimedes density measurement technique when the fluid has a density of 1 g/cm³, the theoretical density is in g/cm³, and all masses are in grams. The volume of the object, V, (in cm³) is:

$$V = M - S, \quad (2)$$

where M is the saturated mass and S is the suspended mass.

From the dry mass, D, and the volume, the bulk density of the object, ρ_b , (in g/cm³) can be calculated as:

$$\rho_b = \frac{D}{V} = \frac{D}{M - S}. \quad (3)$$

The normalized density, N , comparable to the geometrically determined quantity in eqn. (1), is:

$$N = \frac{\rho_b}{\rho_{th}} = \frac{D}{\rho_{th}(M - S)}. \quad (4)$$

The volume of open porosity (in cm^3), V_{op} , or the volume of pores that are in some way connected to the surface of the object, is:

$$V_{op} = M - D. \quad (5)$$

From these equations, the volume fraction of open porosity, v_{op} , can be calculated as:

$$v_{op} = \frac{V_{op}}{V} = \frac{M - D}{M - S}. \quad (6)$$

The impervious volume, V_i , or the volume of the object that has not been penetrated by water (in cubic centimeters), is:

$$V_i = D - M \quad (7)$$

The density of the impervious volume, ρ_i , (in g/cm^3) is the mass of the impervious volume, or D , divided by its volume:

$$\rho_i = \frac{D}{V_i} = \frac{D}{D - M}. \quad (8)$$

In addition to open porosity, or pores that are connected to the surface, the object may also have closed porosity, which consists of isolated pores that are not connected to the surface of the object. If the theoretical density of the material, ρ_{th} , is known, the volume fraction of closed porosity, v_{cp} , can be estimated from ρ_i using a rule of mixtures approach and assuming the density of the pores is zero. The resulting equation for the volume fraction of closed porosity is:

$$v_{cp} = 1 - \frac{\rho_i}{\rho_{th}} \quad (9)$$

As mentioned earlier, the values obtained for v_{cp} are systematically affected by the soak time, possibly due to moisture absorbed by the polymer. Although the values estimated for the quantity of closed porosity are not exact, they do provide a useful estimate of the order of magnitude of the volume of closed porosity present in a polymer compact.

Thermal Properties

Thermal property measurement was performed using a Mettler DSC 30 differential scanning calorimeter (DSC). A scanning rate of 10°C/minute was used for all scans to ensure that the 9-12 milligram samples were heated uniformly as the specific heat capacity was measured as a function of temperature.

Thermomechanical Behavior

A DuPont Thermal Analyst 2100 system equipped with a TMA 943 thermomechanical analyzer was used to measure the dimensional changes of both bulk polymer and compacted powder as a function of time and temperature. A 100 mg mass was used to help maintain contact between the 2.5 mm (0.1 inch) diameter probe and the samples. To reduce the pressure exerted on the sample by the probe and to distribute the pressure evenly across the entire sample, a 0.15 mm thick, 6 mm square piece of glass coverslip was placed between the probe and the sample for “pressureless” tests. For tests with a larger, known pressure, the probe was placed in direct contact with the sample.

Prior to beginning a test, the sample and chamber were cooled to below -20°C using liquid nitrogen to extend the range of meaningful data. In all cases, a heating rate of 5°C/minute was used, as recommended by the manufacturer, to ensure uniformity of the sample temperature during heating. Cooling was performed at approximately 5°C/minute, but slowed down as the temperature approached room temperature, since the equipment relies on natural convection alone for cooling.

Microtensile Testing

Tensile properties were measured by performing microtensile tests with a Polymer Laboratories Minimat™ Tensile Tester. Tests on bulk polycarbonate films were conducted at a crosshead speed of 10 mm/minute. A speed of 1 mm/minute was required to increase

the time to failure of polycarbonate compacts above the 30 second minimum suggested by ASTM D-638, since they failed at a much lower strain. Test specimens were punched from polycarbonate films and hot compacted polycarbonate powder using a self ejecting dogbone-shaped microtensile die having a gage length of 10 mm and a width of 2.72 mm shaped per ASTM Standard D-638M. Due to their fragile nature, tensile strips approximately 6 mm wide with a 10 mm gage length were cut from the other polycarbonate samples (cold compacts, consolidated compacts, and compacts that had experienced pressureless sintering) using a single-edged razor blade.

Characterization of Particle Size Effects

Because there was such a broad particle size distribution, tests were performed to determine whether or not particle size affected molecular weight, an important parameter which influences viscoelastic behavior of polymers. The particles were first sorted through wet sieving, then analyzed using gel permeation chromatography to determine if there was any significant difference in the relative molecular weight distributions for the smallest and largest particle size fractions.

Sieving of particles. Wet sieving of approximately 150 grams of polycarbonate powder was performed by using a fine spray of tap water to help the particles to pass through a series of sieves of the known mesh sizes listed below.

Screen Size	Size of Opening (microns)
140	106
200	75
325	45

The particles were sprayed with water for approximately 30-45 minutes, before removing them from the sieves by spraying the opposite side of the sieve with water and collecting them on a filter paper. The particles were then dried under a vacuum at 100°C for 2 hours and removed from the filter paper. The volume fractions of particles collected through sieving were approximately:

Particle Size Range (microns)	Volume Fraction of Particles (%)
>106	19
75-106	43
45-75	24
< 75	14

Gel Permeation Chromatography. Samples of the largest (greater than 106 microns) and smallest (less than 45 microns) particle size fractions were tested using gel permeation chromatography (GPC) to qualitatively characterize the molecular weight distribution. Samples of approximately 10 milligrams of polycarbonate were mixed with chloroform and run in a GPC column using a polystyrene standard. The following data were obtained for the polystyrene standard at a flow rate of 2 milliliters per minute:

Molecular Weight	Time (minutes)
180,000	10.4
240,000	12.0
95,000	13.2
47,500	14.4
25,000	15.4
9,000	16.4
4,000	18.3
2,510	19.0
760	20.5

From the GPC results for the polycarbonate particles shown in Figure 6, it can be seen that the finer particles contained more lower molecular weight chains, giving them a broader molecular weight distribution and a lower average molecular weight than the coarse particles. This effect was probably due to the grinding performed by DTM Corp. to reduce the particle sizes. (If desired, these results could be converted to actual molecular weights using the data listed above for the polystyrene standard.) Differential scanning calorimetry determined that the difference in molecular weight between the smallest and largest particles was not large enough to cause a measurable change in the glass transition temperature.

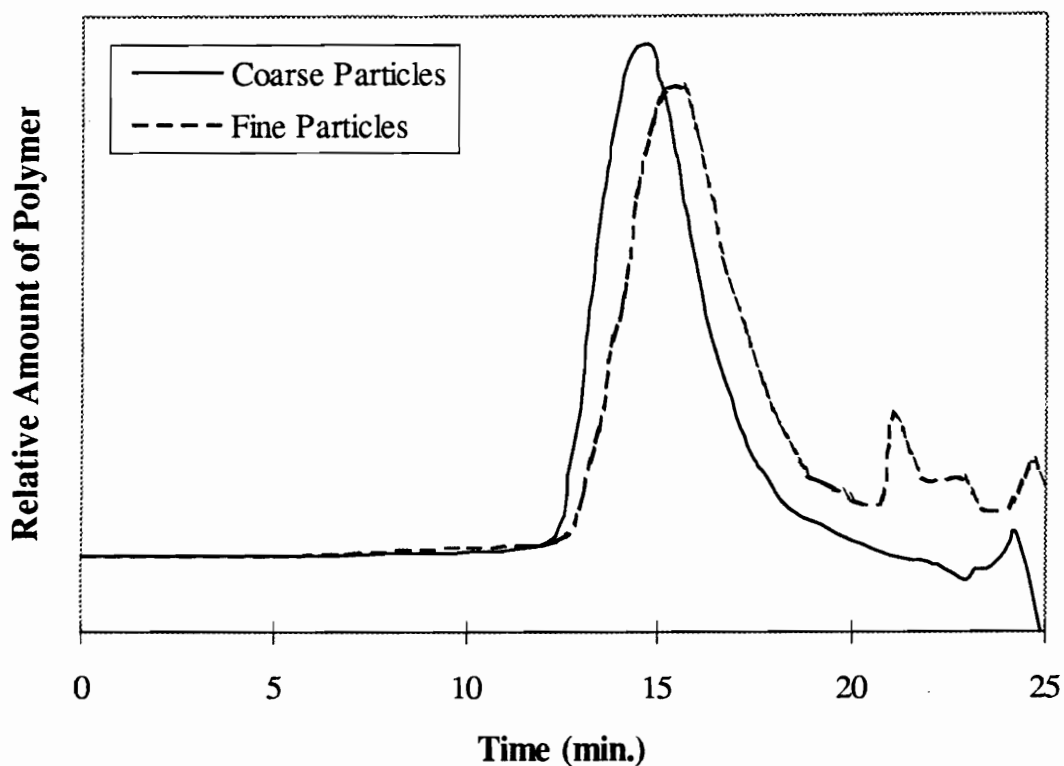


Figure 6 - GPC results for coarse and fine polycarbonate particles.

Environmental Scanning Electron Microscopy

Microstructures of the fractured tensile specimens and cryogenically fractured compacts were evaluated using an ElectroScan™ environmental scanning electron microscope (ESEM). An operating environment of 3.5 torr of water vapor allowed the non-conductive polycarbonate samples to be examined without the application of a conductive coating.

IV. Room Temperature Compaction

Compaction of Polycarbonate Powder

Experiments were performed on unaged polycarbonate powder to examine the effects of altering the compaction time and compact thickness on density and porosity. Results of these tests were used to help choose a compaction time and compact mass for the remainder of the experiments that would result in more reproducible results. Using these processing parameters, the effects of room temperature compaction pressure and physical aging on the thermal properties, physical properties, and morphology of polycarbonate compacts were then examined.

Effect of Compaction Time on Density

The effect of time on compact density was investigated for polycarbonate powder compacted at 40 MPa at room temperature. Compaction times ranged from 30 seconds to 10 minutes, and three compacts were made from 1.5 grams of powder at each of the compaction times. Figure 7 shows the normalized density data obtained on these compacts using the Archimedes technique. At 30 seconds, the density was 79% of the theoretical value, and it slowly increased to about 82% of the theoretical value after 10 minutes of compaction. Although the density changed slightly between 5 and 10 minutes of compaction, it was not strongly influenced by time after 5 minutes. For this reason, a compaction time of 5 minutes was chosen for further compaction tests.

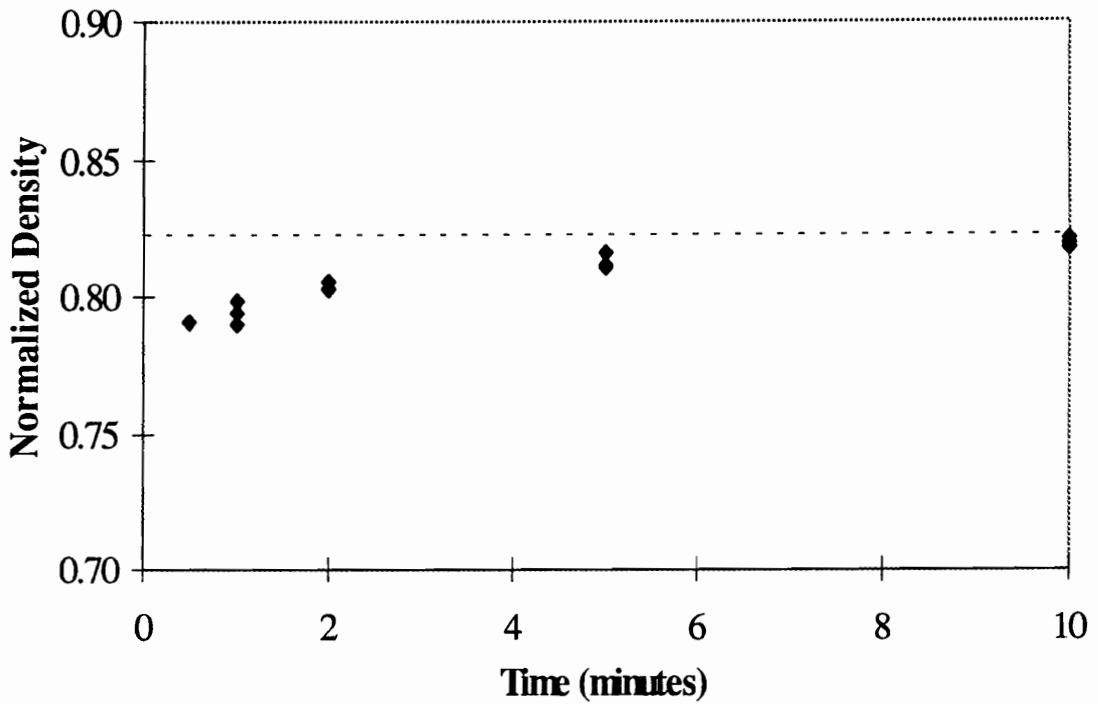


Figure 7 - Effect of compaction time on the normalized density of polycarbonate compacts (compaction pressure: 40 MPa, compact mass: 1.5 gram).

It should be noted that the majority of the porosity in each of the compacts was found to be open, or connected to the surface, with less than 0.3% by volume of closed porosity estimated to be present in all of the compacts.

Effect of Thickness on Density and Porosity

A series of room temperature compaction experiments were performed on various compact sizes at a fixed compaction pressure of 40 MPa to examine the effect of compact

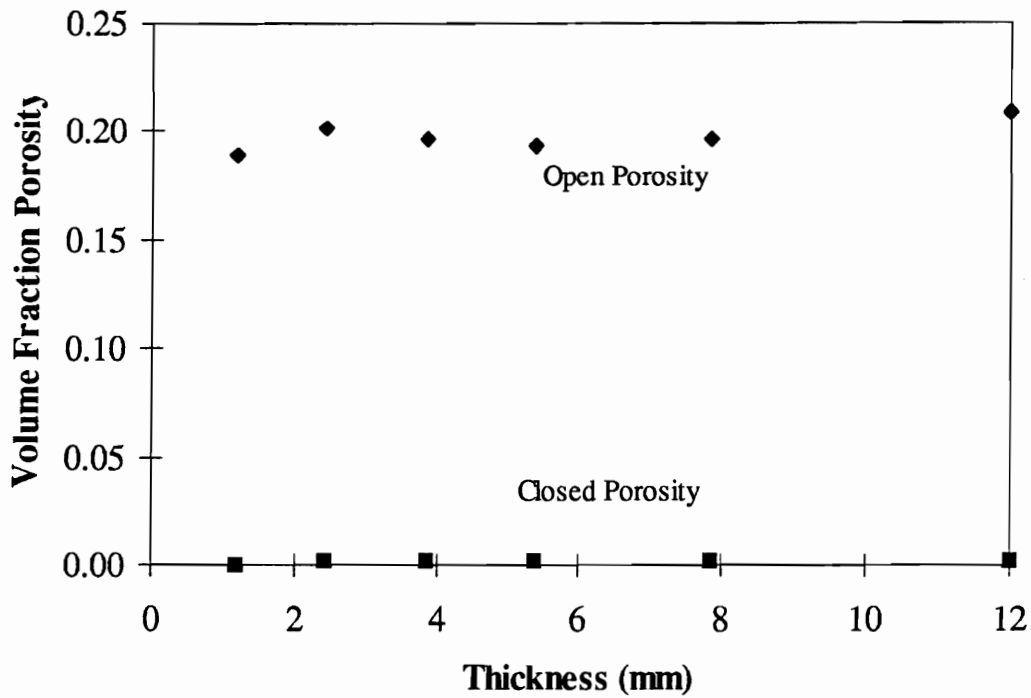


Figure 8 - Effect of compact thickness on the volume fraction of open and closed porosity in polycarbonate compacts (compaction time: 5 minutes.).

thickness on *green*, or as-compacted, density and porosity. The compact masses ranged from 0.7 to 7.5 grams, which corresponded to thicknesses between 1.2 mm and 12 mm. The porosity data are plotted in Figure 8. Note that the volume fractions of open porosity are relatively constant with thickness, while the volume fractions of closed porosity are once again very small, measuring less than 0.3% in all cases. Because these results showed that sample thickness (or mass) did not influence density in the range of masses studied, compacts for most other experiments were made from 1.5 grams of powder, a convenient handling size.

Effect of Compaction Pressure on Density - Unaged Polycarbonate

Compacts made from approximately 1.5 grams of unaged polycarbonate powder were compacted at room temperature over a range of pressures to examine the affect of compaction pressure on green density. (The thicknesses of the compacts ranged from 2.0 to 2.7 mm.) As shown in Figure 9, the compact density increased with pressure and approached a maximum density at high pressures, which was roughly 90% of the theoretical density of the polycarbonate. This density, also known as the *plateau* or *terminal density*, is observed in the compaction of metals, ceramics, and polymers and is

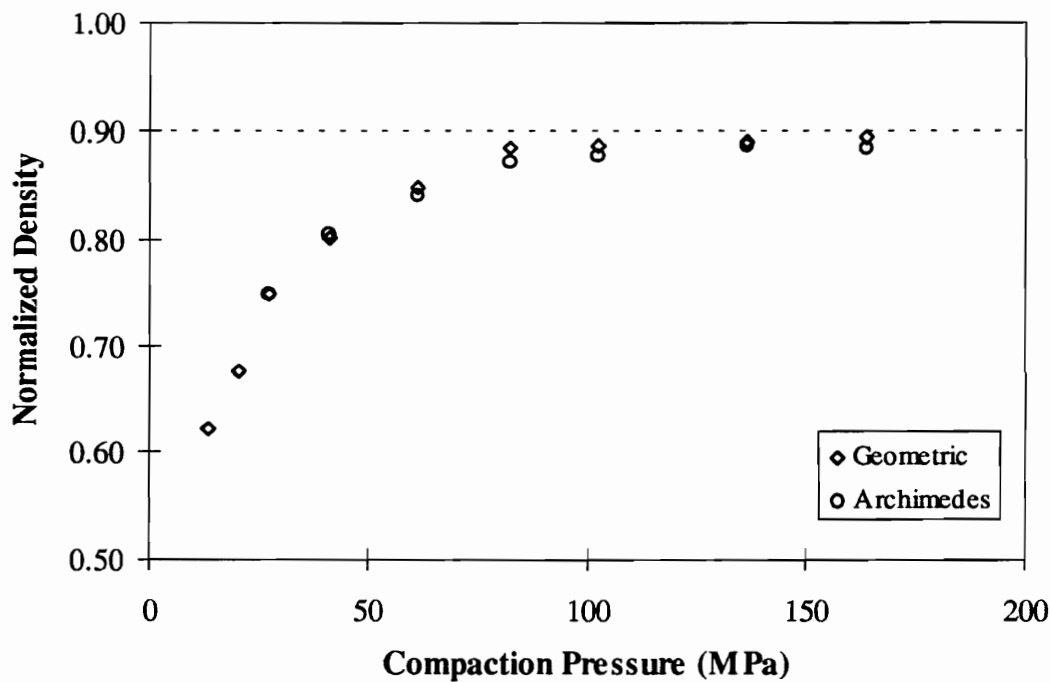


Figure 9 - Effect of compaction pressure on the normalized density of polycarbonate compacts (compaction time: 5 minutes, compact mass: 1.5 gram). Note: Each point represents average measurements made on three different samples. The maximum standard deviation in normalized density was 0.0017 and 0.007 for the geometric and Archimedes data, respectively.

consistent with values obtained for other polymers [6-11,13,14], which tend to be between 85% and 95% of the theoretical density and are generally obtained at compaction pressures in the range of 100 to 500 MPa at room temperature.

Note that the two sets of data points presented in Figure 9, obtained by the geometric and Archimedes methods, are in excellent agreement and are within experimental error of each other. Again, open porosity accounted for the majority of the deviation from the theoretical density, as the volume fraction of closed porosity remained less than 0.3%.

Effect of Compaction Pressure on Density - Aged Polycarbonate

The density versus compaction pressure measurements were repeated on polycarbonate powder aged in a vacuum for 200 hours at 130°C. The data from this series of tests on the aged PC are plotted in Figure 10 along with the data from the unaged PC. As can be seen in this figure, the compacts formed from the aged powder had consistently lower densities than did the compacts made from the unaged powder. The density of the compacts from the aged powder at the highest pressure appeared to be approaching a plateau density of about 85% of the theoretical density, compared to 90% of the theoretical density obtained for the unaged powder. At the two lowest pressures, 13 and 20 MPa, the compacts formed from the aged powder did not have sufficient handling strength to survive during density measurement.

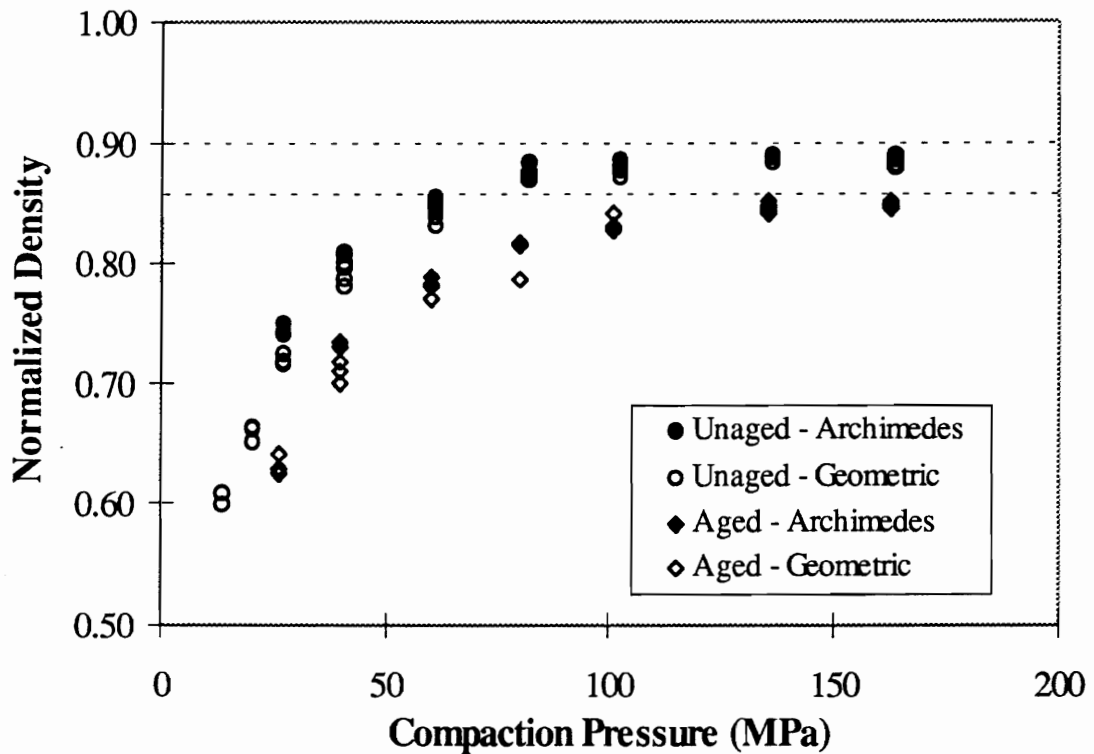


Figure 10 - Effect of compaction pressure on the normalized density of compacts made from unaged and aged polycarbonate powder (compaction time: 5 minutes, compact mass: 1.5 gram).

Effects of Physical Aging on Densification Mechanisms

The stages of compaction of polymeric powders were described by Crawford and Paul [5] as being the same as those described for metals: particle rearrangement, elastic deformation at contact points, plastic deformation at contact points, and bulk compression. These stages, which may occur simultaneously, are illustrated in Figure 11. The differences in compaction behavior between the aged and unaged polycarbonate powders from the current study might be explained by the increases in yield strength that

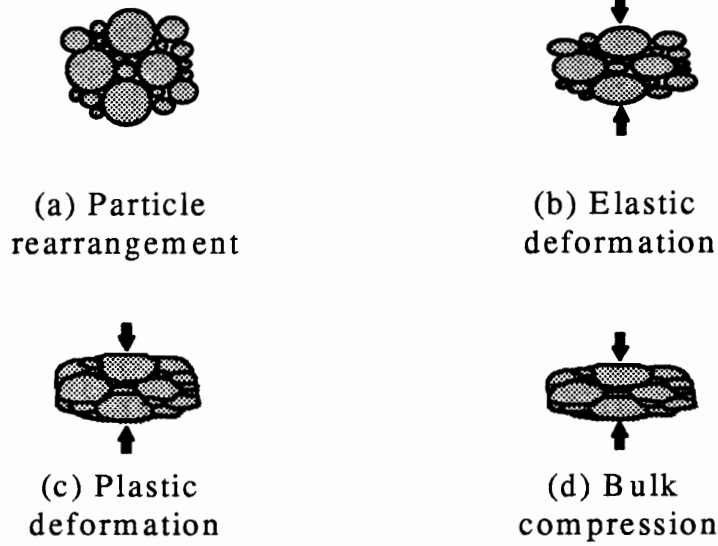


Figure 11 - Stages of compaction for metals, ceramics, and polymers.

result from physical aging, which would change the relative contribution that each stage of compaction makes in the densification process.

For the polycarbonate used in this study, increases in tensile yield strength of 25% were observed in aged films. The compressive yield strength would also be expected to increase due to physical aging. An increase in yield strength would result in a greater amount of particle rearrangement occurring before the compressive stresses became high enough to plastically deform the individual particles. For a given compaction pressure, a higher yield strength would also be expected to result in less particle deformation and possibly a lower degree of mechanical interlocking. This could cause the green strength to be noticeably lower in compacts made from aged powder, especially at very small

compaction pressures, as was observed at the two lowest compaction pressures used in this study (13 and 20 MPa).

The fact that the density was lower for compacts formed from the aged polycarbonate suggests that particle deformation is a very important densification mechanism, with a decrease in the plateau density of 5% of the theoretical density caused by physically aging the powders prior to compaction. This difference in plateau density also suggests that the relative contribution from particle rearrangement versus plastic deformation is different between the aged and unaged powders. In fact, if the relative contributions were the same, then the two data sets in Figure 10 would be able to be scaled horizontally to superimpose on one another.

Effect of Physical Aging on Microstructure

In order to study the effect of physical aging on the morphology of compacted polycarbonate powder, compaction pressures were selected which would result in compacts made from aged and unaged powders having the same density. Room temperature compaction pressures of 60 MPa and 140 MPa for the unaged and aged powder, respectively, were found to result in compacts with a normalized density of 85% of the theoretical density (see Figure 10). Using these compaction pressures, compacts were made and fractured after cooling in liquid nitrogen. The fracture surfaces were then

examined using an environmental scanning electron microscope, viewing the surfaces at an angle of approximately 45°.

Figure 12 shows the resulting microstructures of the aged and unaged compacts. The particles in the compact made from the unaged powder are highly deformed, irregularly shaped, and difficult to distinguish from one another, as shown in Figure 12a. Although the aged particles were subjected to more than double the pressure to form a compact having the same density, they show much less deformation and are easier to identify in the micrograph shown in Figure 12b. These micrographs support the above conclusion that an increase in particle yield strength due to physical aging results in more particle rearrangement and less particle deformation at a given compact density.

Effect of Compaction on Thermal Properties

Differential scanning calorimetry was used to study the effect of room temperature compaction pressure on the thermal properties of the polycarbonate powder. Figure 13 shows DSC scans of as-received and aged polycarbonate, along with the trace for the second heating cycle of the aged material. For clarity, the heat flow versus temperature curves are shifted vertically in all figures. Note that in the as-received condition, the polycarbonate has not been aged significantly, as is evident from the lack of the “ T_g overshoot” endotherm that is characteristic of physical aging. The glass transition



Figure 12 - ESEM Micrographs of polycarbonate compacts made from (a) unaged and (b) aged powder having densities of 85% of the theoretical density of polycarbonate (compaction time: 5 minutes, compact mass: 1.5 grams, compaction pressure: (a) 60 MPa and (b) 140 MPa).

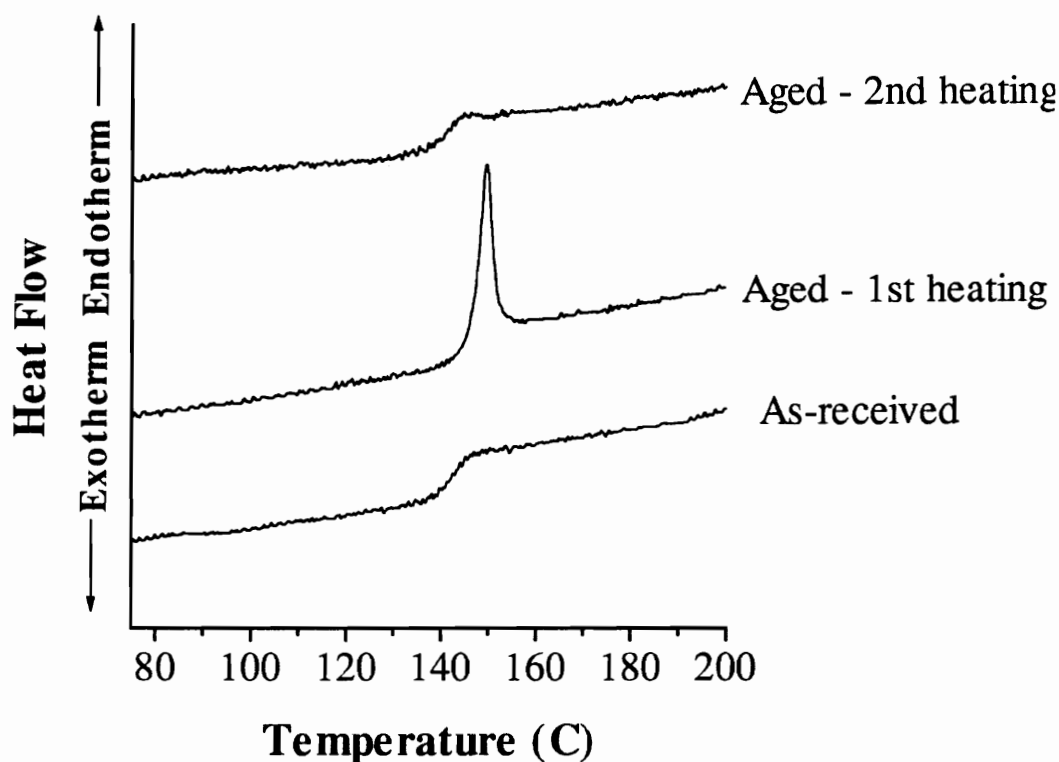


Figure 13 - Differential scanning calorimetry traces for as-received and aged polycarbonate (first and second scans) obtained at a heating rate of 10°C/minute.

temperature (the temperature at which the specific heat capacity value is midway between that of the glass and the liquid states) occurs at about 142°C.

The polycarbonate aged for 200 hours at 130°C exhibited a rather large endothermic peak at the glass transition, whose location did not change due to aging. Upon cooling and reheating the aged polycarbonate, the endothermic peak was no longer present, nor was the glass transition temperature shifted, indicating that the physical aging process was thermally reversible.

Both aged and unaged polycarbonate powders were cold compacted at three different pressures (40, 80, and 160 MPa) at room temperature, and DSC scans were obtained on samples cut from the center of each compact within 5 minutes after the compaction pressure was released. Figure 14 shows the DSC results for the unaged polycarbonate compacts, while Figure 15 shows the results for the compacts made from aged powder. Included for reference in each figure are traces measured for the unaged and aged uncompacted powders.

From Figure 14, it can be seen that for the unaged polycarbonate, as the compaction pressure was increased, a small endothermic peak appeared at the glass transition, similar

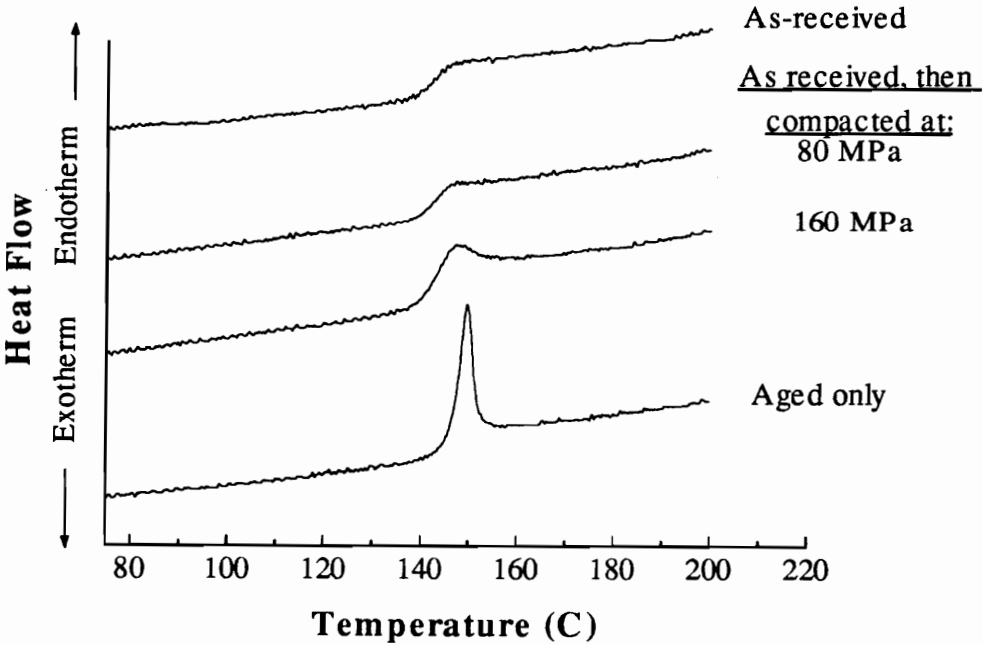


Figure 14 - Effect of compaction pressure on the thermal properties of unaged (as-received) polycarbonate powder (compaction time: 5 minutes, compact mass: 1.5 grams).

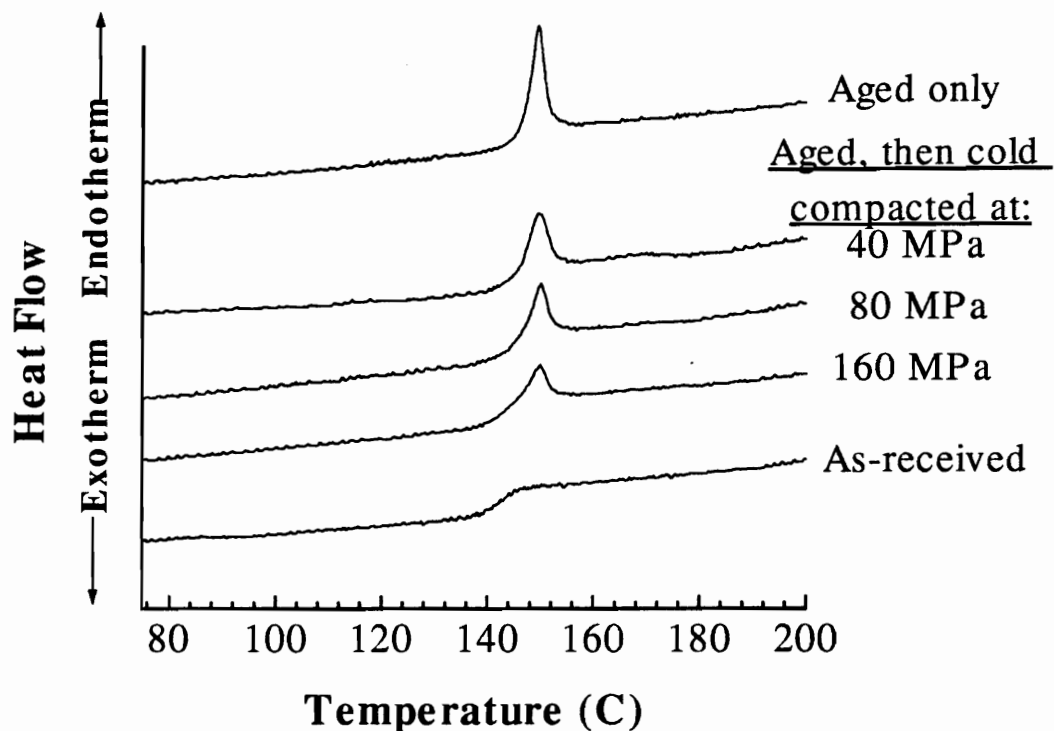


Figure 15 - Effect of compaction on the thermal properties of aged polycarbonate powder (compaction time: 5 minutes, compact mass: 1.5 grams).

to the T_g overshoot present in the physically aged powder. This suggests that the compaction process may be causing a free volume reduction in the polycarbonate due to the small hydrostatic component of the compaction stresses which results from side support provided by the die wall.

In Figure 15, the opposite effect can be observed. When aged polycarbonate powder is compacted, the T_g overshoot decreases in size as the compaction pressure is increased, suggesting a decrease in the apparent degree of physical aging, although the powders were

subjected to compressive loading. Deaging of polycarbonate has been observed to occur due to different types of mechanical loading, such as simple tension or simple compression [42]. It is believed that deaging occurs as a result of volume dilatation, which is caused by certain types of loading. Because the compaction stresses are not purely uniaxial, the shear component of the stress state may be causing the free volume of the polycarbonate to increase during cold compaction, resulting in what appears to be a decrease in the degree of physical aging.

Room Temperature Compaction of Semicrystalline Polymers.

Linear Low Density Polyethylene

LLDPE powder, which has a glass transition temperature well below room temperature, was compacted at room temperature at compaction pressures up to 160 MPa. (A well accepted value for the T_g of polyethylene is -80°C , although reported values range from -130°C to -30°C [43].) Although the same procedure was used as in the polycarbonate experiments, sufficient green strength could not be developed in the compacts to allow them to survive either removal from the die or handling during thickness measurement. At the higher compaction pressures, the compacts initially appeared to have sufficient handling strength, however, within a few minutes of being removed from the die, they, too had very low strength and crumbled during handling. One would expect that compaction of a purely amorphous powder (of sufficient molecular weight) above its glass transition temperature would result in a compact with a green strength approaching that of the bulk

material, as high chain mobility would permit the reptation of chains across particle interfaces and the development of entanglements in a relatively short period of time.

Two factors may be contributing to the fact that the LLDPE powder could not be successfully compacted at room temperature. LLDPE has a fairly high degree of crystallinity (up to 62% by volume for a polyethylene with a low degree of branching [43]), and particle deformation which results in densification and development of green strength is expected to occur primarily in the amorphous phase. This means that a smaller volume fraction of amorphous phase is available to participate in densification and the amorphous material that is present exists in much smaller domains, making it much more difficult to achieve mechanical interlocking between particles.

The second factor which would hinder green strength development in LLDPE is its very low glass transition temperature. Because compaction at room temperature is being done well above the glass transition temperature of the amorphous phase, the amorphous chains have a fair amount of mobility. However, due to the high degree of crystallinity in this material, it is probable that the majority of the amorphous chains are anchored by crystalline lamellae in one or more places along their lengths and that only short lengths of “free” amorphous chains exist between the lamellae in the polymer. These free lengths of amorphous chains would be much shorter than the critical length needed to form entanglements and develop significant strength across particle interfaces.

If these arguments are correct, semicrystalline polymers having glass transition temperatures above room temperature and/or a lower degree of crystallinity would be expected to have higher normalized density and green strength than did the LLDPE. This was verified by performing compaction experiments on Nylon-11 and PEEK.

Nylon-11

As expected, compaction of Laserite™ LN4010 Nylon-11 powder, which has a glass transition temperature above room temperature (50°C) and a lower degree of crystallinity (typically on the order of 40%) than LLDPE (~62%), was more successful. However, time-dependent density changes were observed upon removal of the compacts from the die. This can be seen in the normalized density versus pressure curves shown in Figure 16, which were measured at various times following release of the compaction pressure. (Note that density measurements were made using the geometric technique, as the Archimedes technique does not allow rapid density measurement.)

From Figure 16, it can be seen that the density of the Nylon-11 drops by almost 5% of the theoretical value between 10 minutes and 300 hours after removal from the die, with about half of this change experienced during the first 24 hours. The maximum density obtained by compacting the powder at 160 MPa (measured 10 minutes following compaction) was only about 80% of the theoretical density, compared to the 90% and 85% theoretical

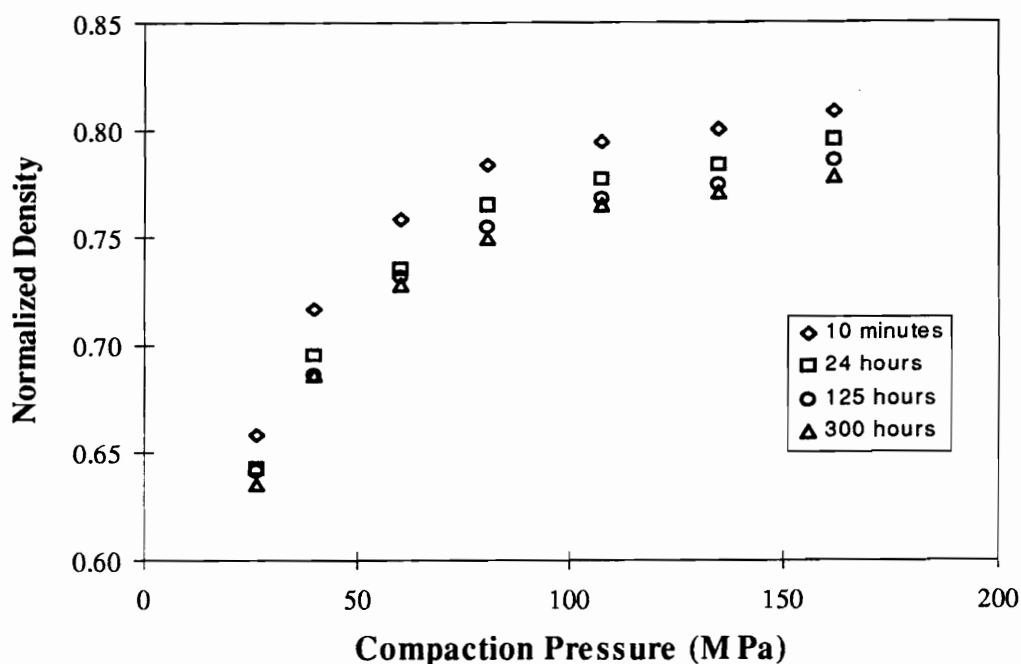


Figure 16 - Effect of compaction pressure on the normalized density of Nylon-11 compacts as measured using the geometric technique at various times after removal of the compaction pressure (compaction time: 5 minutes, compact mass: 1.5 grams). Each point represents average measurements made on three different samples.

density obtained for the unaged and aged polycarbonate powders, respectively, at the same pressure. From this plot, it does not appear that the plateau density of the Nylon-11 powder has been reached by 160 MPa, as it had been for both the unaged and aged polycarbonate.

The normalized density of the Nylon-11 compacts is lower than that of the compacts made from either the unaged or aged polycarbonate (see Figure 10), suggesting a lower degree of particle deformation in the Nylon-11 for a given compaction pressure. Two factors

may have contributed to this effect. The first is the decrease in the volume fraction of the amorphous phase in the Nylon-11, which is the primary site for deformation at lower compaction pressures. The second is the higher yield strength and modulus of the Nylon-11 (see Tables II and III). Since Nylon-11 has less amorphous material that is more difficult to deform, it follows that less particle deformation would be present than in the polycarbonate powder.

Because the glass transition temperature of Nylon-11 is only about 30°C higher than room temperature, the amorphous phase has a limited degree of mobility at room temperature. This allowed partial viscoelastic recovery of the particle deformation at room temperature in a relatively short amount of time (hours and probably even minutes), as the locked-in strains within the particles act as a driving force for recovery. Time-dependent relaxation of the amorphous domains resulted in the macroscopic decreases in compact density with time. This time-dependent recovery is also likely to be experienced by the polycarbonate, however, because the polycarbonate has a much higher glass transition temperature (142°C) than does the Nylon-11 (50°C), it occurs over a much greater time scale in polycarbonate and is not significant over the experimental time scale (days).

Poly(ether ether ketone)

Room temperature compaction was also performed on PEEK. The normalized density is plotted versus compaction pressure in Figure 17. The plateau density of PEEK was found

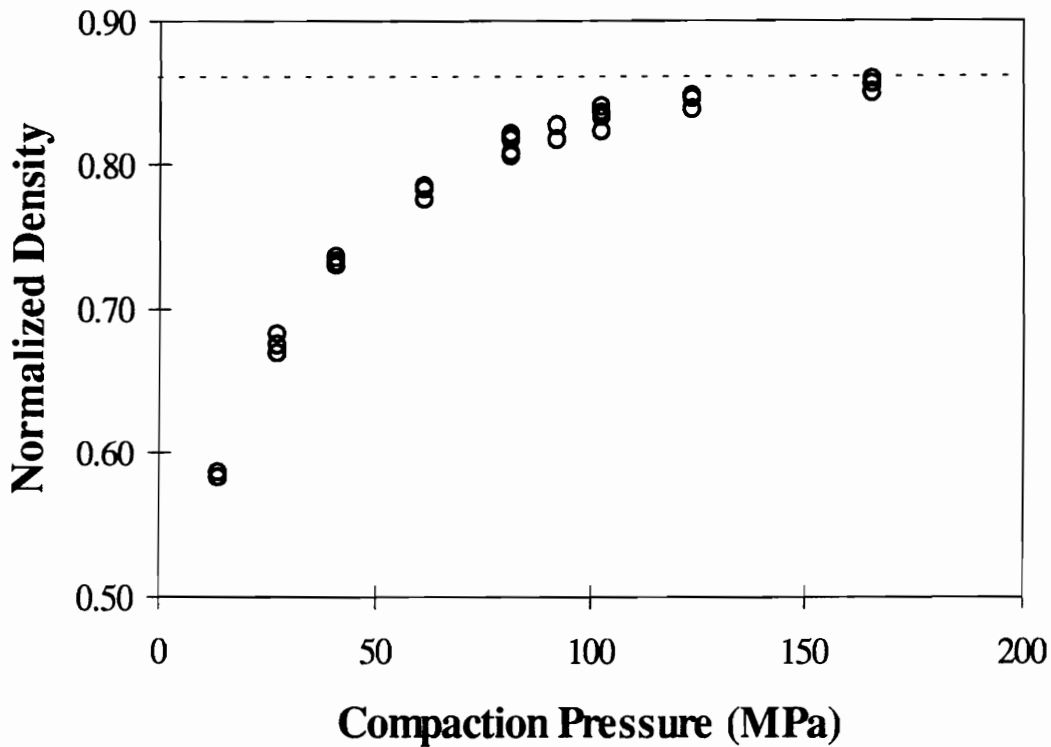


Figure 17 - Effect of compaction pressure on the normalized density of PEEK compacts (compaction time: 5 minutes, compact mass: 1.5 grams).

to be about 86% of the theoretical density, compared to the 90% and 85% measured for unaged and aged polycarbonate, respectively. PEEK has a T_g well above room temperature ($\sim 145^\circ\text{C}$, similar to that of PC) and can attain a maximum of only $\sim 35\%$ crystallinity by volume. This allowed it to be successfully compacted at low pressures, and prevented it from exhibiting significant time-dependent recovery. These results support the prediction that semicrystalline polymers having a T_g well above room temperature would have better handling strength and would show much less

time-dependent recovery than did the Nylon-11, whose T_g was just above room temperature.

Summary of Room Temperature Compaction Results

It was found that differences in the degree of physical aging affect the compaction behavior of polycarbonate powder, with lower pressures being required to achieve sufficient handling strength for the unaged powder compared to the aged powder. Also, compacts made from unaged powder consistently had a higher density than aged powder compacted at the same pressure. This was apparently due to the higher yield strength of the aged polycarbonate, which decreases the plastic deformation experienced by the aged particles relative to the unaged particles. These findings show that the degree of physical aging of thermoplastic polymer powders, which can be influenced by powder handling operations such as drying and long term storage, can ultimately affect the ability of the powder to be successfully compacted at room temperature.

Room temperature compaction was found to affect the thermal properties of both the aged and unaged polycarbonate powder. For relatively high compaction pressures, the height of the endotherm at the glass transition, which is typically indicative of the degree of physical aging, was found to decrease for aged powder and increase for unaged powder for relatively high compaction pressures.

Compaction experiments also revealed that both the degree of crystallinity and the glass transition temperature affect the ability of a semicrystalline polymer to be compacted successfully. The results suggested that the presence of crystallinity led to a lower degree of particle deformation and a lower density for a given compaction pressure. This could result from two factors: a decrease in the volume fraction of amorphous phase, which is the primary site for deformation at lower compaction pressures, and an increase in the yield strength and modulus of the particles, as the crystalline phase acts as a reinforcing phase. In semicrystalline polymers having a very high degree of crystallinity, the portions of amorphous chains that are “free” and mobile may be too short to form entanglements and contribute significantly to strength development across particle interfaces.

Compaction of a purely amorphous powder (of sufficient molecular weight) above its glass transition temperature would result in a compact with a green strength approaching that of the bulk material, as high chain mobility would permit the reptation of chains across particle interfaces and the development of entanglements in a relatively short period of time.

The speed of viscoelastic recovery following removal of the compaction pressure was affected by the glass transition temperature of the polymer. Compacts made from Nylon-11 powder, whose T_g is about 30°C above room temperature, exhibited time-dependent recovery, with dimensional changes resulting in a decrease of almost 5% of the

theoretical density in the time period between 10 minutes and 300 hours after the compaction pressure was removed. In polycarbonate and PEEK, which both have a T_g ~145°C, no significant time-dependent deformation was observed at room temperature following compaction.

V. Sintering of Compacts Formed at Room Temperature

Two types of sintering experiments were done on cold compacted (unaged) polycarbonate powder. The first involved heating the bulk compacts above the glass transition temperature in the absence of an applied pressure and measuring the density and the porosity levels as a function of isothermal hold time. The second consisted of sintering smaller samples at a known heating rate and measuring the change in thickness as a function of time and temperature using a thermomechanical analyzer. The complementary data obtained using these techniques yielded valuable information which showed that the sintering process is quite different in polymer compacts than in metal or ceramic compacts. Selected experiments were repeated on aged polycarbonate and semicrystalline polymers to examine how factors such as yield strength and crystallinity affect the sintering process.

Isothermal Pressureless Sintering of Polycarbonate Compacts

Density Changes during Pressureless Sintering

The normalized density of polycarbonate compacts was measured as a function of pressureless sintering time at 165°C (about 20°C above T_g) for three different room temperature compaction pressures (40, 80, and 160 MPa). Three different specimens were tested at each time and compaction pressure. As shown in Figure 18, although the initial density is relatively high (approaching 90% of the theoretical density for the highest compaction pressure), the density quickly dropped upon heating above T_g . Within the first

few minutes at 165°C, the density of all compacts was between 52% and 58% of the theoretical density, with higher compaction pressures resulting in slightly higher densities measured after 5 minutes at 165°C. Note that these values are on the order of the tap density of the powder, which was reported to be 52% of the bulk density of the polycarbonate (see Table II).

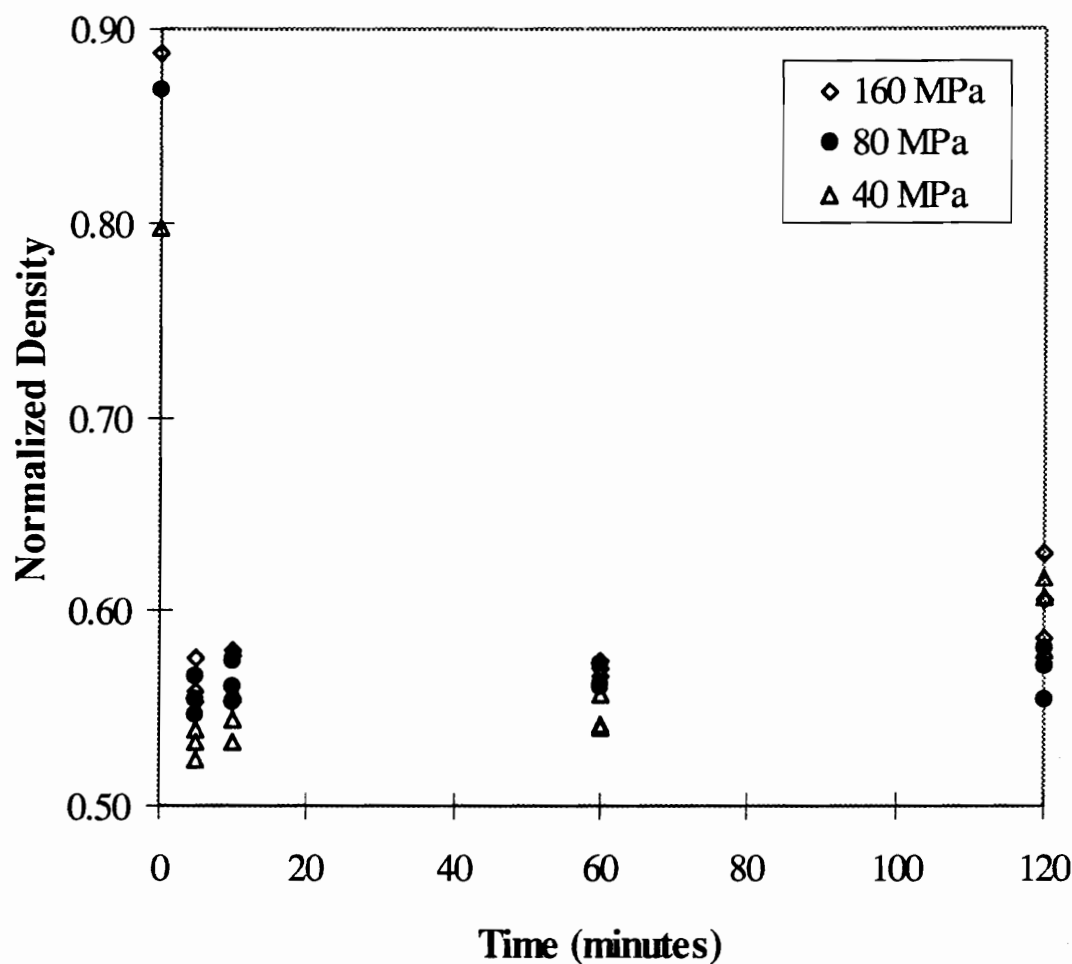


Figure 18 - Effect of pressureless sintering at 165°C on the normalized density of polycarbonate powder compacted at room temperature at compaction pressures of 40, 80, and 160 MPa (compaction time: 5 minutes, compact mass: 1.5 grams).

At times greater than 60 minutes, the density increased slightly with time, as densification due to neck growth between the particles began to overshadow the dimensional recovery experienced by the particles, which dominated the early minutes of heating above T_g . The room temperature compaction pressure (or initial density) did not affect the density following sintering as much as might be expected, with the data points from the three pressures tending to overlap each other.

Note that the data points below 60 minutes were obtained by heating the samples between preheated hot press platens (with no applied pressure), while the data points taken at 60 minutes and above were obtained by heating the samples in a preheated vacuum oven (at ambient pressure). This change in heating technique may be responsible for a slight shift in the data above 5 minutes, but both techniques indicate that pressureless sintering at 165°C results in a dramatic decrease in density.

For all specimens, the deviation of the density from the theoretical value following isothermal sintering was primarily due to open porosity; the volume fraction of closed porosity was below 0.6% in all cases. The fact that closed porosity was almost nonexistent, either before or after sintering, indicated that the expansion of the compacts during heating was not due to trapped air causing pressure to build up within the closed pores.

Microstructural Changes during Pressureless Sintering

To examine the effect of pressureless sintering on the microstructure of room temperature compacted polycarbonate, a set of compacts comparable to the ones shown in the ESEM micrographs in Figure 12 were formed and isothermally sintered at 165°C with no applied pressure. The resulting compacts were cryogenically fractured and examined using the ESEM to obtain the micrographs shown in Figure 19. Note that both the (a) unaged and (b) aged compacts have lost the mechanical interlocking present prior to sintering (Figure 12), and necks appear to be growing between some of the particles. Several small broken contacts points can also be seen along the fracture surface of both compacts.

Dynamic Sintering of Polycarbonate Compacts

Thermomechanical analysis (TMA) was performed on polycarbonate compacts formed under the same compaction conditions as the compacts that were “isothermally” sintered at 165°C. This type of test simulated a “dynamic sintering” process in which the dimensional changes could be measured as a function of time and temperature at a known heating rate. It yielded more information about the kinetics of the viscoelastic recovery and densification processes than did the isothermal sintering tests on the bulk compacts. As discussed earlier, during TMA, the samples were heated at a rate of 5°C/minute and subjected to the various hold temperatures for 20 minutes prior to cooling at about 5°C/minute. The very small pressures exerted by the probe on the specimen was less than 40 Pa (0.006 psi).

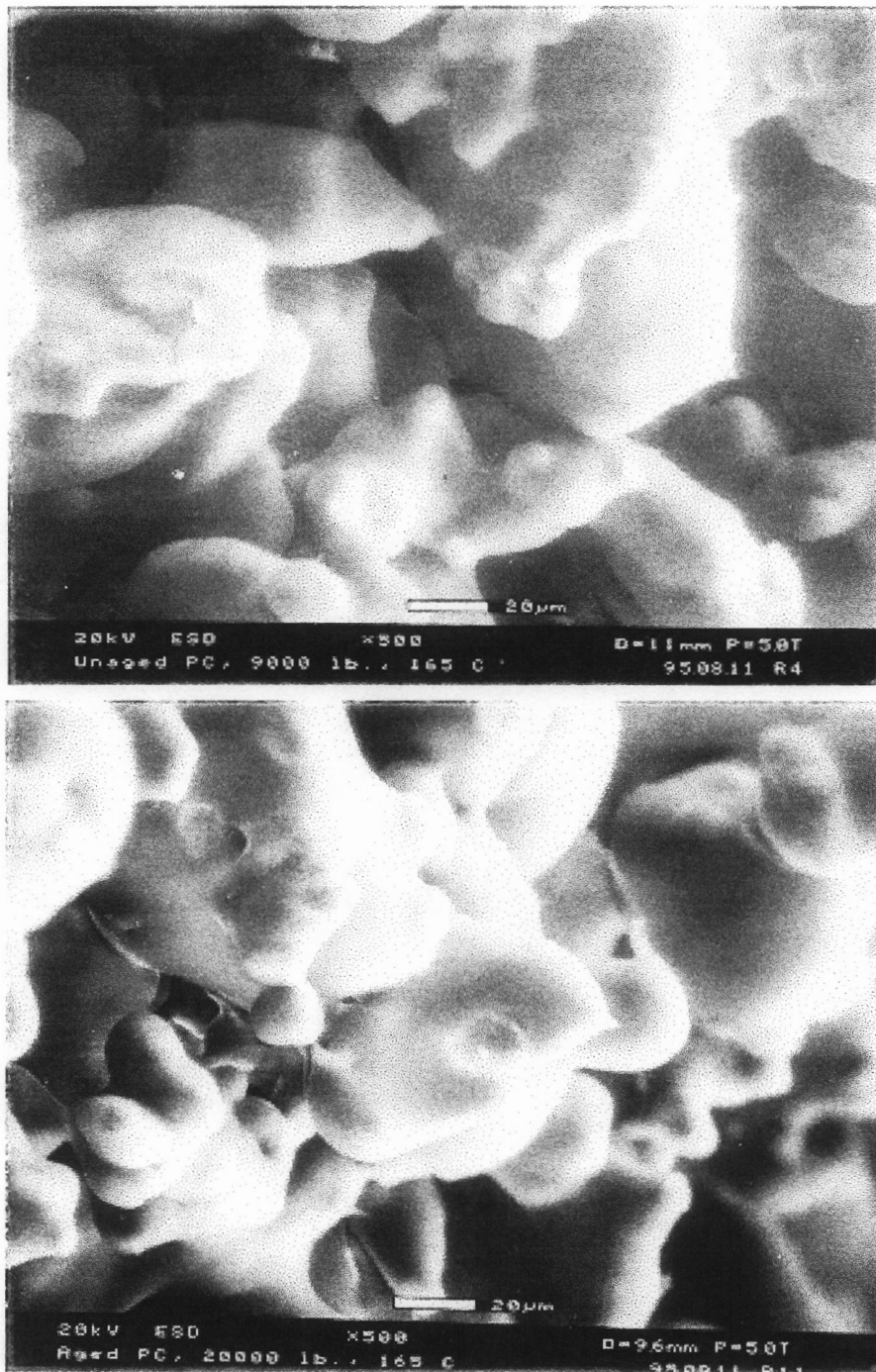


Figure 19 - ESEM Micrographs of polycarbonate compacts made from (a) unaged and (b) aged powder after pressureless sintering for 20 minutes at 165°C (compaction time: 5 minutes, compact mass: 1.5 grams, compaction pressure: 60 MPa, density prior to sintering: 85% of the theoretical density of polycarbonate).

TMA of Bulk Polycarbonate Films

For comparison with data obtained on polycarbonate compacts, TMA was performed on bulk unaged polycarbonate film made from the LPC3000 powder. Figure 20 shows the resulting percent thickness change versus temperature. The thermal expansion coefficients for the glassy and liquid states were about 70 and 300 x 10⁻⁶ m/m/°C, respectively. The glass transition temperature can also be estimated from this data as the extrapolated point where the thickness versus temperature curve changes slope. From the data presented in

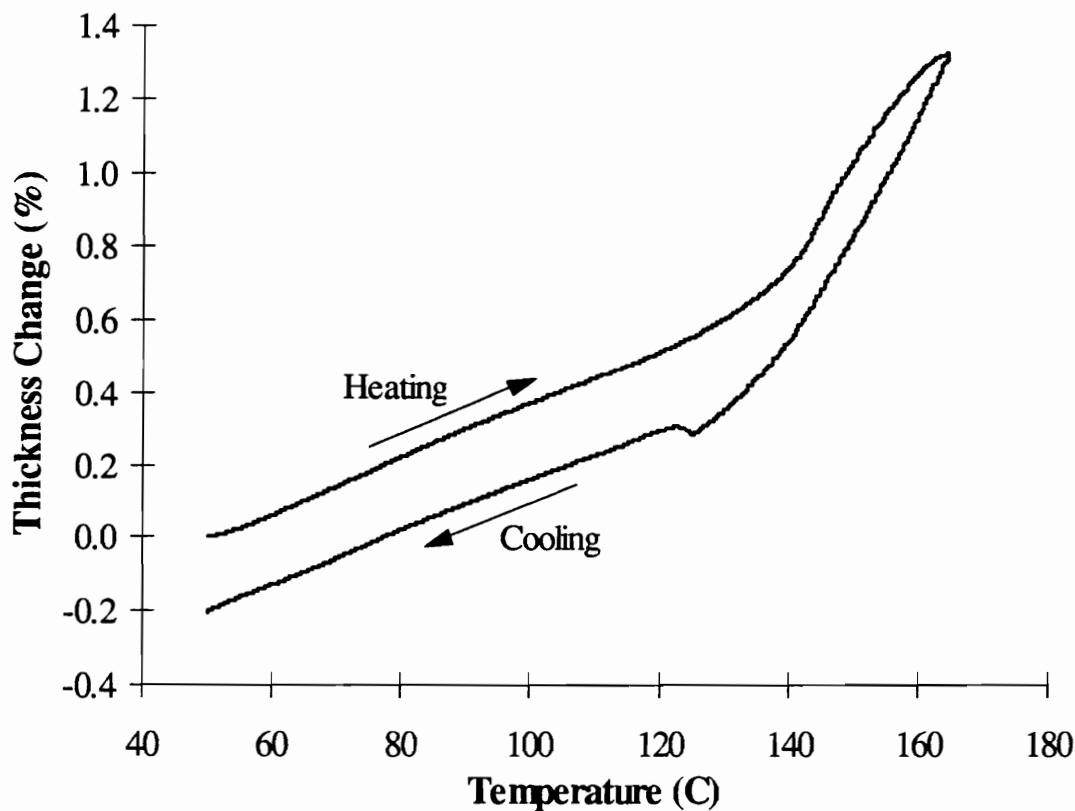


Figure 20- TMA trace for bulk (unaged) polycarbonate film scanned at heating and cooling rates of 5°C/minute (pressure exerted by probe: < 40 Pa (0.006 psi)).

this figure, the glass transition temperature is on the order of 138°C, which is fairly consistent with the value of 142°C obtained through differential scanning calorimetry at a scanning rate of 10°C/minute.

TMA of Room Temperature Compacted Polycarbonate

Figure 21a shows plots of the change in thickness versus temperature for unaged polycarbonate powder compacted at room temperature at a pressure of 80 MPa. The three curves shown in this figure represent the response of the compacts to heating at 5°C/minute and holding for 20 minutes at temperatures of 100°C, 150°C, and 180°C prior to cooling. Figure 21b shows the corresponding values of normalized density versus temperature estimated from this TMA data. (It should be noted that the dimensional changes experienced by the compacts in the thickness direction were much larger than those measured in the radial direction, as measured during isothermal sintering of the bulk compacts. Changes in the diameters of the compacts isothermally sintered at 165°C were always less than 5% and have been ignored in calculating normalized densities.)

Transition from Reversible to Irreversible Expansion. From Figure 21, it can be seen that a transition occurs at about 50°C during the initial heating cycle, well below the glass transition (142°C). At this temperature, the slope of the curves changes significantly, indicating a large increase in the coefficient of thermal expansion, or α , which jumped

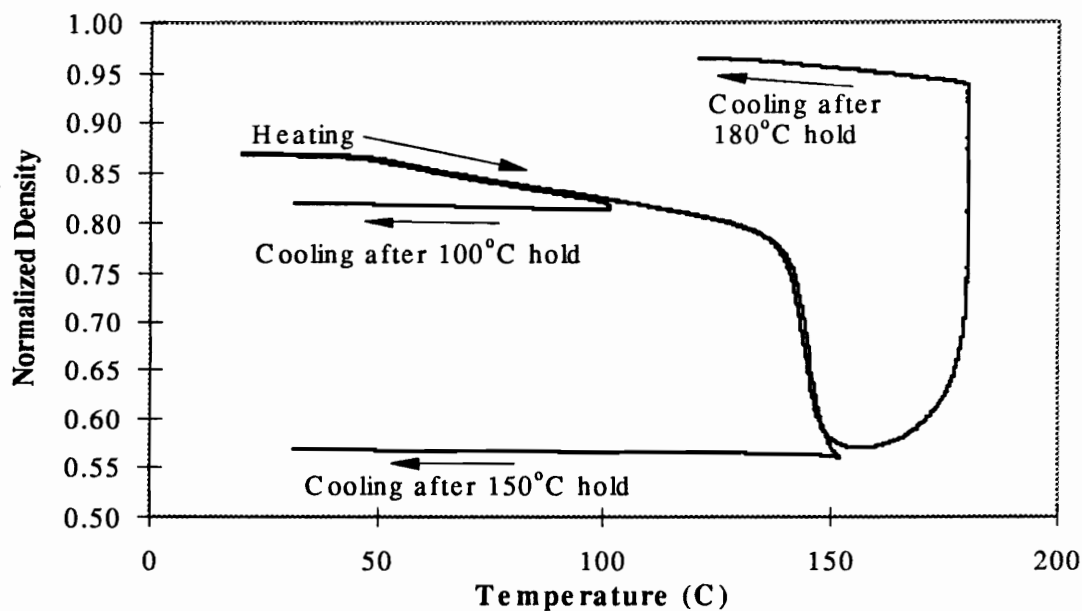
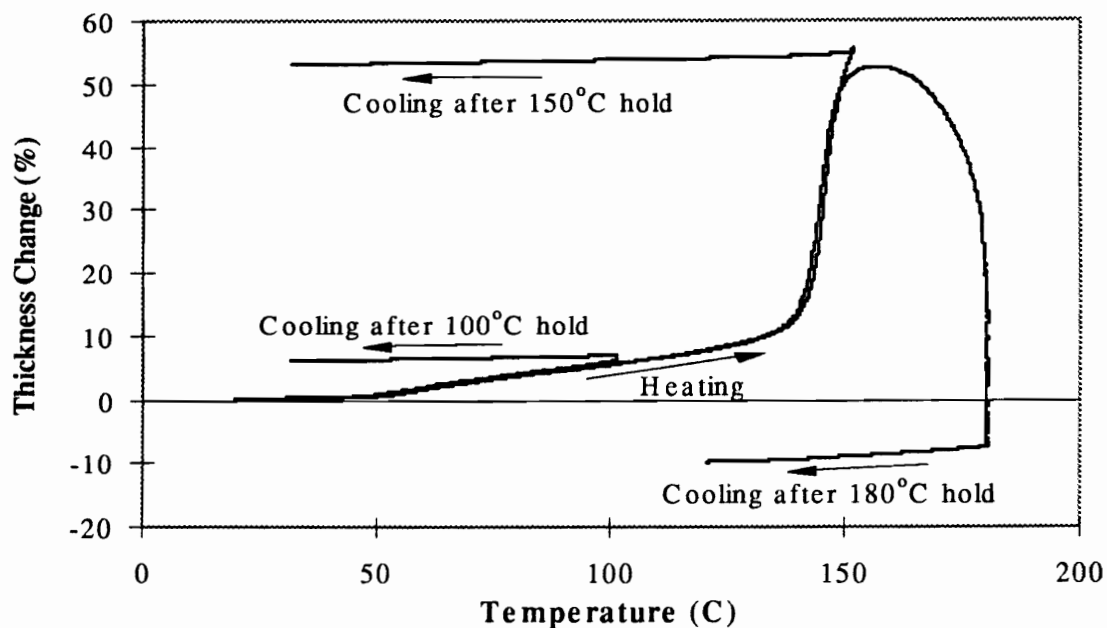


Figure 21 - (a) Thickness change and (b) estimated normalized density (fraction of theoretical density) during TMA testing of polycarbonate compacts formed at room temperature at a compaction pressure of 80 MPa from unaged powder (compaction time: 5 minutes, compact mass: 1 gram, pressure exerted by probe: < 40 Pa (0.006 psi)).

from about 140×10^{-6} m/m/°C below the transition to about 1150×10^{-6} m/m/°C above the transition.

Upon cooling from the various hold temperatures, α dropped back down to values similar to those measured below the transition during the initial heating stage. This low-temperature transition marks the change from reversible thermal expansion to irreversible expansion. The large values observed above the transition temperature are a sum of two components, the first due to bulk thermal expansion of the polycarbonate and the second due to irreversible recovery of the particles, as shown schematically in Figure 22.

Above the transition temperature, two factors may be contributing towards non-recoverable expansion. It is possible that the very large locked-in strains which exist locally at the sites of the original contact points between particles have caused an effective lowering of the glass transition in these high stress regions, giving the chains sufficient mobility to begin to recover deformation well below the glass transition temperature of the bulk compact. Localized losses in mechanical interlocking caused by non-uniform thermal expansion may also be occurring due to the complex states of locked-in strain in the particles, resulting in reorganization of the particles which contribute to the macroscopic dimensional changes.

Expansion above the Transition Temperature. Dimensional changes in the compacts continued steadily as the compacts were heated above the transition temperature, as shown in Figure 21. A 20 minute hold at 100°C resulted in a permanent expansion on the order of 5% for the polycarbonate compacted at room temperature at 80 MPa. Note that this dimensional change occurred as the sample was being heated up, but did not significantly increase during the 20 minute hold time, suggesting that this low-temperature expansion occurred quickly relative to the scan rate of 5°C/minute.

When the compacts were further heated above the glass transition (140-150°C), they rapidly expanded and had estimated densities approaching that of the tap density of the

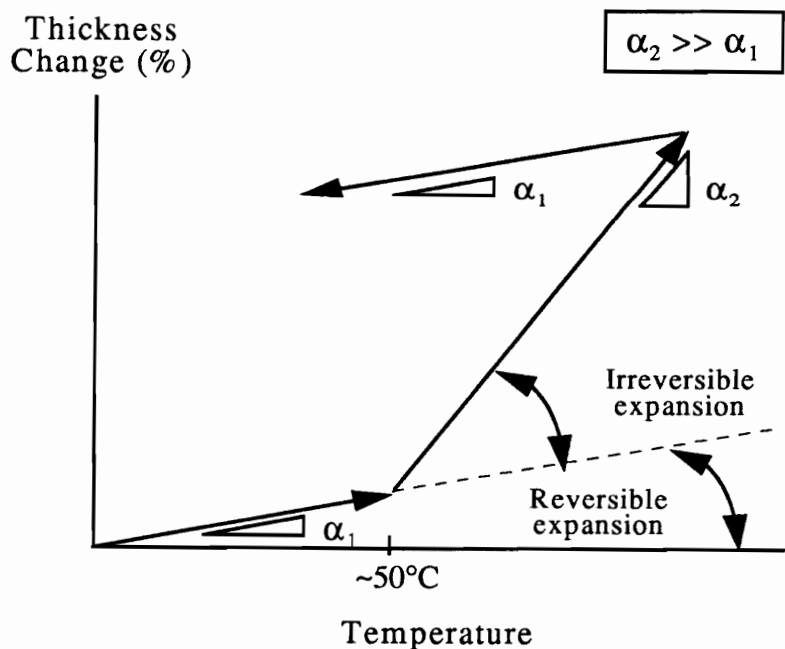


Figure 22 - Schematic showing transition from reversible to irreversible expansion which occurs at about 50°C in cold compacted polycarbonate.

powder. Increases in thickness of up to 55% were recorded. Unlike the irreversible expansion that occurred at lower temperatures, these dimensional changes were nonlinear with temperature. They were much larger in magnitude than the low temperature expansion, suggesting that they occurred as a result of recovery in the majority of the material, not just the regions of highest locked-in strain.

In Figure 23, the data from Figure 21 for the 150°C hold temperature have been re-plotted to show the change in thickness and the temperature versus time. Note that dimensional

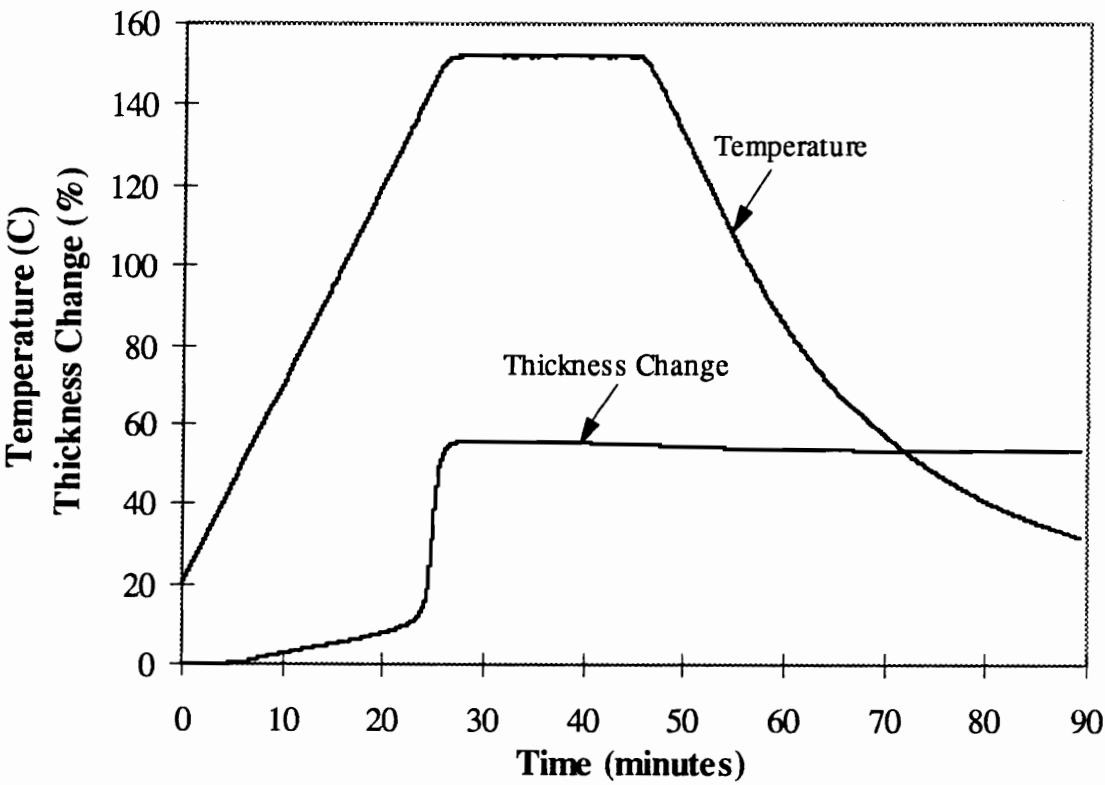


Figure 23 - Change in thickness as a function of time during TMA testing of room temperature compacted polycarbonate (compaction time: 5 minutes, compaction pressure: 80 MPa, pressure exerted by probe: < 40 Pa (0.006 psi)).

recovery at the glass transition temperature is extremely rapid, with the sample attaining its maximum expansion at about the same time its temperature reached the hold temperature. Since the compact was only about 10°C above the glass transition temperature at the hold temperature, the densification process, which would cause the thickness to begin to decrease with time, is very slow relative to the time scale of this experiment. Densification would have resulted in a much larger negative slope during the remainder of the isothermal hold.

When held at temperatures well above the glass transition temperature (180°C), the compacts did begin to densify during the thermomechanical analysis, with final densities approaching 98% of the theoretical density. However, this densification was aided by the very small pressure exerted on the sample by the probe. In fact, in earlier TMA scans when glass coverslips were not used to distribute the loads over the entire sample, it was found that the area underneath the probe became indented during the 180°C hold, even with an applied load of only 100 mg (approximately 200 Pa or 0.03 psi) used to maintain contact between the sample and the probe. This caused the probe to “climb” back out of the indentation site as the sample was cooled below T_g , making the sample erroneously appear to expand during cooling.

Effect of Compaction Pressure on Recovery. The effect of room temperature compaction pressure on expansion behavior during TMA was examined by testing unaged

polycarbonate compacted at 40 and 160 MPa under the same conditions as the 80 MPa compacts at hold temperatures of 100°C, 150°C, and 180°C.

Figure 24 shows the estimated normalized densities of polycarbonate compacts compacted at the three compaction pressures as a function of temperature for the 150°C hold temperature. The curves start at different initial densities, due to the differences in compaction pressure (refer to Chapter IV for details on how compaction pressure affects density) and are very similar to each other below the glass transition temperature, as they maintain the initial difference in normalized density as a function of temperature.

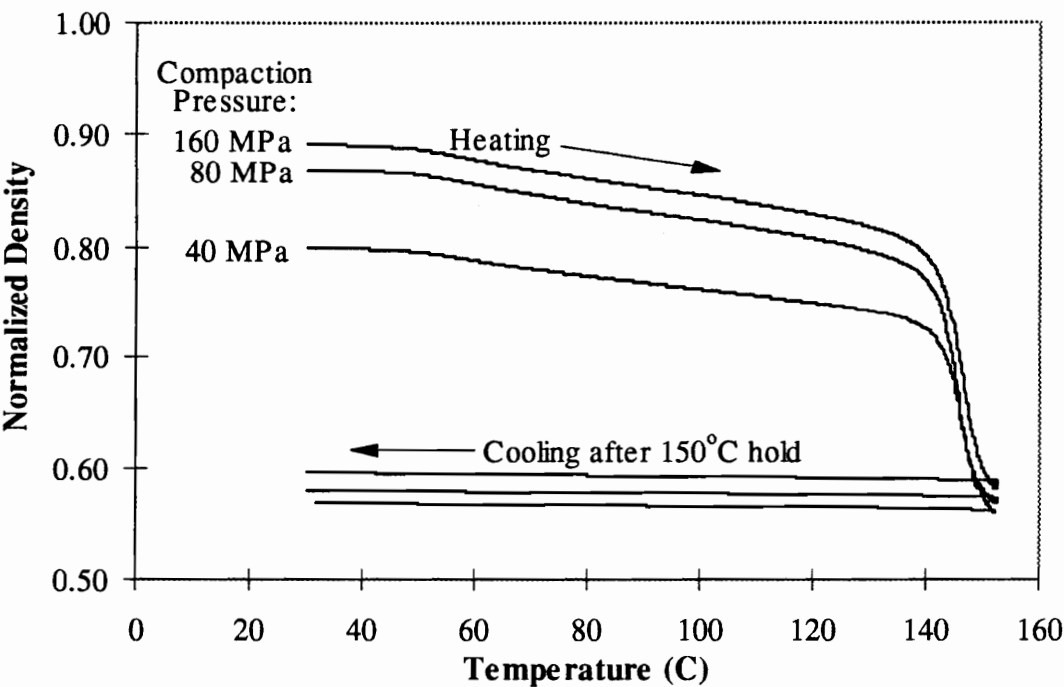


Figure 24 - Normalized density (fraction of theoretical density) estimated from TMA data for compacts formed from unaged polycarbonate powder at room temperature at compaction pressures of 40, 80, and 160 MPa (compaction time: 5 minutes, compact mass: 1 gram, pressure exerted by probe: < 40 Pa (0.006 psi)).

However, once the glass transition temperature is reached, recovery is greater in the compacts formed at higher pressures, and the final densities are closer in value, although the higher compaction pressures still resulted in slightly higher densities.

Values of the transition temperature where recovery becomes irreversible are summarized along with the coefficients of thermal expansion above and below the transition during heating and during cooling in Table V for unaged polycarbonate compacted at 40, 80, and 160 MPa. Changes in thickness and normalized densities at the 100°C and 150°C hold temperatures for these samples are included in Table VI. Note that as observed in Figure 24, the thermal expansion and transition temperature values are very similar, indicating that compaction pressure does not significantly affect thermal expansion or recovery below the glass transition temperature, although it affects recovery upon heating above T_g , as evident from the expansion data in Table VI.

These results can be interpreted as indicating that the factors that influence low temperature recovery (localized areas of very high locked-in strains and depressed T_g and/or mechanical interlocks that are broken due to non-uniform thermal expansion) are not significantly affected by compaction pressure over the range of pressures studied (40-160 MPa). However, higher compaction pressures create a higher degree of deformation and locked-in strain in the particles, resulting in a larger percentage thickness change, but a higher normalized density, upon heating above T_g .

Table V- Summary of TMA thermal expansion data obtained on room temperature compacted (unaged) polycarbonate powder (compaction time: 5 minutes, compact mass: 1 gram).

Compaction Pressure (MPa)	Coefficient of Thermal Expansion (10^{-6} m/m/°C)			Transition Temperature (°C)
	Initial Heating: Below Transition	Initial Heating: Above Transition	Cooling: Above & Below Transition	
40	140	1160	120	57
80	140	1150	120	57
160	130	1060	120	61

Table VI- Summary of TMA recovery data obtained on room temperature compacted unaged polycarbonate powder (compaction time: 5 minutes, compact mass: 1 gram).

Compaction Pressure (MPa)	Initial Normalized Density	Thickness Change @ 100 C (%)	Thickness Change @ 150 C (%)	Normalized Density after 110 C hold	Normalized Density after 150 C hold
40	0.80	8	47	0.74	0.50
80	0.88	7	55	0.83	0.53
160	0.89	7	53	0.83	0.54

Effect of Physical Aging on Recovery. The effect of physically aging the polycarbonate powder (prior to room temperature compaction) on expansion during TMA testing was examined. Aged polycarbonate compacted at 40, 80 and 160 MPa was tested under the same conditions as the compacts formed from unaged polycarbonate at hold temperatures of 100°C, 150°C, and 180°C. Figure 25 shows the estimated normalized densities of polycarbonate compacts formed from unaged and aged powder compacted at 80 MPa as a function of temperature for the 150°C hold temperature.

Although the initial densities were different (refer to Chapter IV for details on how physical aging affects density), they are very similar to each other below the glass transition temperature. As in the case of unaged polycarbonate compacted at different pressures, the curves maintained the initial difference in normalized density as a function of temperature below T_g . However, once the glass transition temperature was reached, recovery was greater in the compacts formed from unaged powder, which exhibited a greater degree of particle deformation (refer to Figure 12). The final densities were closer

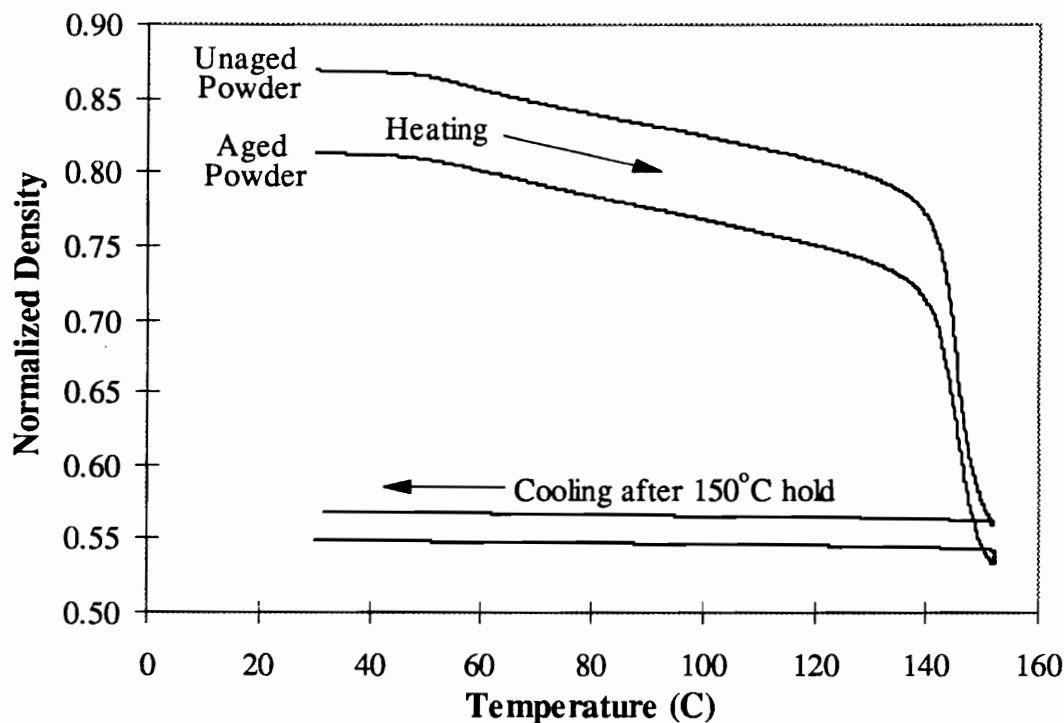


Figure 25 - Normalized density (fraction of theoretical density) estimated from TMA data for compacts formed from aged and unaged polycarbonate powder at room temperature at a compaction pressure of 80 MPa (compaction time: 5 min., compact mass: 1 gram, pressure exerted by probe: < 40 Pa (0.006 psi)).

in value, although the compact formed from the unaged powder still maintained a slightly higher density.

Table VII summarizes values of the transition temperature and the coefficients of thermal expansion above and below the transition during heating and during cooling for aged polycarbonate compacted at 40, 80, and 160 MPa. Consistent with Figure 25, these values are very similar, indicating that physically aging the powders prior to compaction does not significantly affect thermal expansion or recovery below the glass transition temperature.

Table VII - Summary of TMA thermal expansion data obtained on room temperature compacted aged polycarbonate powder (compaction time: 5 minutes, compact mass: 1 gram).

Compaction Pressure (MPa)	Coefficient of Thermal Expansion (x 10 ⁻⁶ m/m/°C)			Transition Temperature (°C)
	Initial Heating: Below Transition	Initial Heating: Above Transition	Cooling: Above & Below Transition	
40	120	1140	110	57
80	130	1200	110	59
160	130	1150	120	59

Table VIII - Summary of TMA recovery data obtained on room temperature compacted aged polycarbonate powder (compaction time: 5 minutes, compact mass: 1 gram).

Compaction Pressure (MPa)	Initial Normalized Density	Thickness Change @ 100 C (%)	Thickness Change @ 150 C (%)	Normalized Density after 110 C hold	Normalized Density after 150 C hold
40	0.75	7	40	0.70	0.50
80	0.82	8	47	0.76	0.52
160	0.85	7	49	0.79	0.53

Changes in thickness and normalized density at the 100°C and 150°C hold temperatures for these samples are included in Table VIII. The density data from Table VI and Table VIII have been plotted in the bar graph in Figure 26 for easier comparison between compacts made from unaged and aged powder. From this figure, it can be seen that as was true of altering the compaction pressure with the unaged powder, physical aging does not affect the factors that influence low temperature recovery, although it does affect recovery upon heating above T_g .

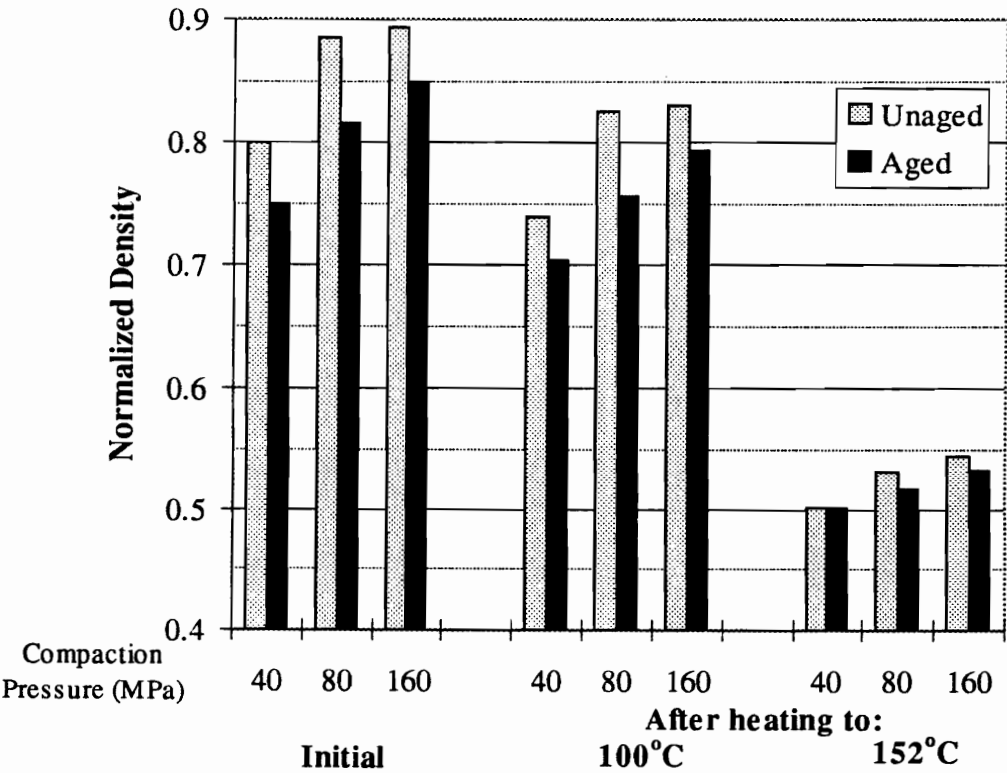


Figure 26- Effect of physical aging of polycarbonate particles prior to compaction on the dimensional changes during TMA analysis for compaction pressures of 40, 80, and 160 MPa (compaction time: 5 minutes, compact mass: 1 gram, TMA load: < 0.2 kPa (0.03 psi)).

Dynamic Sintering of Semicrystalline Polymers

Nylon-11

Thermomechanical analysis was performed on Nylon-11 compacts formed at 160 MPa at room temperature. The estimated normalized density versus temperature curves are presented in Figure 27 for isothermal hold temperatures of 100°C, 150°C, and 180°C. Note that in the vicinity of the glass transition temperature (50°C), the slope of the curves changed drastically, due to an apparent increase in the coefficient of thermal expansion.

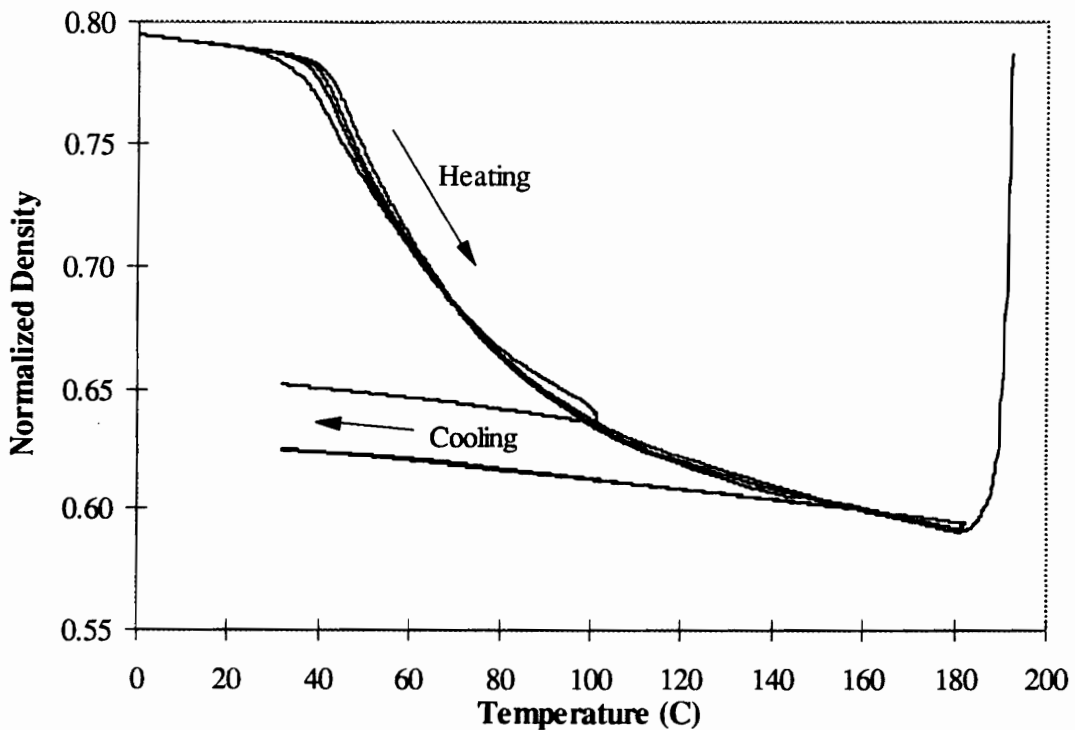


Figure 27 - Estimated normalized density (fraction of theoretical density) during TMA testing of Nylon-11 compacts formed at room temperature for isothermal hold temperatures of 100, 150, and 180°C (compaction pressure: 160 MPa, compaction time: 5 minutes, compact mass: 1 gram, pressure exerted by probe: < 40 Pa (0.006 psi)). Testing was performed 24-30 hours after the compaction pressure was removed.

Several similarities can be seen when comparing the Nylon-11 data in Figure 27 and polycarbonate data from Figure 21b: (1) the expansion above the glass transition temperature is irreversible, with the density of the Nylon-11 compacts dropping from 79% of the theoretical density to about 65% theoretical density after heating to 100°C, (2) the thermal expansion coefficient (or slope of density versus temperature curve) measured upon initial heating at low temperatures was very close to that exhibited during cooling, suggesting that the expansion consists of a reversible and irreversible component, and (3) only very small changes in density were observed during the isothermal holds, as expansion was fast relative to the time scale of the test.

Unlike polycarbonate, Nylon-11 must be heated well above its glass transition temperature to achieve the largest drop in density, due to reinforcement provided by the crystalline phase (which has a peak melting temperature of 190°C). After heating the compacts to 100°C (or 50°C above T_g) the minimum possible density had not yet been reached. Upon heating to 150°C, small drops in density occurred, although no further change was noted when heating to 180°C. The lowest recorded density in the Nylon-11 compacts was about 59% of the theoretical density, compared to a tap density of 56% for the powder. Heating to an isothermal hold temperature of 200°C resulted in bulk flow of the Nylon-11, which erroneously made the sample appear to densify at this temperature. In the case of (amorphous) polycarbonate, heating 10°C above the glass transition temperature was sufficient to obtain the lowest density, which was also comparable to the tap density of the

powder. Decreases in density above the bulk T_g of Nylon-11 are most likely to be the result of a broader glass transition and the reinforcement caused by the presence of crystallinity.

An interesting feature of the Nylon-11 density versus temperature curves is an inflection point where the change in density with temperature decreases at higher temperatures. This indicates that fewer chains are participating in the recovery process at higher temperatures, as they have already been heated above their effective glass transition temperatures. Densification mechanisms, such as cold crystallization and neck formation and growth, may also be affecting the slope of the curves above T_g , but probably to a much lower extent. Neither significant neck growth nor development of crystallites shared by particles are believed to have occurred during these tests, as the TMA samples were extremely weak and crumbly when removed from the test apparatus.

Poly(ether ether ketone)

Thermomechanical analysis was performed on PEEK compacts formed at 80 MPa at room temperature. Figure 28 shows the estimated normalized density versus temperature curves for isothermal hold temperatures of 100°C, 150°C, and 180°C. Note that the scale on the graph covers a much smaller range of normalized density than did the previous TMA curves for other compacts, as PEEK exhibited much less expansion during testing, with a

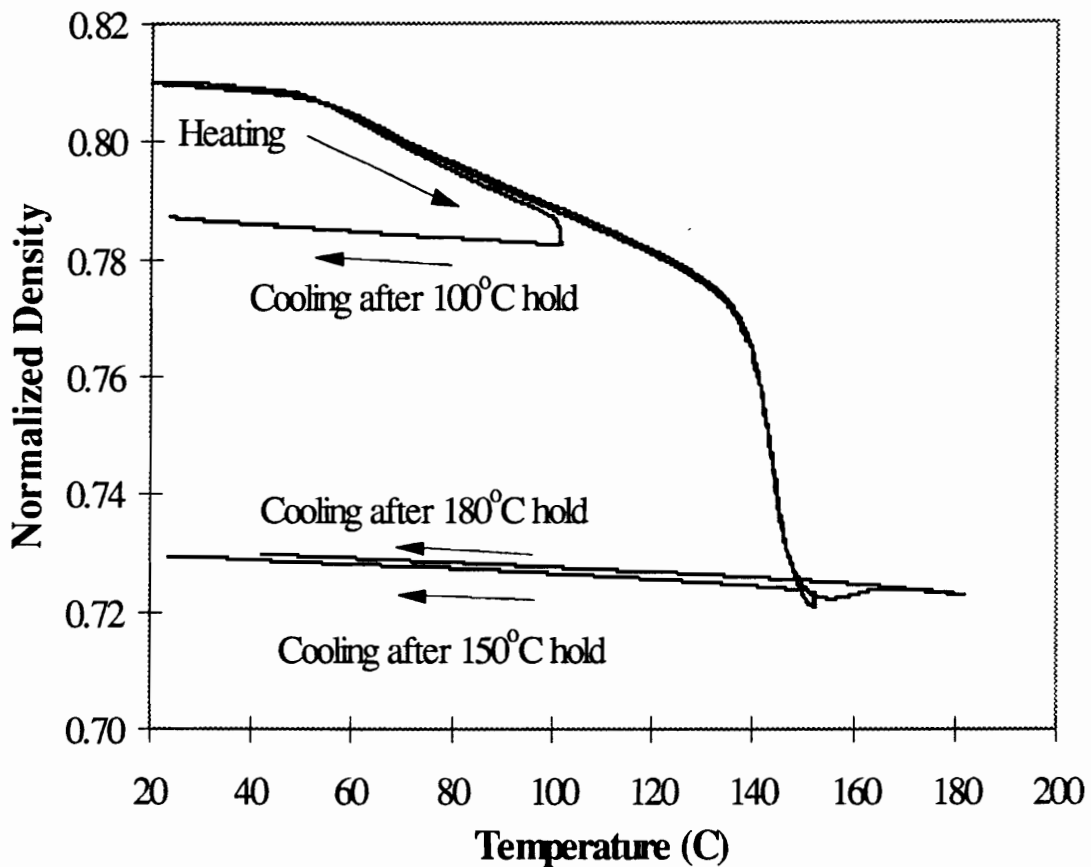


Figure 28 - Estimated normalized density (fraction of theoretical density) during TMA testing of PEEK compacts formed at room temperature for isothermal hold temperatures of 100, 150, and 180°C (compaction pressure: 80 MPa, compaction time: 5 minutes, compact mass: 1 gram, pressure exerted by probe: <40 Pa (0.006 psi)). Testing was performed 24-30 hours after compaction pressure was removed.

maximum drop in density of less than 10% of the theoretical density. The fact that PEEK expanded less during TMA testing than did polycarbonate and Nylon-11 suggests that less particle deformation and more particle rearrangement occurred during the compaction of PEEK particles, as PEEK has a lower volume fraction of amorphous phase compared to

polycarbonate and a higher modulus and yield strength than both polycarbonate and Nylon-11 (see Tables II-IV).

From Figure 28, it can be seen that PEEK, like polycarbonate and Nylon-11, exhibits irreversible expansion when heated above 50°C, as is evident by the change in slope of the density versus temperature curve. The fact that this temperature is approximately constant for the three different polymers suggests that the temperature at which expansion becomes irreversible is affected by recovery during storage following compaction. Had the storage time or temperature been significantly decreased, it is likely that the transition temperature would have been lower. In fact, significant variations in transition temperature (up to 10°C) were noted in polycarbonate compacts stored for different amounts of time (in the range of 10 minutes to several days) at room temperature. This observation prompted the standardization of the “rest” time prior to TMA testing to approximately 24 hours, when the transition temperature was no longer highly dependent on storage time at room temperature.

An interesting feature of the TMA curve for PEEK is the small increase in density which starts near PEEK’s glass transition temperature (145°C) during heating and continues in the specimen held isothermally at 150°C during the hold period and in the specimen held at 180°C during continued heating above 150°C. This small change can be attributed to

cold crystallization occurring in the PEEK, which apparently was not fully crystallized prior to the start of the TMA test.

Discussion

The results from this portion of the study have shown that the reason pressureless sintering has been largely unsuccessful in the past is due to recovery of the deformation caused by compaction. Recovery begins at temperatures well below the glass transition temperature and becomes very large at temperatures above T_g . Room temperature compaction pressures can create large degrees of “plastic” deformation in the particles, as shown in Figure 9. However, when the deformed particles are heated just above the glass transition temperature, the time constants for motion of the polymer chains increase rapidly. Plastic strains that could not be recovered in reasonable time scales at room temperature can suddenly diminish above T_g in the absence of an applied pressure, and the particles can come close to recovering their original shapes. (Note that if the compacts are heated well above T_g , neck formation and growth will begin to occur, as the reduction of surface area acts as a driving force for particle coalescence.)

The dimensional recovery of room temperature compacted particles at temperatures above T_g can be explained in terms of rubbery elasticity. For rubbery materials, the loss of configurational entropy upon deformation raises the energy of the system. An entropic force opposes the deformation and acts to lower the system energy. When the external

force causing the deformation is removed, the entropic force causes dimensional recovery in the rubbery state.

Room temperature compaction of polycarbonate powder causes a large amount of localized deformation, which increases its configurational entropy. Because the polycarbonate is glassy at room temperature, the molecules have virtually no mobility to return to their equilibrium, random coil-like configurations. However, since the average molecular weight of the polycarbonate is above that of the critical molecular weight for entanglements, it behaves as a rubber above the glass transition temperature, with the entanglements forming the rubbery network. When heated above T_g in the absence of a compaction pressure, the driving force to increase configurational entropy aids the particles in approaching their original shapes, thereby, greatly reducing the beneficial effects of room temperature compaction. To make compaction and coalescence of polymer powders a viable processing method, the dimensional recovery of the particles exhibited above T_g must be reduced.

One might argue that dimensional recovery in the compacts studied here is driven by a lowering of the total energy in the particles due to a reduction in surface area as opposed to entropic recovery. However, the decrease in energy due to changes in the surface area of the particles in these compacts is insignificant compared to that caused by the increase in configurational entropy, because the particles are relatively large (an average of 90 μm)

and the particles do not change shape drastically enough during compaction to greatly affect the total surface area.

To demonstrate that configurational entropy is, in fact, the predominant driving force for recovery in this study, compaction and recovery experiments were performed on 2.54 cm (1 inch) diameter extruded polycarbonate rod, which has minimal surface area compared to the compacts formed from the polycarbonate powder. The rod was cut into 2.54 cm (1 inch) long pieces and compressed at room temperature (in the Carver Laboratory Press) to a final length of 1.27 cm (0.5 inches), then heated up to 170°C for 30 minutes in a vacuum oven at ambient pressure.

Figure 29 shows typical pieces of rod before compaction, after compaction, and after heating. Note that the bulk rod recovers its original shape when heated above T_g , as did the compacts. Since a reduction of surface area in the rod could not have driven recovery, one can conclude that configurational entropy must be the predominant driving force.

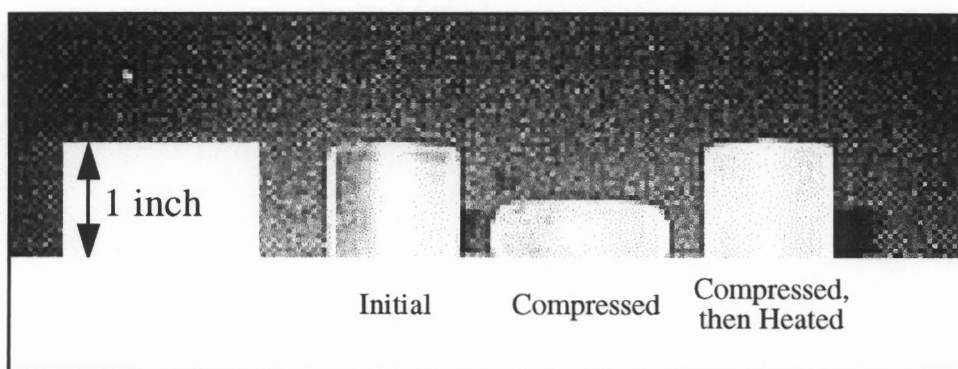


Figure 29 - Extruded polycarbonate rod as cut, after compression to 50% of original length, and after recovery at 170°C for 30 minutes.

Summary

Pressureless sintering was performed on polycarbonate powder compacted at room temperature. It was found that all PC compacts exhibited irreversible expansion when heated to temperatures even well below the glass transition. Thermomechanical analysis was used to study this recovery process, which began at temperatures as low as 50°C. The transition between reversible thermal expansion and irreversible recovery is marked by a large increase in the coefficient of thermal expansion and was found to be affected by the storage time following removal of the compaction pressure.

When the compacts were further heated above the glass transition (140-150°C), they rapidly expanded and had densities approaching that of the tap density of the powder, with increases in thickness of up to 55% observed. If heated well above the glass transition temperature (180°C), the compacts began to densify during thermomechanical analysis, aided by the very small pressure exerted by the probe.

Physical aging causes an increase in yield strength, and crystallinity reduces the volume fraction of amorphous material and improves mechanical properties the semicrystalline polymers studied relative to those of polycarbonate. Both physical aging and crystallinity resulted in lower green density for a given compaction pressure and sometimes caused a noticeable reduction in the handling strength of the compacts. The decrease in green density and strength and decrease in recovery during sintering were caused by a decrease

in particle deformation in the compacts formed from the physically aged polycarbonate and the semicrystalline polymers compared to that which occurred in the compacts formed from unaged polycarbonate.

The relative difference between the glass transition temperature and the compaction temperature were found to affect time-dependent recovery following removal of the compaction pressure. Polycarbonate and PEEK, which were compacted well below T_g during room temperature compaction, did not exhibit the time-dependent recovery noted in the Nylon-11, which had a T_g just above room temperature.

Possible Ways to Improve the Compaction and Sintering Processes

From a review of the literature and results presented in this chapter, it was apparent that pressureless sintering of room temperature compacted polymers at relatively low temperatures (just above the glass transition temperature of amorphous polymers or melting temperature of semi-crystalline polymers) is not feasible. When thermoplastic polymers are compacted at room temperature, they deform both plastically and viscoelastically, with dimensional changes observed upon removal of the room temperature compaction pressure or upon heating of the compact to relatively low temperatures.

Possible methods of controlling particle recovery during sintering are *hot compaction* (compacting the powder at elevated temperatures) and *consolidation* of room temperature

compacted powders (heating just above the glass transition temperature with a very small applied pressure to combat recovery). Hot compaction has been investigated by several groups of researchers [2,6,13,14] and was found to improve green strength and density (refer to the Literature Survey for a description of this research), but its affect on post-sintering properties was not studied. Consolidation of room temperature compacted polymer powders has not yet been discussed in the literature.

Based on previously discussed arguments, it was not expected that hot compaction would improve sintered properties unless it was performed at temperatures at or above the glass transition region, as low configurational entropy would continue to drive particle recovery upon heating above T_g . If such high compaction temperatures were required, then hot compaction would offer little advantage over conventional hot pressing of polymer powders. Therefore, the experimental studies on hot compaction were confined to compaction temperatures below T_g .

Consolidation of room temperature compacted polymer powder, on the other hand, could be shown to offer processing advantages if it was found that relatively low consolidation temperatures and pressures were required to eliminate particle recovery. Since dimensional recovery occurred in such a short period of time relative to the amount of time that would be needed for reptation and healing to occur, a short consolidation step just above T_g (with a small applied pressure) followed by a higher temperature, pressureless “annealing” stage would make a reasonable processing method.

Both hot compaction and consolidation were investigated using the LPC3000 polycarbonate powder, and the experimental results are summarized and discussed in the next two chapters.

VI. Hot Compaction of Polycarbonate Powder

Hot compaction experiments were performed on the LPC3000 polycarbonate powder to study the effect of compaction temperature on green and sintered properties, including density, porosity, and strength. Further experiments examined the effect of hot compaction temperature and pressure on dimensional recovery during isothermal and dynamic sintering.

Hot Compaction of Polycarbonate Powder

Polycarbonate compacts were formed over a range of pressures at compaction temperatures of 100°C and 125°C. In Figure 30, normalized green density is plotted as a function of compaction pressure at these compaction temperatures, along with the room temperature data from Figure 9. All densities were obtained using the Archimedes technique, and each point represents the average density of three samples.

From Figure 30, it can be seen that compaction temperature strongly influenced green density. The largest effects were observed at the lower compaction pressures, where differences of up to 20% of the theoretical density were measured between the compacts formed at room temperature and 125°C. As the compaction pressure was increased, differences between the green density obtained at room temperature and elevated temperatures decreased. At 160 MPa, hot compaction yielded a normalized density about 5% of the theoretical density higher than did room temperature compaction. At high

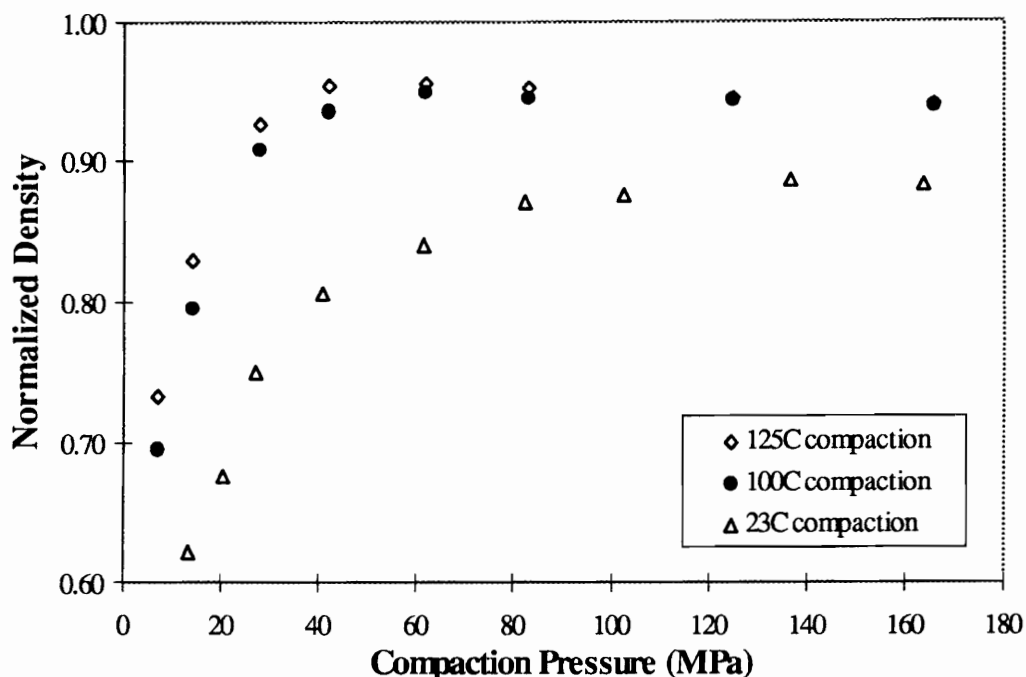


Figure 30 - Effect of compaction temperature on the normalized density of polycarbonate powder as a function of compaction pressure and temperature (preheat time: 5 minutes, compaction time: 5 minutes, compact mass: 1.5 grams). Each point represents the average density of three compacts. The maximum standard deviation was less than 0.4 and 0.7% normalized density for the hot and room temperature compaction data, respectively.

compaction pressures (greater than 60 MPa), the compacts formed at 100°C and 125°C samples had very similar densities.

Increasing the compaction temperature lowered the particle yield strength, and, therefore, affected the relative amounts of particle rearrangement and deformation that occurred during compaction. Differences in density brought about by changing the compaction temperature were similar to those observed by altering the state of physical aging, as was

discussed earlier. As was shown in Figure 10, the density of compacts made from unaged polycarbonate powder was higher at all compaction pressures than the density of compacts made from aged powder. This was attributed to the lower yield strength of the unaged particles, which allowed more particle deformation to occur at a given compaction pressure. When comparing ESEM micrographs of the fracture surfaces of room temperature compacted polycarbonate, previously shown in Figure 12a, and (unaged) polycarbonate compacted at 125°C, shown in Figure 31, it is obvious that more particle deformation had, in fact, taken place in the hot compacted polycarbonate.

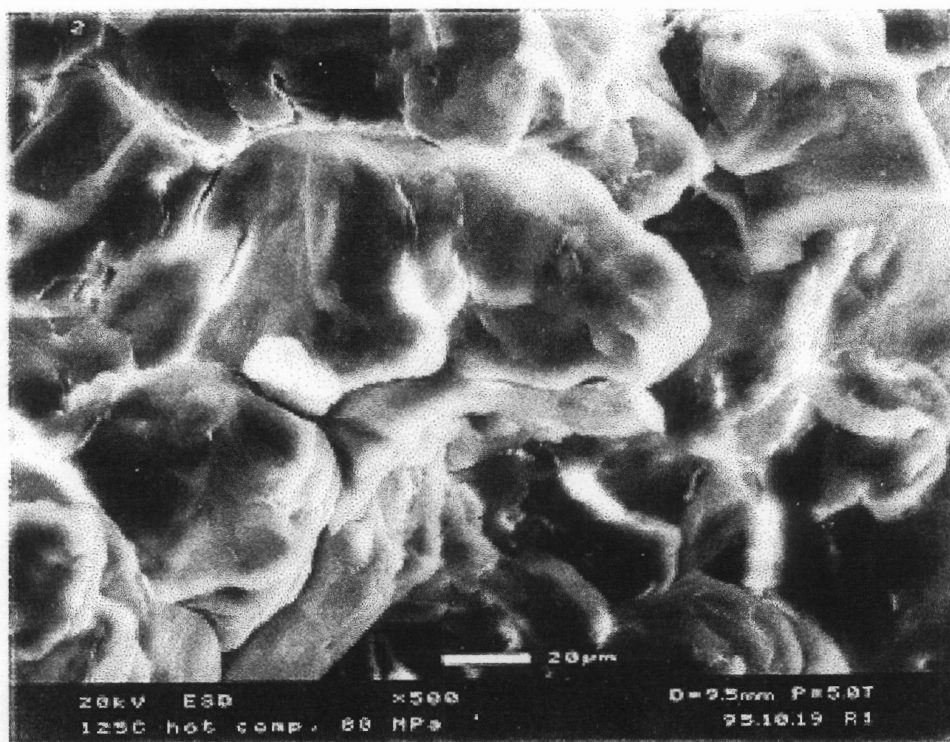


Figure 31- ESEM micrograph of polycarbonate compact formed at 125°C using unaged powder. (compaction time: 5 minutes, compact mass: 1.5 grams, compaction pressure: 80 MPa, green density: 96% of the theoretical density of polycarbonate).

Note that the density of the hot compacted polycarbonate peaks at moderate pressures (40 MPa for 125°C and 60 MPa for 100°C) and decreases very slightly at higher pressures. This small decrease in density is not a result of increased closed porosity, as might be expected. All compacts were found to have closed porosity values of less than 0.3% by volume. Similar decreases in the density of hot compacted polyphenylene sulfide were reported by Mokashi and Jog [13] at high compaction pressures.

A possible explanation for the slight decrease in density with hot compaction pressure is that the densification of polycarbonate compacts is more time-dependent at 100°C and 125°C than it was at room temperature. The density at the moderate pressures may be increasing with time as the particles flow to fill in voids that are present after the compaction pressure has been applied. At the highest compaction pressures, a larger component of hydrostatic pressure may be preventing some of this flow from occurring once the compaction pressure has been applied.

This suggests that the plastic deformation mechanism shown in Figure 11 contributes more to densification at moderate compaction pressures than at higher pressures, while bulk compression takes the place of plastic deformation at the higher compaction pressures. To determine if this is true, one could change the rate at which the pressure is applied at the highest compaction pressures. If the density increased as the loading rate was decreased, this would indicate that the above explanation is correct.

Isothermal Pressureless Sintering of Hot Compacted Polycarbonate

The normalized density of hot compacted polycarbonate compacts was measured as a function of pressureless sintering time at 165°C (about 20°C above T_g) for the 100°C and 125°C compaction temperatures and a compaction pressure of 80 MPa, to examine the effect of compaction temperature on recovery. These experiments were repeated for pressures of 40 MPa and 160 MPa for the 125°C compaction temperature to study the effect of hot compaction pressure on recovery. Three different specimens were tested at each time and compaction pressure. As was mentioned earlier, sintering was performed using the hot press for test times less than one hour and the vacuum oven for sintering times of one hour and greater, possibly causing a shift in the data between the 10 minute and 60 minute data points.

Effect of Compaction Temperature on Sintered Density

Normalized density is plotted in Figure 32 as a function of sintering time for compacts formed at 80 MPa at 100°C and 125°C, along with the results previously reported for polycarbonate compacted at room temperature at the same compaction pressure (from Figure 18). As was true in the case of the room temperature compacted polycarbonate, the density of the hot compacted polycarbonate quickly dropped upon heating above T_g . Within the first few minutes at 165°C, the density of all compacts reached a minimum, with higher compaction temperatures resulting in higher densities measured after 5 minutes at 165°C.

The sintered densities of compacts formed at 125°C were over 10% of the theoretical density larger than those formed at room temperature, demonstrating that altering the compaction temperature can have lasting effects on density. The compacts pressed at 125°C had normalized densities up to 5% of the theoretical density greater than those formed at 100°C after sintering, even though the initial densities were almost identical. This indicates that even though the initial densities were the same, the morphologies and/or states of residual stress of the compacts were not.

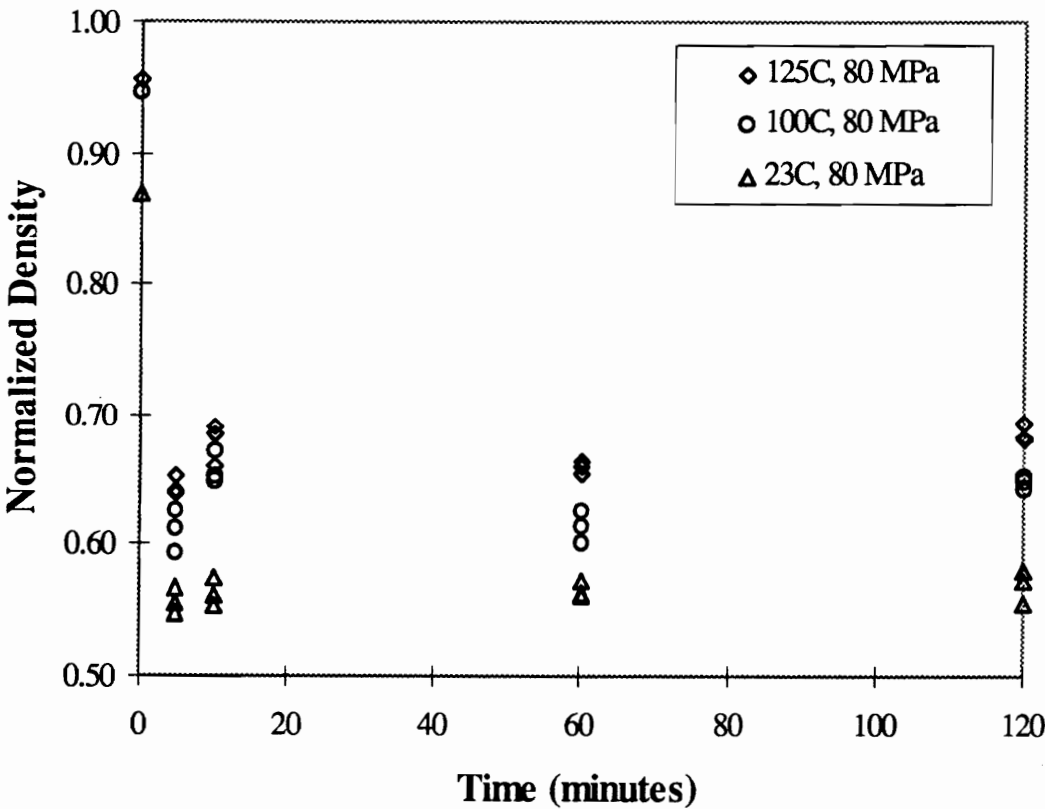


Figure 32 - Effect of compaction temperature on the normalized density of polycarbonate compacted at 80 MPa during pressureless sintering at 165°C (compaction time: 5 minutes, compact mass: 1.5 grams).

Despite the fact that raising the compaction temperature resulted in improvements in sintered density, compacting at elevated temperatures below T_g did not entirely eliminate dimensional recovery, as the polymer molecules still existed in non-equilibrium, low configurational entropy conformations following compaction. In an earlier discussion, it was noted that in order to entirely eliminate recovery, compaction would have to be performed above T_g .

Effect of Compaction Pressure on Sintered Density

In Figure 33, normalized density is plotted as a function of sintering time for compacts formed at 125°C at pressures of 40, 80, and 160 MPa. From this figure, it can be seen that the hot compaction pressure does not have nearly as large an effect on the sintered density as did the compaction temperature for compaction pressures of 40 MPa or larger. These results suggest that by 40 MPa, the majority of deformation that can occur during hot compaction at 125°C has taken place. Further increases in pressure led to bulk compression of the compact rather than localized yielding at the contact points.

Microstructural Changes during Pressureless Sintering

To examine the effect of pressureless sintering on the microstructure of hot compacted polycarbonate, a compact comparable to the one shown in the ESEM micrograph in Figure 31 was formed by hot compacting at 125°C and 80 MPa. It was then isothermally

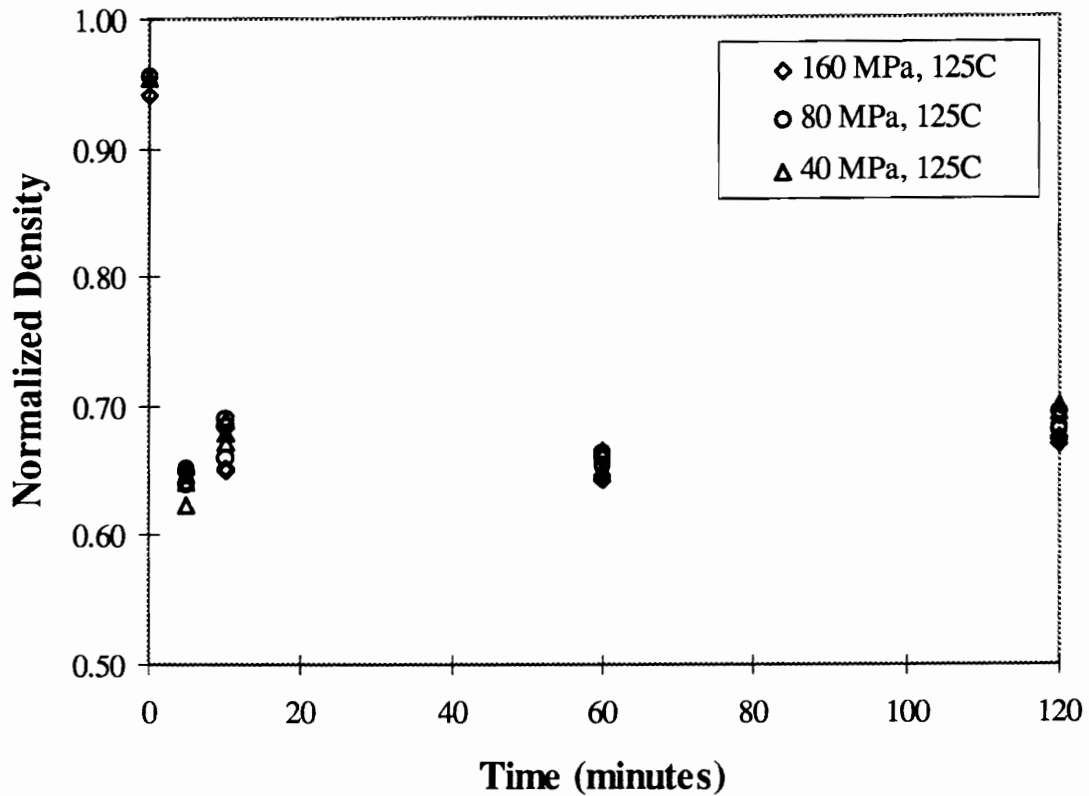


Figure 33- Effect of compaction pressure on the normalized density of polycarbonate compacted at 125°C during pressureless sintering at 165°C. (compaction time: 5 minutes, compact mass: 1.5 grams).

sintered at 165°C in the hot press for 20 minutes with no applied pressure. The ESEM micrograph in Figure 34 shows the resulting microstructure of the cryogenically fractured surface.

As was the case with room temperature compacted polycarbonate (Figure 19), mechanical interlocking between the particles has been lost during sintering, and the particles have recovered much of their original shape. A major difference between the room temperature



Figure 34- ESEM micrograph of polycarbonate compact hot compacted at 125°C made from unaged powder following pressureless sintering for 20 minutes at 165°C (compaction time: 5 minutes, compact mass: 1.5 grams, compaction pressure: 80 MPa, density prior to sintering: 96% of the theoretical density of polycarbonate.)

and 125°C compacts is the much larger number of contact points evident in the hot compacted polycarbonate (Figure 34) following sintering. From these micrographs and the data from Figure 32, one might conclude that the improvements in sintered density in the hot compacted polycarbonate resulted from strength developed at the necks between the particles prior to large-scale recovery, as opposed to differences in the configurational

entropy of the room temperature and elevated temperature compacted polycarbonate. To examine this hypothesis, microtensile strength tests were performed on polycarbonate compacts subjected to various processes.

Effect of Processing on Microtensile Strength

Although the green strength of the polycarbonate compacts was fairly low, by carefully cutting out tensile bars from the compacts with a single-edged razor blade, tensile strengths could be estimated at various stages of processing. A summary of the average yield strength for 5 specimens at each stage of processing is presented in Figure 35. For comparison, the average strength of bulk polycarbonate film made from the same powder was 60 MPa as-processed (unaged) and 75 MPa following physical aging.

Note that the polycarbonate compacts formed from aged and unaged polycarbonate powder at room temperature had very low strengths of 0.7 MPa and 1.3 MPa, respectively. The green strength of the compacts formed at room temperature results from mechanical interlocking between the particles caused by non-elastic deformation. Because physical aging increases the yield strength of polycarbonate, less particle deformation occurs for a given compaction pressure in aged powder, and as expected, the green strength is lower than in compacts formed from unaged powder.

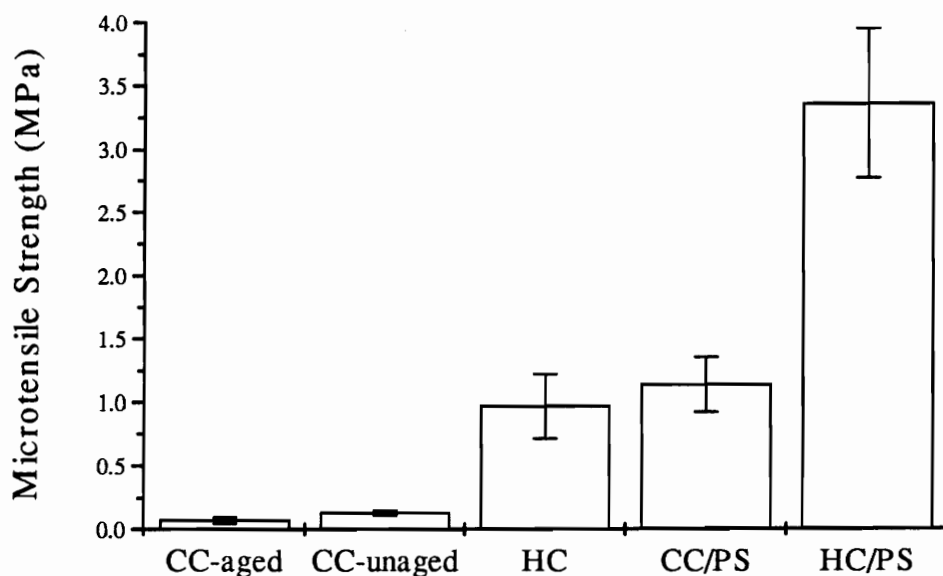


Figure 35 - Microtensile strengths of polycarbonate compacts at various stages of processing: CC - cold (room temperature) compacted, HC - hot compacted at 125°C, PS -following pressureless sintering for 20 minutes at 165°C, aged - powder aged before compaction. (compaction pressure: 160 MPa for all specimens; all powder unaged prior to compaction unless otherwise noted)

When the compaction temperature was raised to 125°C, the tensile strength of the compacts increased by an order of magnitude. Since this temperature is too low to cause diffusion of chains across particle interfaces during the 5 minute compaction time, the increase in strength can be attributed to an increase in particle deformation and mechanical interlocking. This is consistent with the findings for the room temperature compacted aged and unaged powder, with an increase in yield strength and modulus due to physical aging resulting in less deformation and lower green strength. For the hot compacted

polycarbonate, raising the compaction temperature had a similar effect on deformation and green strength due to the lowering of the yield strength and modulus with temperature.

Although pressureless sintering (for 20 minutes at 165°C) was found to greatly decrease density, microtensile tests showed that it did, in fact, raise tensile strength. In contrast with the hot compacted polycarbonate, the order of magnitude increase in strength over room temperature compacted polycarbonate was a result of neck formation and growth between the particles during pressureless sintering. These necks were observed in the ESEM micrographs in Figure 19, which showed the fracture surface of room temperature compacted polycarbonate following pressureless sintering. Note that in the sintering of metallic and ceramic powders, higher density is generally an indication of higher strength. Based on results from this study, this is definitely not true of polymers.

If neck formation and growth were responsible for increases in strength, then the more necks present, the higher the sintered strength should be. Since a much larger number of necks was evident in the hot compacted polycarbonate (Figure 34) than the room temperature compacted polycarbonate (Figure 19) following pressureless sintering, the hot compacted/pressureless sintered compacts should have an even higher strength. From Figure 35, it can be seen that this is indeed true. Raising the compaction temperature to 125°C increased the sintered strength by a factor of 3.

Dynamic Sintering of Hot Compacted Polycarbonate

Thermomechanical analysis was performed on hot compacted polycarbonate formed under the same compaction conditions as the compacts that were isothermally sintered at 165°C. As with the previous TMA tests on room temperature compacted polycarbonate, the samples were heated at a rate of 5°C/minute and subjected to the various hold temperatures for 20 minutes, prior to being cooled at about 5°C/minute.

Effect of Compaction Temperature on Recovery

Figure 36 shows plots of the change in estimated normalized density versus temperature for (unaged) polycarbonate powder compacted at room temperature, 100°C, and 125°C at a pressure of 80 MPa. An isothermal hold temperature of 150°C was used for all three specimens. From this figure it can be seen that compaction temperature greatly affects the temperature at which recovery becomes irreversible (evident by a change in the slope of the density versus temperature curves). The transition temperature was about 50°C for the compact formed at room temperature, 100°C for compacts formed at 100°C, and 125°C for compacts formed at 125°C.

As noted earlier, dynamic sintering tests were performed about 24 hours after the compaction pressure was removed from each specimen. It is possible that if the room

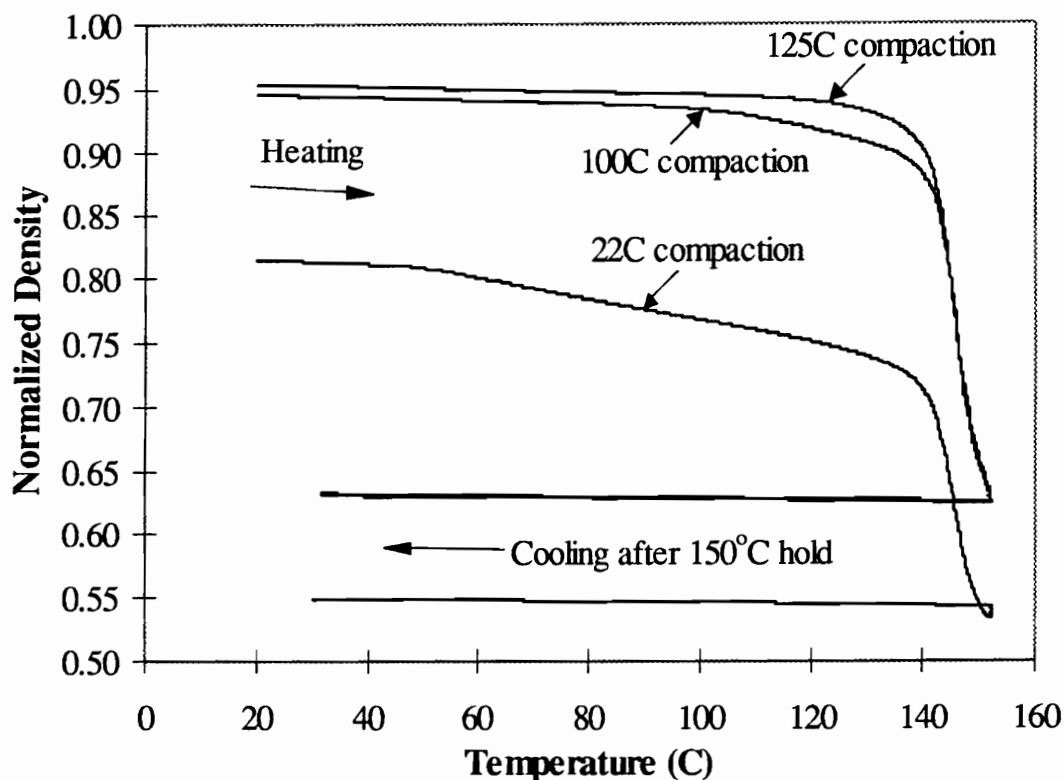


Figure 36 - Normalized density (fraction of theoretical density) estimated from TMA data for compacts formed from unaged polycarbonate powder at room temperature, 100°C, and 125°C at a compaction pressure of 80 MPa (compaction time: 5 min., compact mass: 1 gram, pressure exerted by probe: < 40 Pa (0.006 psi)).

temperature compact was tested immediately after the pressure was removed, the transition to irreversible recovery may have been much closer to room temperature. In fact, significant decreases in the transition temperature (up to 10°C) were observed when the rest time prior to testing was shortened to a under an hour. This finding supports the idea that although the glass transition temperature of the bulk compact is unchanged following compaction, very small localized areas of high deformation have locally reduced

glass transition temperatures. This allows them to recover at temperatures well below the bulk glass transition temperature range in relatively short periods of time (hours at room temperature).

When the specimens were heated to higher temperatures, the compacts formed at 100°C and 125°C followed very similar density versus temperature curves, exhibiting large-scale recovery just above the glass transition temperature (142°C). Final densities for the two were very similar and were estimated to be about 63% of the theoretical density of bulk polycarbonate.

Note that the dynamic sintering results in Figure 32 do not exactly match the “isothermal” sintering results in Figure 32, in part because the heating rates were much slower (and more controlled) in the dynamic sintering experiments and the hold temperature was 150°C for the data in Figure 36 instead of 165°C. However, both the isothermal and dynamic experiments did show a higher final density when the compaction temperature was raised to 100°C or 125°C compared to that measured for room temperature compacted polycarbonate. In both cases, the hot compacts had sintered densities about 10% higher than the room temperature compacts formed at the same compaction pressure.

Effect of Compaction Pressure on Recovery

Figure 37 shows plots of the change in estimated normalized density versus temperature for (unaged) polycarbonate powder compacted at 100°C at compaction pressures of 40, 80, and 160 MPa. The isothermal hold temperature for these tests was once again 150°C. Unlike the compaction temperature, the compaction pressure did not have a large effect on recovery during dynamic sintering for the range of pressures studied. Small differences in initial density persisted up to the glass transition region, when large-scale recovery began to occur. The compacts formed at the different pressures followed almost identical

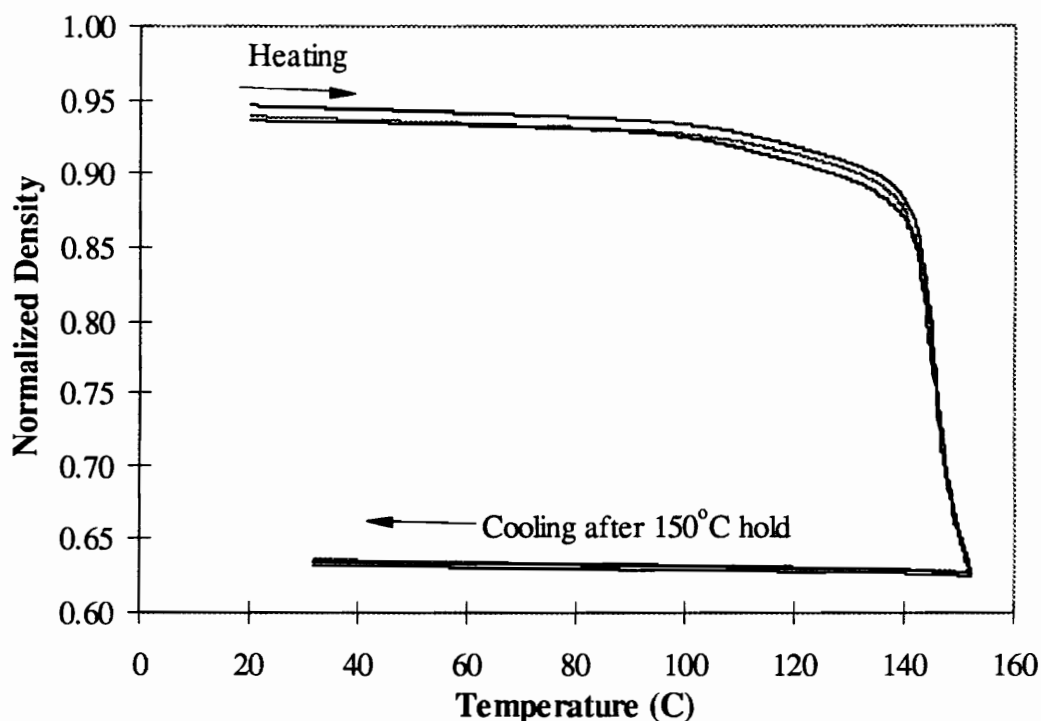


Figure 37 - Normalized density estimated from TMA data for compacts formed from unaged polycarbonate powder at 100°C at compaction pressures of 40, 80, and 160 MPa (compaction time: 5 min., compact mass: 1 gram, pressure exerted by probe: < 40 Pa (0.006 psi)).

cooling curves, with no significant variations in final density observed between the specimens.

Results obtained for polycarbonate compacted at 125°C at 40, 80, and 160 MPa (which are not shown) were very similar, with compaction pressure having an insignificant effect on the cooling curve and final density. These findings support the conclusion previously made (based on isothermal sintering results) that the majority of particle deformation takes place in polycarbonate by 40 MPa at the elevated compaction temperatures. Above this pressure, bulk (elastic) compression of the compact is the major source of deformation.

Summary

Hot compaction was found to greatly increase the green density of polycarbonate compacts by allowing more particle deformation to take place at a given compaction pressure. Raising the compaction temperature to 100°C or 125°C increased the density of compacts subjected to pressureless sintering at 165°C, however, it did not eliminate the majority of the dimensional recovery in the compacts. Hot compaction pressure did not have a large effect on green or sintered density above 40 MPa, as bulk compression of the compact, rather than localized yielding, primarily takes place above this pressure.

Microtensile strength tests showed that cold compacted polycarbonate had the lowest tensile yield strength. Raising the compaction temperature to 125°C or performing

pressureless sintering for 20 minutes at 165°C raised the strength of cold compacted polycarbonate by an order of magnitude, but for different reasons. Increasing the compaction temperature resulted in more particle deformation and mechanical interlocking, while performing pressureless sintering allowed the development of necks between particles. The highest strength was obtained by sintering the hot compacted polycarbonate. Results from these tests showed that unlike metallic and ceramic compacts, polymer compacts having the highest density do not necessarily have the highest strength.

It was concluded that the small improvements in sintered density through hot compaction resulted from a greater number of necks being formed between particles during sintering. However, to completely eliminate dimensional recovery, the compaction temperature would have to be increased to the glass transition temperature so that the polymer molecules would remain in their high entropy, equilibrium states following compaction. As mentioned earlier, compacting above T_g would not yield any processing advantages over conventional hot pressing of powders, so it was not a major focus of this study.

VII. Consolidation of Cold Compacted Polycarbonate

Polycarbonate compacts formed at room temperature were *consolidated*, or sintered with an applied pressure, in an attempt to reduce dimensional recovery upon heating above the glass transition temperature. One set of experiments was done on bulk compacts in the hot press (similar to the “isothermal” sintering tests) to examine the effect of consolidation pressure on compact density. “Dynamic” consolidation experiments were performed using thermomechanical analysis to simulate consolidation with known applied pressures and controlled temperature profiles. Although both of these experimental techniques have some limitations (see the Experimental Methods chapter), they were useful in predicting how polymer compacts would respond to sintering when a small pressure was applied.

Isothermal Consolidation of Polycarbonate Compacts

Polycarbonate compacts formed at room temperature at a compaction pressure of 80 MPa were consolidated for 15 minutes at an average temperature of approximately 165°C using the preheated bottom platen of the hot press. Preheated steel blocks of known mass were placed on top of the compacts as quickly as possible after the compacts were placed on the hot platen to provide heating and a fairly uniform consolidation pressure. As discussed in the Experimental Methods chapter, neither variations in the temperature across the thickness of the compacts nor variations in the consolidation pressure could be totally eliminated and were responsible for some non-uniformities in the consolidated compacts.

Figure 38 shows (a) the normalized density (measured using the Archimedes technique) and (b) the thickness as a function of consolidation pressure. At the smallest consolidation pressures (less than 5 kPa or 0.7 psi), almost no improvement had been made compared to the results obtained through pressureless sintering (Figure 18). However, as the consolidation pressure was raised to about 22 kPa (3.2 psi), dramatic improvements in the final densities and thickness changes were observed, with only a 5% increase in thickness (or decrease in percent theoretical density) measured.

It should be noted that the diameters of the compacts were measured before and after consolidation, and increases in the diameter were between 2% and 5% for all compacts, with a 2% increase in diameter common for compacts consolidated with no load or a very small load. This indicated that the consolidation pressures used in these experiments were not large enough to cause large-scale bulk flow of the compact.

Due to difficulties encountered in applying larger heated masses, the effects of consolidating at small, but higher pressures could not be investigated on the bulk compacts to determine what load would be required to totally eliminate recovery. However, based on the data in Figure 38, thickness increases should certainly be insignificant at a consolidation pressure of 50 kPa (7 psi), a very low pressure.

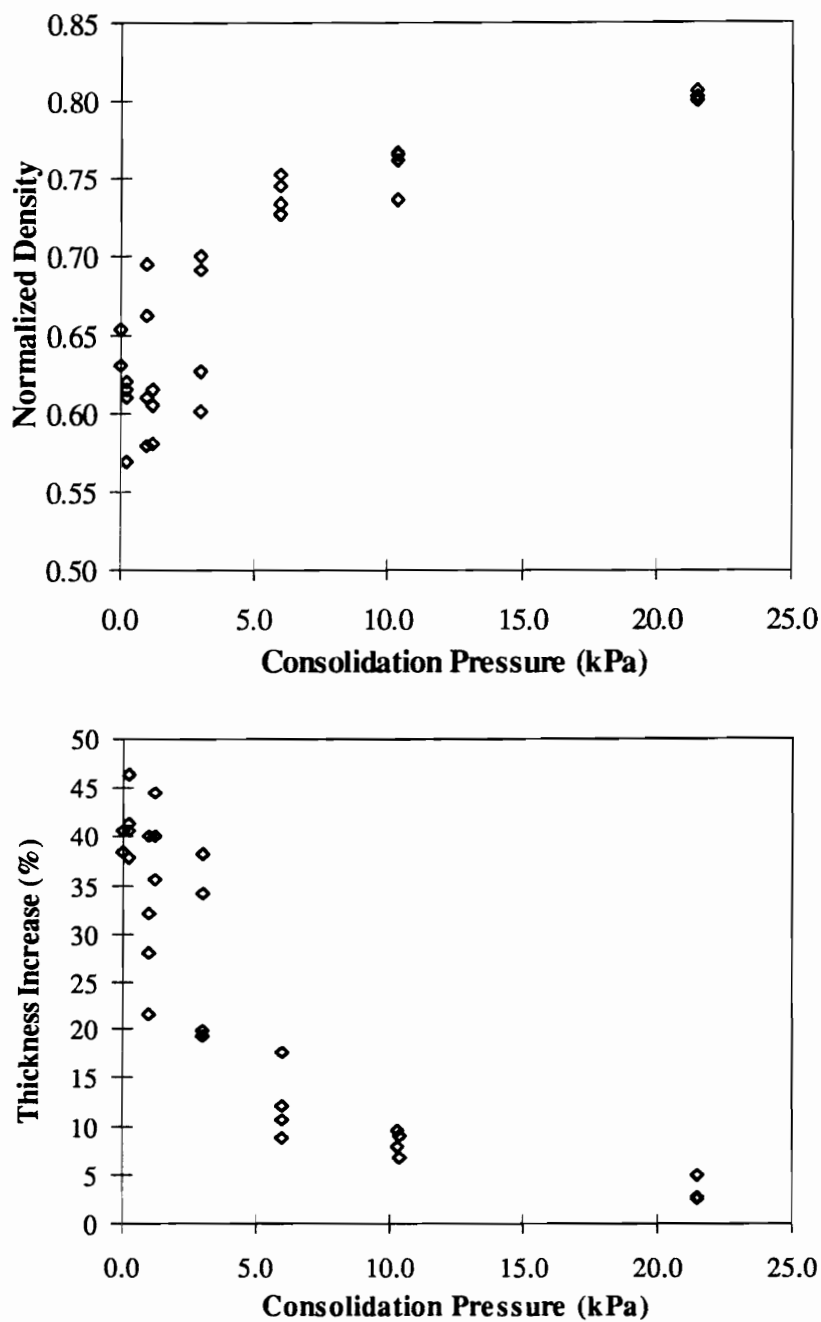


Figure 38 - Effect of consolidation pressure on the dimensional recovery of polycarbonate compacts consolidated at 162°C for 15 minutes following room temperature compaction at 80 MPa (compaction time: 5 min., compact mass: 1.5 grams, initial compact density: 87% of the theoretical density).

Dynamic Consolidation of Polycarbonate Compacts

Polycarbonate compacts formed at room temperature at a compaction pressure of 80 MPa were also subjected to dynamic consolidation using a controlled temperature profile with various applied pressures. As was the case with previous TMA tests, a heating rate of 5°C/minute was used to ramp up to the isothermal hold temperature, which was held for 20 minutes. Rather than using glass coverslips to distribute the load over the entire specimen, the probe alone was used to apply relatively large loads to an area of known, constant cross section in the center of each specimen. The data presented here are in the form of thickness change and temperature versus time plots, where the thickness changes and times have been shifted to zero at a temperature of 100°C for convenience.

Figure 39 shows the effect of consolidation pressure on the thickness increase during thermomechanical testing of polycarbonate compacts held isothermally at 152°C, which is about 10°C above the glass transition temperature. The actual temperature profile, which was the same for all scans, is included in this figure for reference. Note that large-scale recovery began when the specimen reached the glass transition temperature, at an adjusted time of approximately 8 minutes. The maximum thickness change, which was measured shortly after the glass transition temperature was exceeded, decreased with consolidation pressure from about 37% to 14%, for consolidation pressures of 4 kPa (0.6 psi) and 100 kPa (14.5 psi), respectively.

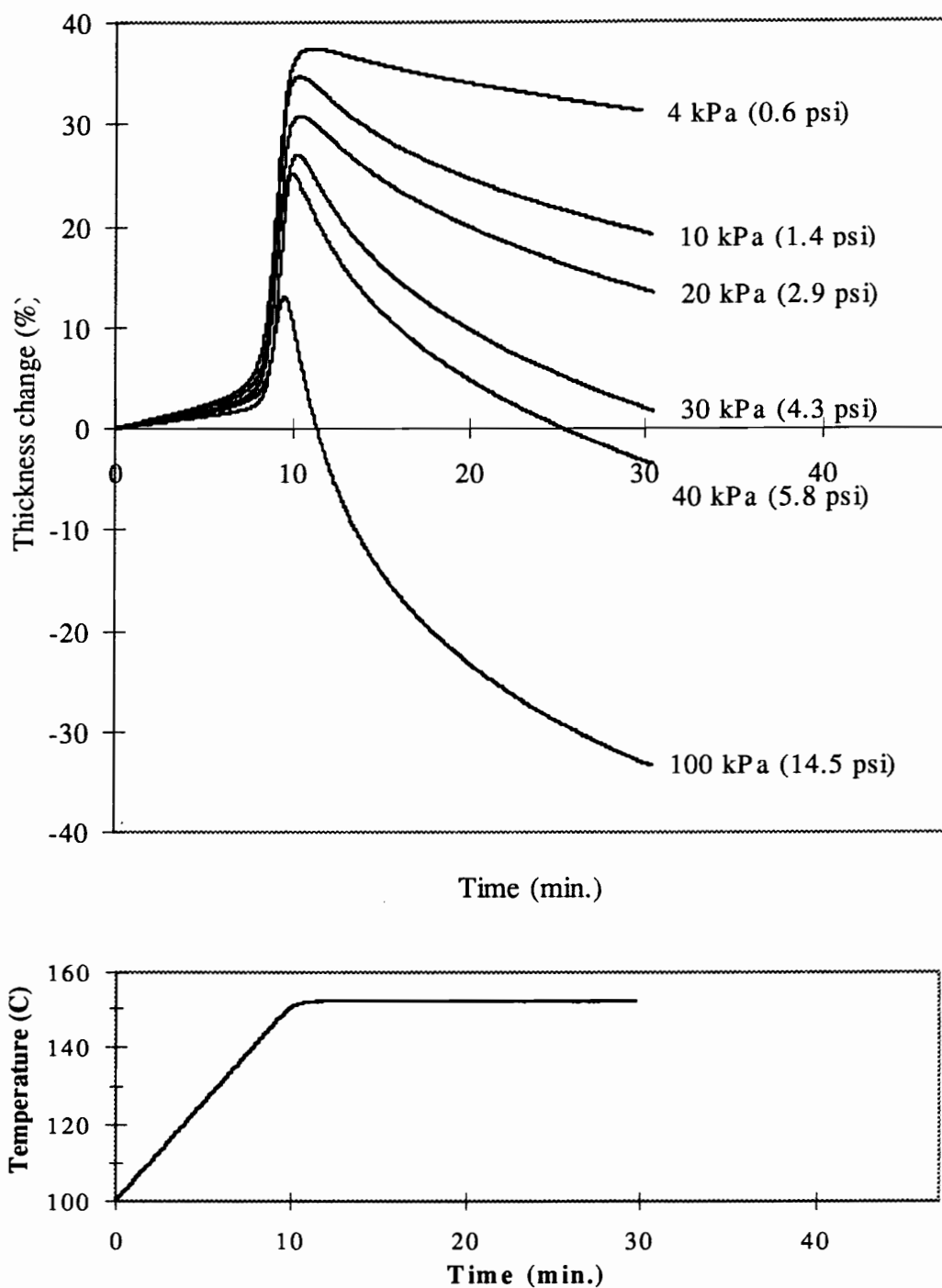


Figure 39 - Effect of TMA load on dimensional recovery during TMA scan with a 152°C isothermal hold and temperature profile as shown. (compaction pressure: 80 MPa, compaction time: 5 min., compact mass: 1 gram, initial compact density: 87% of the theoretical density).

At the highest consolidation pressure of 100 kPa, the thickness change becomes negative and large (-35%), much higher than would be necessary to achieve 100% of the theoretical density. This indicated that in addition to decreasing the thickness, large consolidation pressures can cause flow of the particles perpendicular to the direction of the applied load if no side support is provided. For dynamic consolidation tests, it is unclear at what load significant particle flow began to occur, however, in the isothermal consolidation tests previously described, very little flow was observed at consolidation pressures up to 22 kPa.

Note that each isothermal consolidation data point in Figure 38 is the equivalent of a point on a dynamic sintering curve in Figure 39 at an adjusted time of ~ 27 minutes (or 15 minutes after the isothermal hold temperature was reached). Although the isothermal data in Figure 38 suggest that expansion at T_g is proportional to the final thickness change, Figure 39 shows that the maximum expansion does in fact occur near T_g and that the final dimensions are affected by time-dependent deformation which occurs during the isothermal hold at temperatures above T_g .

Figure 40 shows data from dynamic sintering tests performed on polycarbonate compacts at an isothermal hold temperature of 162°C, which was 20°C above the glass transition temperature and 10°C higher than the isothermal hold temperature used to obtain the data

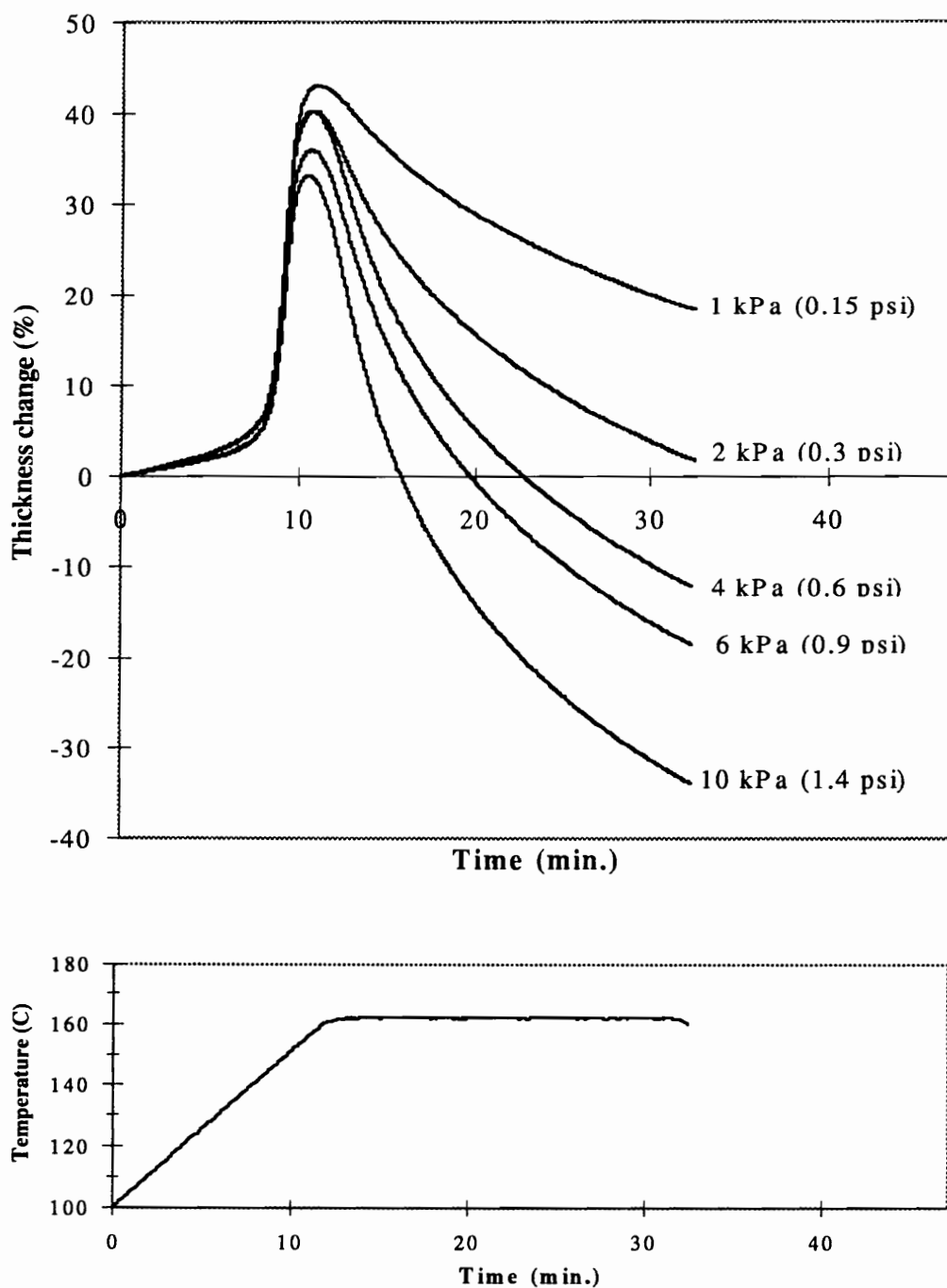


Figure 40 - Effect of TMA load on dimensional recovery during TMA scan with a 162°C isothermal hold and temperature profile as shown. (compaction pressure: 80 MPa, compaction time: 5 min., compact mass: 1 gram, initial compact density: 87% of the theoretical density).

in Figure 39. Note that increasing the hold temperature by 10°C did not affect the maximum thickness change, which occurred near T_g (below the isothermal hold temperatures), but it did greatly affect dimensional changes due to time-dependent deformation during the isothermal hold.

Figure 41 shows a plot of the maximum thickness change (which occurred near T_g) versus consolidation load for the dynamic consolidation tests performed with the two different

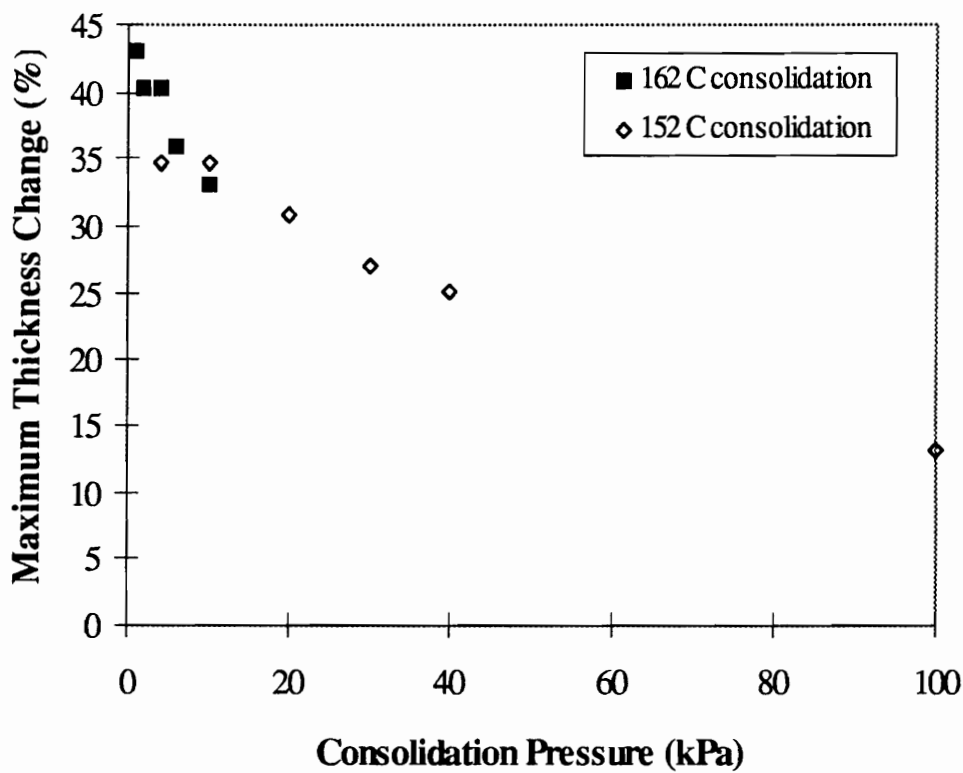


Figure 41 - Effect of the consolidation pressure on the maximum thickness change measured during thermomechanical analysis. (Data taken from Figures 35-36.)

hold temperatures. Increasing the load decreased the maximum thickness increase, but even a consolidation pressure of 100 kPa (14.7 psi) did not entirely eliminate the dimensional recovery which occurs at the glass transition temperature. Since the 100 kPa load was shown to be high enough to cause flow of the particles (as was evident by the large, negative thickness change in Figure 39), it appears that to eliminate dimensional recovery at T_g , a mold capable of providing side support is required during consolidation.

As is evident in Figure 40, increasing the consolidation temperature by only 10°C greatly enhanced the ability of the load to decrease the thickness change while the compacts were held above the glass transition temperature. For example, the curve for the specimen subjected to a consolidation pressure of 40 kPa (Figure 39) is similar to that obtained by increasing the hold temperature by 10°C and decreasing the pressure to 4 kPa (Figure 40). This data serves as a warning that increasing the consolidation temperature increases the likelihood that distortion of the compact will occur if proper side support is not provided.

Figure 42 provides a comparison of data obtained by isothermally consolidating compacts in the hot press and dynamically consolidating the TMA samples. In this plot, the percent change in thickness measured after 15 minutes at the isothermal hold temperature (at an adjusted time of 27 minutes in the dynamic tests) is plotted versus

the consolidation pressure. At low consolidation loads, the two techniques yielded similar results. As the pressure was increased, the isothermal tests resulted in a desirable leveling off of the thickness change of the bulk compacts. However, the dynamic TMA tests resulted in penetration of the probe into the specimens, as was evident by a negative thickness change at higher pressures. The differences in consolidation behavior at higher pressures reflect differences in the consolidation conditions, such as temperature profile, load distribution, boundary conditions and friction, which appear to be very important variables in consolidation.

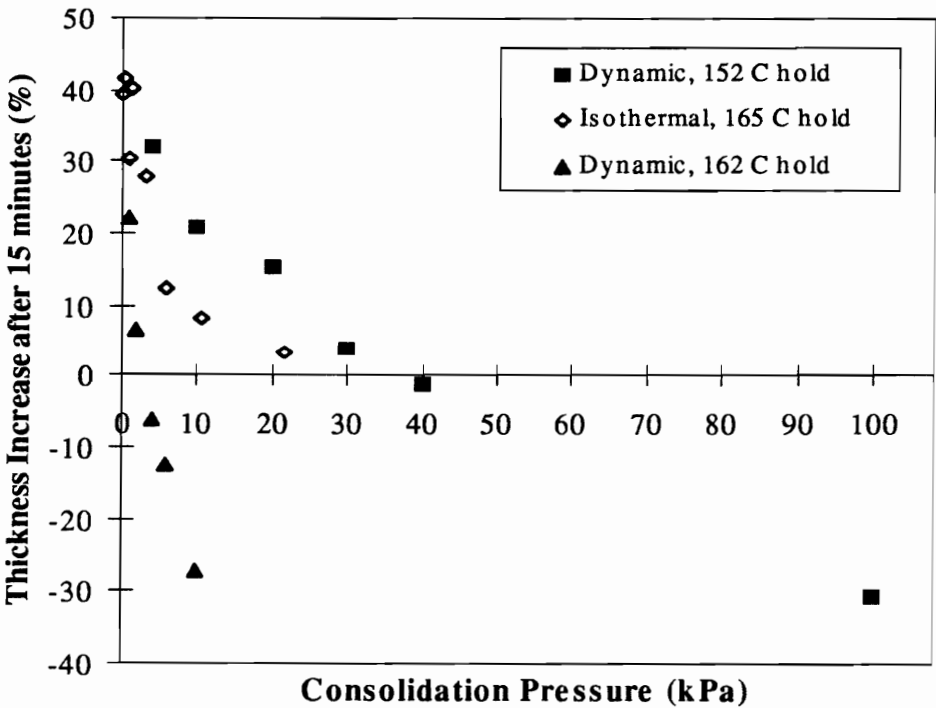


Figure 42 -Percent thickness increase measured after 15 minute hold at the indicated temperature (compaction pressure : 80 MPa, compaction time: 5 minutes, compact mass: dynamic -1 gram, isothermal - 1.5 grams). (Data taken from Figures 34-36).

Difficulties in Theoretically Modeling the Consolidation Process

Theoretical modeling of the consolidation process to predict the required consolidation pressures from fundamental principles would be extremely difficult. Some of the more troublesome complications are:

- *Temperature dependence of relaxation.* Relaxation is a time- and temperature-dependent process. Recovery of deformation imposed by compaction begins even well below T_g (as was discussed with regard to the transition from reversible to irreversible expansion), although it occurs more quickly at temperatures approaching the glass transition temperature. Both the temperature at which significant recovery begins to occur and the total amount of recovery that will occur during heating are dependent on the thermal history of the compact. Also, recovery times may be significantly influenced by the state of locked-in strain and may vary across each particle.
- *Temperature dependence of material properties.* Because large-scale recovery begins in the glass transition region, the material properties in this region are of interest. However, properties of polymers are extremely sensitive to temperature near T_g . Although it is possible to measure dynamic mechanical properties such as modulus as a function of temperature, static mechanical properties critical to a model, such as yield strength, would be very difficult to accurately measure at temperatures near T_g .
- *Non-uniformity of stress and strain.* Deformation experienced by the particles is very non-uniform and varies across each particle. The actual sizes and shapes of the

particles are irregular due to grinding, making modeling even more difficult. Although the compact might be thought of as a bulk material, the particles are not strongly bonded together and may move relative to each other, especially if the consolidation pressure is high. At high enough temperatures (or for long enough times), the polymer may “flow,” due to viscoelastic behavior. Frictional forces and boundary conditions must also be considered in a model.

- *Non-uniformity of temperature.* The temperature across the compact varies with both time and position, causing recovery to occur non-uniformly with time and position.

With all of the difficulties associated with theoretically modeling the consolidation process from fundamental principles, simple consolidation experiments, such as those used to collect the data in Figure 38, could be used to more accurately estimate the required consolidation pressures. However, if one wished to model the consolidation process to calculate the required consolidation pressure, the following steps might be taken:

Characterize the material:

- Determine viscoelastic properties of the polymer as a function of temperature and stress
- Determine the particle shapes and size distributions
- Determine the recovery temperature as a function of locked-in strain

Model the compaction process:

- Relate the global stresses to the local stresses on particles, taking into account the boundary conditions (friction at wall, mold geometry, etc.)
- Relate stresses on the particles to locked-in strains in the particles as a function of compaction pressure, time, and temperature.

Model the consolidation process:

- Calculate the temperature distribution in the compact as a function of time and temperature for the desired consolidation conditions
- Find the degree of recovery of locked-in strain as a function of time and temperature
- Calculate the local stresses required to eliminate recovery as a function of time and temperature
- Relate the local stresses to global stresses to find the pressures exerted on the mold by the particles during consolidation

Strength development in the consolidated compact occurs as the chains cross the interfaces between particles and form entanglements (see the Literature Review). To model strength development during an annealing stage (after recovery had been eliminated during consolidation), one might:

- Use a reptation-based theory to model strength development as a function of annealing time, temperature, and pressure
- Use a fracture mechanics approach to discount strength based on the largest remaining voids following annealing

Summary

Isothermal consolidation tests on bulk polycarbonate compacts showed that small pressures (22 kPa or 3.2 psi) could be used to limit the final dimensional recovery during consolidation at 165°C, without causing significant distortion of the compacts. Dynamic consolidation tests revealed that although consolidation pressures can be used to reduce the maximum thickness increase experienced by the compact at the glass transition temperature, they cannot be used to entirely eliminate this expansion without causing significant flow of the compact perpendicular to the load direction. It was concluded that molds capable of exerting small pressures (less than 50 kPa or 7.3 psi) and capable of providing side support to the compacts would be desirable to use during consolidation. Steps that might be taken to model the consolidation process were outlined.

VIII. Summary and Conclusions

Room Temperature Compaction

Unaged Polycarbonate

Results from compaction experiments performed on unaged polycarbonate showed that:

- Compact density was not strongly affected by compaction time after 5 minutes.
- For compacts 1.2 to 12 mm thick, thickness did not affect the density or levels of open and closed porosity.
- Compaction at high pressures resulted in a plateau density of $\sim 90\%$ of the theoretical density of polycarbonate.

These results were consistent with behavior observed in the compaction of metallic and ceramic particles.

Physically Aged Polycarbonate

Studying the compaction behavior of aged polycarbonate allowed the effect of yield strength and modulus on compaction to be examined. It was concluded that:

- Physical aging resulted in lower compact density for a given compaction pressure and a 5% decrease in plateau density.
- More particle deformation occurred in compacts made from the unaged (lower yield strength and modulus) powder compared to compacts made from aged powder having the same density, as observed using the ESEM.

- The decrease in particle deformation and mechanical interlocking resulted in a lower green strength for compacts formed from physically aged powder compared to those formed from unaged powder.

These findings show that the degree of physical aging, which is affected by common powder handling operations, such as drying and storage, can influence the ability of polymer powders to be successfully compacted at room temperature. Also, one would anticipate that polymers having a higher yield strength and modulus would experience a greater amount of particle rearrangement and a lower degree of particle deformation and mechanical interlocking during compaction than those with a lower yield strength and modulus.

Differential scanning calorimetry was used to examine thermal properties of unaged and aged polycarbonate powder before and after room temperature compaction. It was found that immediately following compaction:

- The endothermic peak at T_g , which is typically indicative of the degree of physical aging, decreased when physically aged powder was compacted.
- A small endothermic peak at T_g similar to that observed in physically aged powder appeared when unaged powder was compacted at high pressures.

It is believed that the apparent de-aging and aging effects are due to different components of the compaction stresses. Apparent de-aging results from shear stresses causing volume

dilatation, while apparent aging occurs due to the hydrostatic compressive stresses causing volume reduction.

Semicrystalline Polymers

Room temperature compaction experiments on semicrystalline polymers having a range of glass transition temperatures revealed that both the presence of crystallinity and the T_g affect compaction behavior. Specifically:

- The presence of crystallinity led to a lower density at a given compaction pressure, due to a lower degree of particle deformation compared to (amorphous) polycarbonate. This effect could have resulted from the lower volume fraction of amorphous phase and the higher modulus and strength of the semicrystalline polymers.
- Linear low density polyethylene, which has a T_g well below room temperature and a relatively high degree of crystallinity, could not be successfully compacted at room temperature, as the amorphous phase recovered from deformation rapidly after the compaction pressure was removed and because the free lengths of amorphous chains were probably short relative to the critical length required to form entanglements (and strength) across particle interfaces.
- Nylon-11, which has a $T_g \sim 30^\circ\text{C}$ above room temperature, showed time-dependent recovery of deformation at room temperature following the removal of the compaction pressure.

- Poly(ether ether ketone), whose T_g is close to that of polycarbonate ($\sim 145^\circ\text{C}$), responded in a similar manner to polycarbonate, compacting readily at room temperature and showing no significant time-dependent recovery following compaction. However, as with the other semicrystalline polymers, it had a lower density than did polycarbonate for a given compaction pressure.

Thus, the presence of crystallinity affected the compaction behavior due to a change in mechanical properties, while the glass transition temperature affected compaction by influencing relaxation times. These findings suggest that the degree of crystallinity, which is affected by the powder processing and storage conditions, can influence the ability of semicrystalline polymer powders to be successfully compacted at room temperature.

Sintering of Compacts Formed at Room Temperature

Polycarbonate Compacts

Experiments in which bulk polycarbonate compacts were isothermally sintered at 165°C in the absence of an applied pressure revealed that:

- Heating polycarbonate compacts above T_g caused them to quickly expand and approach the tap density of the powder, regardless of the magnitude of the compaction pressure.

- Changes in compact microstructure resulting from pressureless sintering above T_g included: large-scale recovery of particle deformation, loss of mechanical interlocking, and development of necks between particles.

Dynamic sintering tests on compacted polycarbonate (24 hours after compaction) using a temperature ramp to 165°C showed that:

- Small-scale, irreversible recovery of particle deformation begins at ~50°C, well below T_g . At the onset of this recovery, the thermal expansion coefficient increased by almost an order of magnitude.
- Large-scale, irreversible recovery of particle deformation, which took place at T_g , occurred quickly relative to the time scale of the test and resulted in an increase in compact thickness of as much as 50%.
- Compaction pressure and physical aging had a larger effect on the initial compact density than they did on the sintered density.

Irreversible recovery can be explained in terms of rubbery elasticity. Room temperature compaction causes a decrease in configurational entropy, which raises the energy of the polymer. The large increase in chain mobility at T_g allows the chains to increase in configurational entropy, as the particles recover from deformation. Factors which decrease the amount of particle deformation, such as decreasing the compaction pressure,

physically aging the powder, and increasing the particle yield strength and modulus, lower the amount of dimensional recovery that occurs upon heating to T_g .

Semicrystalline Polymers

Dynamic sintering tests on Nylon-11 and PEEK (24 hours after compaction) revealed that:

- Like polycarbonate, the semicrystalline polymers exhibited small-scale dimensional recovery beginning at $\sim 50^\circ\text{C}$ and large-scale recovery starting at T_g .
- The temperature at which expansion becomes irreversible appears to be influenced primarily by the thermal history, including storage time and temperature.
- Because the semicrystalline polymers experienced less particle deformation during compaction, they exhibited much less recovery during pressureless sintering, with PEEK dropping in density by only 10% of its theoretical density when heated above its T_g , compared to the 30% decrease measured in polycarbonate compacts.
- Nylon-11 exhibited large-scale expansion over a broader range of temperature than did polycarbonate and PEEK and had to be heated to its melting temperature to achieve maximum expansion.
- Small increases in density observed in PEEK compacts heated above T_g were attributed to cold crystallization occurring in the particles.

From these results, it is clear that crystallinity influences the behavior of semicrystalline polymers during sintering. Crystallinity affects the degree of particle deformation in the

compacts following compaction, which influences the amount of recovery that can take place during sintering. It also alters the dynamics of recovery during sintering by imposing constraints on the amorphous phase. Cold crystallization can occur in some compacts, causing changes in the dimensions during sintering that are not directly related to recovery of deformation.

Hot Compaction of Polycarbonate Powder

Hot compaction of polycarbonate at 100°C and 125°C was investigated. It was found that elevated compaction temperatures (below T_g) caused the following effects:

- For a given compaction pressure, the green density increased when compaction was performed above room temperature, with the largest effects noticed at the lowest pressures. A 5% difference in plateau density was measured for compaction temperatures of 100°C and 125°C.
- More particle deformation was observed to occur at a given compaction pressure in compacts formed at elevated temperatures.
- Increases in green and sintered strength were observed in compacts formed at elevated temperatures due to the increased particle deformation, which resulted in a higher degree of mechanical interlocking in green compacts and the formation of more necks in sintered compacts.

- The density of sintered compacts was higher when the compacts were formed above room temperature, however, raising the compaction temperature did not eliminate the majority of the dimensional recovery that occurs during pressureless sintering.

Thus, as anticipated, hot compacting compacts at temperatures below T_g did not solve the dimensional recovery problems experienced during the sintering of polymeric powders. In order to eliminate recovery during sintering, compaction would have to be done above T_g so the polymer molecules could remain in high entropy, equilibrium states. However, this would offer no processing advantages over conventional hot pressing of powders.

Consolidation of Polycarbonate Powder

Consolidation, or sintering with an applied pressure, was performed on compacts formed at room temperature. It was found that:

- Isothermal consolidation at 165°C for 15 minutes with very small applied pressures (~ 22 kPa or 3.2 psi) limited the dimensional recovery of the compacts without causing significant distortion of the compacts.
- Dynamic consolidation tests revealed that although consolidation pressures can be used to reduce the maximum thickness increase experienced by the compact at the glass transition temperature, they cannot be used to entirely eliminate this expansion without causing significant flow of the compact perpendicular to the load direction.

It was concluded that molds capable of exerting small pressures (less than 50 kPa or 7.3 psi) to limit recovery and providing side support to reduce distortion should be satisfactory for consolidation at temperatures 10-20°C above T_g .

Based on the complications that would be encountered in theoretically modeling the consolidation process, it was concluded that simple consolidation experiments would be more accurate in predicting the pressure required to limit dimensional recovery during consolidation.

Possible Applications of Compaction and Sintering Technology

Based on the results from this study, it can be concluded that compaction and sintering of polymeric materials can be useful for some applications, including:

- Processing high viscosity polymers at reduced temperatures, resulting in energy savings;
- Reducing degradation of some polymers during processing, by lowering the required processing temperatures;
- Reducing shipping costs of polymer powder, by compacting powder prior to shipping and breaking up the compacts prior to use (suggested by General Electric of NY);
- Producing inexpensive temperature exposure indicators (for shipping and storage) or irreversible temperature-activated switches, which would irreversibly expand when heated above the glass transition of the powder; and
- Forming polymers with a large amount of uniformly distributed open porosity.

Contributions of this Research

Although compaction and sintering of polymeric powders has been investigated since the early 1970's, this processing method is not widely used, possibly because the fundamental mechanisms which control compaction and sintering have never been fully understood. This study has made significant contributions to our understanding of compaction and sintering of polymers. It was demonstrated that mechanical properties (strength, modulus) and physical characteristics (degree of physical aging, glass transition temperature, presence of crystallinity) of the particles, and thus, powder processing, storage, and handling techniques, affect the ability of the polymer to be successfully compacted. The difficulties encountered in sintering polymeric compacts were explained in terms of a loss of configurational entropy of the polymer molecules during compaction, which caused large-scale dimensional recovery in the particles upon heating above T_g . Hot compaction (above room temperature, but below T_g) was not found to be useful in eliminating recovery during pressureless sintering. However, consolidation of compacts formed at room temperature (by heating 10-20°C above T_g and applying a small pressure (less than 50 kPa)) was shown to be a promising processing method.

References

1. J.P. Jog, "Solid-state processing of polymers: a review," *Adv. Polym. Technol.*, 12(3), 281-289 (1993).
2. T. Maeda and S. Matsuoka, "Study on cold-compaction molding of polymeric powders," *J. Fac. Eng., Univ. of Tokyo*, XXXII(3), 191-226 (1975).
3. S. Mazur (DuPont Central Research & Development), manuscript in preparation to be included in the book, *Polymer Particle Technology*.
4. J.S. Hirschhorn, **Introduction to Powder Metallurgy**, American Powder Metallurgy Institute, New York, 1969.
5. R.J. Crawford and D.W. Paul, "Cold compaction of polymeric powders," *J. Mat. Sci.*, **17**, 2267 (1982).
6. J.L. Throne, "Study of the compaction and sintering of two high-performance thermoplastic polyimides," *Advances in Polym. Tech.*, **9**(4), 281-291 (1989).
7. R.J. Crawford and D.W. Paul, "Solid phase compaction of polymers," *J. Mat. Sci.*, **14**, 2693-2702 (1979).
8. D.M. Bigg and M.M. Epstein, "Molding polymeric powders by compaction and sintering," *Science and Technology of Polymer Processing; Proceedings of the International Conference on Polymer Processing*, held at MIT, August 1977, 897-918, MIT Press (1979).
9. G.S. Jayaraman, J.F. Wallace, P.H. Geil, and E. Baer, "Cold compaction molding and sintering of polystyrene," *Polym. Eng. and Sci.*, **16**(8), 529-536 (1976).

10. R.W. Truss, Han, K.S., Wallace, J.F., and Geil, P.H., "Cold compaction molding and sintering of ultra high molecular weight polyethylene," *Polym. Eng. and Sci.*, **20**(11), 747-755 (1980).
11. G.W. Halldin and I.L. Kamel, "Powder processing of ultra-high molecular weight polyethylene I. Powder characterization and compaction," *Polym. Eng. and Sci.*, **17**(1), 21-26 (1977).
12. S.S. Hambir, J.P. Jog, and V.M. Nadkarni, "Strength development in powder processing of poly(tetrafluoroethylene)," *Polym. Eng. and Sci.*, **34**(13), 1065-1069 (1994).
13. S.Y. Mokashi and J.P. Jog, "Solid-state compaction of polyphenylene sulfide," *Polym.-Plast. Technol. Eng.*, **32**(6), 647-656 (1993).
14. J.J. Reilly and I.L. Kamel, "Characterization and cold compaction of polyether-etherketone powders," *Polym. Eng. and Sci.*, **29**(20), 1456-1465 (1989).
15. R.J. Crawford and D.W. Paul, *Eur. Poly. J.*, **17**, 1023 (1981)
16. S. Radhakrishnan and V.M. Nadkarni, "Modification of surface structure and crystallinity in compression molded poly(phenylene sulfide)," *Polym. Engr. and Sci.*, **24**(18), 1383-1389 (1984).
17. J.P. Jog, A. Lodha, and V.M. Nadkarni, "Structure development in powder processing of polyphenylene sulfide," *Advances in Polym. Techn.*, **11**(1), 41-52 (1991/1992).

18. J. Scheirs, S.W. Bigger, and O. Delatycki, "Structural morphology and compaction of nascent high-density polyethylene produced by supported catalysts," *J. Mat. Sci.*, **26**(12), 3171-3179 (1991).
19. G.W. Kuczynski, B. Neuville, and H.P. Toner, "Study of sintering of poly(methyl methacrylate)," *J. Appl. Polym. Sci.*, **14**, 2069-2077 (1970).
20. N. Rosenzweig and M. Narkis, "Observation and analysis technique for studying sintering of polymeric particles," *J. Appl. Polym. Sci.(Notes)*, **26**, 2787-2789 (1981).
21. N. Rosenzweig and M. Narkis, "Sintering rheology of amorphous polymers," *Polym. Engr. and Sci.*, **21**(17), 1167-1170 (1981).
22. N. Rosenzweig and M. Narkis, "Coalescence phenomenology of spherical polymer particles by sintering," *Polymer (Polymer Communications)*, **21**, 988-989 (1980).
23. J. Frenkel, *J. Phys. (USSR)*, **9**, 385 (1945).
24. N. Rosenzweig and M. Narkis, "Dimensional variations of two spherical polymeric particles during sintering," *Polym. Engr. and Sci.*, **21**(10), 582-585 (1981).
25. D.M. Gale, "Fabrication of poly(*p*-phenylene) by powder-forming techniques," *J. Appl. Polym. Sci.*, **22**, 1955-1969 (1975).
26. J. Rausch, Jr., and W.J. Farrissey, *Soc. of Plastics Engineers Annual Tech. Conf.*, *34th*, 644-646 (1976).
27. P. de Gennes, "Reptation of a Polymer Chain in the Presence of Fixed Obstacles," *J. Chem. Phys.*, **55**, 572 (1971).

28. R.P. Wool and K.M. O'Conner, "A Theory of Crack Healing in Polymers," *J. Appl. Phys.*, **52**(10), 5953-5963 (1981).
29. Y.H. Kim and Wool, R.P., "A Theory of Healing at a Polymer-Polymer Interface," *Macromolecules*, **16**, 1115-1120 (1983).
30. H. Zhang and R.P. Wool, "Concentration profile for a polymer-polymer interface. I. Identical chemical composition and molecular weight," *Macromolecules*, **22**, 2018 (1989).
31. R.P. Wool, B.L. Yuan, and O.J. McGarel, *Polym. Eng. And Sci.*, 29(19), 1340-1367 (1989).
32. H.H. Kausch and M. Tirrell, "Polymer Interdiffusion," *Annu. Rev. Mater. Scie.*, **19**, 341-377 (1989).
33. A.C. Loos and P.H. Dara., "Processing of thermoplastic matrix composites," *Review of Progress in Quantitative Nondestructive Evaluation*, **6B**, 1257-1265 (1987).
34. W.I. Lee and G.S. Springer, "A model for the manufacturing process of thermoplastic matrix composites," *J. Comp. Mat.*, **21**, 1017-1055 (1987).
35. M.C. Li and A.C. Loos, "Thermoplastic composite consolidation," *CCMS-94-01 (VPI-E-94-02)*, Center for Composite Materials Report Series, Virginia Tech (1994).
36. S.C. Mantel and G.S. Springer, "Manufacturing process models for thermoplastic matrix composites," *J. Comp. Mat.*, **26**(16), 2348-2377 (1992).

37. S.C. Mantel, Q. Wang, and G.S. Springer, "Processing thermoplastic composites in a press and by tape laying - experimental results," *J. Comp. Mat.*, **26**(16), 2378-2401, (1992).
38. C.A. Butler, R. Pitchumani, J.W. Gillespie, Jr., and A.R. Wedgewood, "Coupled effects of healing and intimate contact on the strength of fusion-bonded thermoplastics," *Proceedings of the 10th Annual ASM/ESD Advanced Composites Conference*, Dearborn, Michigan, 7-10 November, 1994, 595-604 (1994).
39. Laserite™ LPC3000 Data Sheet, DTM Corp., Austin, Texas (1994).
40. Laserite™ LN4010 Data Sheet, DTM Corp., Austin, Texas (1994).
41. Vixtrex PEEK 150PF Powder Data Sheet, Vixtrex USA, Inc., West Chester, PA (1996).
42. T.L. Smith, T. Ricco, G. Levita, and W.K. Moonan, *Proceedings, 6th Ann. Conf. on Deformation, Yield, and Fracture of Polymers*, Churchill College, Cambridge, 1-4 April, 1985, Plastics and Rubber Institute, London, 2.1 (1985).
43. "Physical constants of poly(ethylene)," in *Polymer Handbook, Third Edition*, edited by J. Brandry and E.H. Immergut, 1989.

Vita

Linda Wagnecz Vick was born on August 22, 1963 to Sylvia and Alexander Wagnecz. She grew up in Mine Hill, New Jersey, and graduated as valedictorian from Dover High School in 1981. While studying mechanical engineering at Virginia Tech, she spent her summers working with a materials research group at Picatinny Arsenal in Dover, New Jersey. Linda graduated magna cum laude in June, 1985, receiving a Bachelor of Science degree in Mechanical Engineering from Virginia Tech. She earned her Master of Science degree in Engineering Mechanics in 1987 from Virginia Tech, with Dr. Wayne Stinchcomb serving as her advisor. Her master's thesis topic was *Mechanical Behavior and Damage Mechanisms of Woven Graphite-Polyimide Composite Materials*.

Linda worked as a materials scientist at Litton Poly-Scientific in Blacksburg, Virginia for 4½ years. Her duties included failure analysis, product development, applied research, and technical support for the fiber optic and slip ring product lines. Returning to Virginia Tech in 1992, Linda served as a research associate at the Center for Intelligent Materials Systems and Structures in the Mechanical Engineering Department. She became a full time graduate student in 1993, with Dr. Ron Kander as her advisor in the Materials Engineering Science program.

Linda's immediate plans are to stay in the Materials Science and Engineering Department at Virginia Tech as research associate, working on several polymer-related industrial research projects with Dr. Kander.

Linda W. Vick